
Doctoral Dissertations

Student Theses and Dissertations

Spring 2018

Experimental and numerical investigation on tar production and recycling in fixed bed biomass gasifiers

Jia Yu

Follow this and additional works at: https://scholarsmine.mst.edu/doctoral_dissertations

 Part of the [Chemical Engineering Commons](#)

Department: Chemical and Biochemical Engineering

Recommended Citation

Yu, Jia, "Experimental and numerical investigation on tar production and recycling in fixed bed biomass gasifiers" (2018). *Doctoral Dissertations*. 2693.

https://scholarsmine.mst.edu/doctoral_dissertations/2693

This thesis is brought to you by Scholars' Mine, a service of the Missouri S&T Library and Learning Resources. This work is protected by U. S. Copyright Law. Unauthorized use including reproduction for redistribution requires the permission of the copyright holder. For more information, please contact scholarsmine@mst.edu.

EXPERIMENTAL AND NUMERICAL INVESTIGATION ON TAR PRODUCTION
AND RECYCLING IN FIXED BED BIOMASS GASIFIERS

by

JIA YU

A DISSERTATION

Presented to the Graduate Faculty of the
MISSOURI UNIVERSITY OF SCIENCE AND TECHNOLOGY

In Partial Fulfillment of the Requirements for the Degree

DOCTOR OF PHILOSOPHY

In

CHEMICAL ENGINEERING

2018

Approved by

Dr. Joseph Smith, Advisor
Dr. Muthanna Al-Dahhan
Dr. Douglas Ludlow
Dr. Christi Luks
Dr. Gregory Gelles

© 2018

JIA YU

ALL RIGHTS RESERVED

PUBLICATION DISSERTATION OPTION

This dissertation consists of the following three articles, formatted in the style used by the Missouri University of Science and Technology:

Paper I: Pages 7–53, Validation and Application of a Kinetic Model for Biomass Gasification Simulation and Optimization in Updraft Gasifiers, published by Chemical Engineering and Process – Process Intensification. 2018, 125: 214-226.

Paper II: Pages 54-99, Kinetic Modeling and Simulation of Biomass Gasification in Downdraft Fixed Bed Gasifiers, to be submitted to Chemical Engineering and Process – Process Intensification.

Paper III: Pages 100-132, Experimental Investigation of Tar Recycling in Pilot-scale Biomass Gasifiers: Prospects, Operating Procedures, Process Variations and Controls, to be submitted to Chemical Engineering Journal.

ABSTRACT

Bioenergy has been utilized for domestic purposes since pre-recorded history and it catches the highlight in the recent decades because it naturally benefits the world climate and energy security. Gasification is one of the key technologies to efficiently and economically convert biomass into syngas and further into biofuels. Despite these outstanding advantages, biomass gasification suffers from the formation of unfavorable byproduct tar and the consequential tar elimination. Moreover, the collected tar is toxic and thus requires storage and strict deposit method to avoid environmental pollution.

To understand the mechanisms of biomass gasification and tar production, simulations with Aspen Plus were conducted for both downdraft and updraft gasifiers, which are presented in the Paper I and II, respectively. The kinetic models are implanted with reaction kinetics to ensure their ability to approximate the tar production, which are superior to the widely used Gibbs Energy Minimization model for predicting syngas compositions. Paper III focuses on the investigation of the impact of tar recycling on syngas compositions under various operating conditions including different reactor scales (4", 8", 12"), different biomass feedstocks (pellets, picks, and flakes) and different equivalence ratios (0.15, 0.20, 0.25).

ACKNOWLEDGEMENTS

First, I gratefully acknowledge the Wayne and Gayle Laufer Endowment for the generous financial support for this project. I would like to thank my Ph.D. committee members: Dr. Joseph Smith, Dr. Muthanna Al-Dahhan, Dr. Douglas Ludlow, Dr. Christi Luks and Dr. Gregory Gelles. Their guidance and constructive critiques enhanced my work and are definitely better for this project. I would like to give my special thanks to my advisor, Dr. Joseph Smith, who gave his full support throughout my time as a Ph.D. candidate. He and his wife, Eileen Smith, always shared their braveness and life experiences with me, which encouraged me to solve problems both in my research and my personal life. Now, I have become a better woman.

I would like to thank my labmates who gave me all the help during my research time and I enjoyed so much working with them, especially Haider Al-Rubaye. Haider offered his time and skills helping me settle the methodology and the setup design. I enjoyed working with him a lot. I would also like to thank all the colleagues from the chemistry department: S. Roark, Dr. P. Whitefield, E. Schmittzhe, Dr. K. Woelk, Dr. J. Winiarz, Dr. T. Bone. I could not make it this far without your kind help.

Most importantly, I express a deep sense of appreciation to my family. My parents, Fei Yu and Hongxiang Sun, have been my strongest supporters during the past 29 years, and they still will be in the future. I am grateful for the extraordinary love of my husband, Dr. Xi Gao. You have been the light from the other side of the tunnel in the past, and I look forward to the next adventure together with you. No matter how far I go, home is always where I return.

TABLE OF CONTENTS

	Page
PUBLICATION DISSERTATION OPTION	iii
ABSTRACT.....	iv
ACKNOWLEDGEMENTS.....	v
LIST OF ILLUSTRATIONS.....	x
LIST OF TABLES	xii
 SECTION	
1. INTRODUCTION	1
1.1. RESEARCH MOTIVATION	3
1.2. RESEARCH OBJECTIVES	5
 PAPER	
I. VALIDATION AND APPLICATION OF A KINETIC MODEL FOR BIOMASS GASIFICATION SIMULATION AND OPTIMIZATION IN UPDRAFT GASIFIERS	7
ABSTRACT.....	8
1. INTRODUCTION	9
2. MODEL DEVELOPMENT.....	17
2.1. MINIMIZING GIBBS FREE ENERGY MODEL (MGFE MODEL) ..	17
2.2. REACTION MODEL (RXN MODEL).....	17
2.2.1. Schematic of the Kinetic Model.	18
2.2.2. Drying and Devolatilization.	19
2.2.3. Gasification and Combustion.	21

3. MODEL VALIDATION	27
3.1. SIMULATION OBJECTS.....	27
3.2. VALIDATION.....	28
4. MODEL APPLICATION AND OPTIMIZATION.....	31
4.1. EQUIVALENCE RATIO INFLUENCES.....	31
4.2. GASIFICATION TEMPERATURE INFLUENCE	33
4.3. BIOMASS MIXTURE INFLUENCE	34
4.4. MOISTURE CONTENT INFLUENCE	37
4.5. GASIFICATION CONDITIONS INFLUENCES ON TAR YIELD	38
5. CONCLUSIONS.....	41
ACKNOWLEDGEMENTS	42
NOTATION	43
REFERENCES	45
II. KINETIC MODELING AND SIMULATION OF BIOMASS GASIFICATION IN DOWNDRAFT FIXED BED GASIFIERS	54
ABSTRACT.....	55
1. INTRODUCTION	56
2. MODEL DESCRIPTION	65
2.1. MINIMIZING GIBBS ENERGY MODEL (GEM MODEL)	65
2.2. REACTION MODEL (KINETIC MODEL)	66
2.3. SIMULATION STRATEGY AND DETAILS	66
2.3.1. Test Cases.....	66
2.3.2. Structure of Downdraft Gasifier.....	67
2.3.3. Aspen Plus Simulation (Kinetic Model).....	69

3. RESULTS AND DISCUSSION	75
3.1. MODEL VALIDATION	75
3.2. ER EFFECT	80
3.3. TEMPERATURE EFFECT	81
3.4. MOISTURE CONTENT EFFECT	82
3.5. EFFECT OF BIOMASS COMPOSITION	84
3.6. TAR.....	86
4. CONCLUSIONS.....	89
ACKNOWLEDGEMENTS	90
NOTATION	91
REFERENCES	93
III. EXPERIMENTAL INVESTIGATION OF TAR RECYCLING IN PILOT- SCALE BIOMASS GASIFIERS: PROSPECTS, OPERATING PROCEDURES, PROCESS VARIATIONS AND CONTROLS	100
ABSTRACT.....	101
1. INTRODUCTION	102
2. METHODOLOGY	105
2.1. BIOMASS MATERIALS	105
2.2. EXPERIMENTAL DESIGN	106
2.3. GAS SAMPLING AND MEASURING SYSTEM.....	109
3. RESULTS AND DISCUSSION	112
3.1. EQUIVALENCE RATIO	112
3.2. THE SYNGAS COMPOSITIONS	112
3.3. TEMPERATURE PROFILE	113

3.4. TAR.....	114
3.4.1. Tar Compositions.	114
3.4.2. Tar Amount.	115
3.5. CHAR SIZE DISTRIBUTION.	116
3.6. THE AGGLOMERATION PHENOMENA OF THE CHAR PARTICLES	118
4. PROCESS CONTROL	122
4.1. PREPROCESSING OF THE BIOMASS	122
4.2. TROUBLESHOOTING.....	123
5. THE SHUTDOWN TIME	127
6. CONCLUSION.....	130
REFERENCES	131
SECTION	
2. OVERALL CONCLUSION	133
APPENDICES	
A. FORTRAN CODE IN THE PYROLYSIS CALCULATOR BLOCK.....	134
B. GC ANALYTICAL METHOD	137
REFERENCES	140
VITA.....	143

LIST OF ILLUSTRATIONS

SECTION	Page
Figure 1.1. Applications of synthesis gas	2
 PAPER I	
Figure 1. (a) Structural diagram of an updraft gasifier, (b) simulator schematic for the RXN model	20
Figure 2. (a) Flowsheet for drying and breaking down; (b) flowsheet for pyrolysis; (c) streams and operation blocks corresponded to reactor facts; and (d) Aspen flowsheet for gasification and oxidation zones.....	25
Figure 3. Case I syngas compositions for CO, CO ₂ , H ₂ and CH ₄	29
Figure 4. Case II syngas compositions for (a) CO; (b) CO ₂ ; (C)CH ₄ ; (d)H ₂	30
Figure 5. The RXN simulations for Case II (a) LHV and (b) η at different ERs	33
Figure 6. Reduction zone temperature influence on (a) syngas composition (wet basis); (b) syngas composition (dry basis); (c) extra energy needed and extra energy produced.....	35
Figure 7. Syngas compositions and lower heating value for different ratio of wood pellets and sewage sludge mixtures	37
Figure 8. Moisture content influence on (a) syngas compositions of wood pellets gasification; (b) LHV, dry gas production and η	38
Figure 9. Impact on tar amounts due to: (a) ER value, (b) reduction zone temperatures, (c) tar compositions	40
 PAPER II	
Figure 1. Schematic diagram of a downdraft gasifier.....	68
Figure 2. Model scheme of a downdraft gasifier	71
Figure 3. Aspen Plus flowsheet for downdraft biomass gasification with air	72
Figure 4. Comparison among experimental data, Kinetic Model and GEM Model results on (a)CO (b)H ₂ (c)CH ₄ of case 1; (d) CO (e)H ₂ (f)CH ₄ of case 2	77

Figure 5. (a) Syngas compositions, (b) LHV and η at different reduction zone temperature	82
Figure 6. Product composition of (a) CO, (B) H ₂ , (c) CH ₄ , and (d) LHV and η for Biomass 1-4	84
Figure 7. Product composition of (a) CO, (B) H ₂ , (c) CH ₄ , and (d) LHV and η for Biomass 5-8.	85
Figure 8. Volume fraction of tar for (a) Biomass 1 at different gasifying temperatures, (b) Biomass 1 at different ERs, (c) Biomass 1-4, (d) Biomass 5-8.	88
 PAPER III	
Figure 1. Relative content of different substance groups in gasification tar	104
Figure 2. Biomass feedstocks and gasifier cores	105
Figure 3. Flowsheet of the gasification process.....	107
Figure 4. Typical temperature profiles.....	113
Figure 5. Bio-tar produced during the gasification.....	114
Figure 6. Amount of tar production every 15mins	115
Figure 7. Char particles after sieving.....	117
Figure 8. Size distribution for three types of feedstock	119
Figure 9. Char size distribution.....	120
Figure 10. Agglomeration phenomena for pellets, picks and flakes.....	121
Figure 11. Bridging phenomenon when processing picks	122
Figure 12. Shutdown time comparison	128

LIST OF TABLES

PAPER I	Page
Table 1. Experiments and simulations for the updraft gasifiers in past decades	12
Table 2. Reactions involved in biomass gasification and their kinetic parameters	26
Table 3. Proximate and ultimate analysis of biomass in the two experiments	28
PAPER II	
Table 1. Summary of experimental investigations on downdraft gasifier and processsimulations on all bed types in the past decades	60
Table 2. Proximate and ultimate analysis of hazelnut shell.....	67
Table 3. Proximate and ultimate analysis of pine wood	67
Table 4. Lists the Aspen Plus units.....	70
Table 5. Reactions involved in biomass gasification and their kinetic parameters	73
Table 6. Analysis and errors for other Aspen Plus models.....	78
Table 7. Composition analyses of biomass samples 1-8.....	83
PAPER III	
Table 1. Proximate and ultimate analysis for feedstocks.....	106
Table 2. Calibrated gas flow for the control valve setting.....	108
Table 3. Physical properties of gasified char	116
Table 4. Troubleshooting and rectification	123
Table 5. The cooling down time for each gasification setups.....	129

1. INTRODUCTION

Human beings have been utilizing bioenergy for domestic purposes from pre-recorded history. The relationship between humankind and fire was documented in the myth of Prometheus, who defies the gods by stealing fire and giving it to man. Starting from burning wood, we take the use of the combustion heat to warm shelters, cook food and make tools. The usage of language and controlled fire makes us humanity. The development of the human history has been closely related to fire since then. Until 2016, bioenergy still supplies 10% of the global energy supply, as most developing countries are mainly using biomass for cooking [1]. In the most recent decades, bioenergy is shifting from the indigenous energy source into a more modern and effective commodity. There are usually two characteristics of biomass energy that attract the world's attention. The major benefit of adoption biomass energy is to bring the energy security and diversity of a country to a higher level. Biomass can be converted into solid, liquid and gaseous fuels, some of them are easy to transport and thus relieve the demand pressure off fossil fuels [2]. The other advantage is to reduce the greenhouse gases (GHG) emissions. The harvested biomass, if left in the field, decomposes and gives off the same amount of GHG as if burnt or converted to biofuels. As almost the same amount of forest is grown every year, the biomass is carbon-neutral if there is no additional forest harvest [3].

Biomass gasification is an economic and effective way to convert biomass into combustible gases. The produced synthesis gas (i.e. syngas) could be used to produce high-value chemicals (such as ammonia, methanol, dimethyl ether (DME)) and liquid

carbohydrates. Syngas can also be used by some other devices, such as gas turbines, internal combustion engines, and fuel cells, to produce electricity or heat. See details in Figure 1.1.

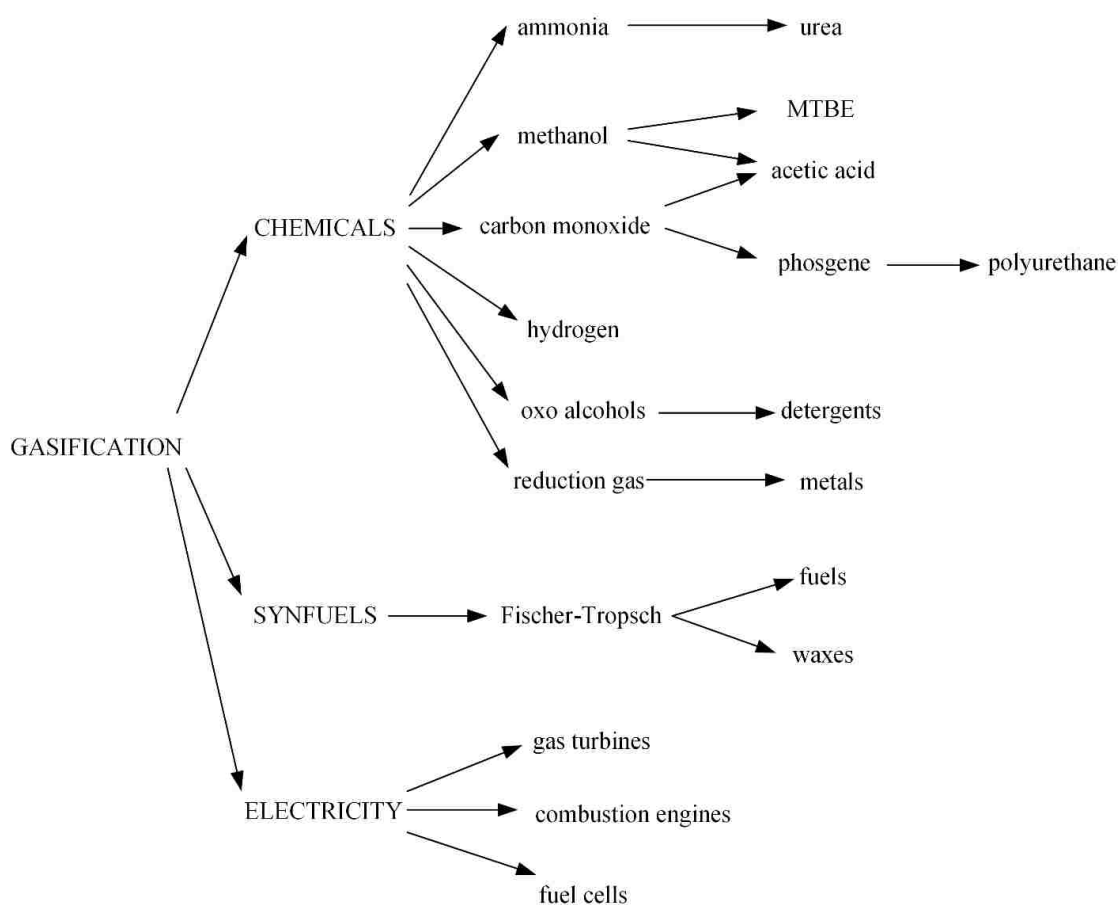
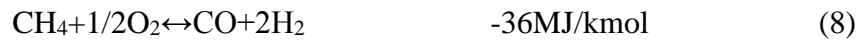


Figure 1.1. Applications of synthesis gas

Gasifiers are the main devices used in the gasification process, in which biomass is converted to syngas, consisting mainly of CO, H₂, CO₂, N₂, tar, ashes and small particulates [4]. Several types of gasifiers have been developed, which includes entrained flow gasifiers

[5-7], fluidized bed gasifiers [8-12], and fixed bed gasifiers [13, 14]. Fixed bed gasifiers can be further divided into downdraft [15-21] or updraft [22-26] based on the gas flow direction. The downdraft gasifier is commonly selected since it produces syngas with low tar content, and is suitable for engine applications [27]. In the gasification process, the produced syngas generally conserves 75% to 88% of the heat from the original fuel [28].

There are several basic chemical reactions:



An operation parameter, equivalence ratio (ER), has been proved to be a critical operating parameter, which dominant the gasification temperature and syngas production. It is defined as the ratio of oxygen provided to oxygen required for stoichiometric combustion. In our experimental design, ER is also controlled between 0.10-0.35 to fully understand the gasification performances.

1.1. RESEARCH MOTIVATION

Gasification produces include not only fuel gases, char and chemicals, but also some unfavorable byproducts such as tar. For all the gasifier types, the economical tar

removal process is still considered to be the main technological barrier [23]. In the gasification process, high molecular weight compounds are condensed to form tar if the temperature drops below 450°C. Two strategies are developed to remove the tar: (1) apply removal apparatus to clean the syngas [29], these apparatus include but not limited to: Cyclones, rotating particle separators (RPS), electrostatic precipitators (ESP), spray towers, packed column scrubber, wash tower, impingement scrubbers ceramics, fiberglass and sand; (2) improve the gasification technology to reduce the tar formation [30]. Most tar is deposited in the pipeline and the rest remains as an aerosol in the syngas. The tar causes metallic corrosion, clogs filters, valves, and internal combustion engines. Most tar is deposited in the pipeline and the rest remains as an aerosol in the syngas. Thus, it is necessary for process models to predict tar residue production.

There are adequate experimental investigations on gasification process. For the numerical analysis, researchers developed Gibbs Energy minimization model (GEM Model) to approximate the syngas compositions and a uniformed bed temperature. The model assumes all reactions in the gasification process are assumed to reach chemical equilibrium before the syngas leaves the reactor. The equilibrium model is not reliable on the full span of ER (0.10-0.35). Since the GEM Model assumes that all reactions reach equilibrium, it cannot be used to approximate the tar residues because tar is an intermediate byproduct. In this case, models nested with kinetic information is needed for the approximation of tar amount and its compositions.

Tar residues are mainly polycyclic aromatic hydrocarbons. Even after the cleanups, tar compositions are toxic and requires strict deposit method to prevent pollution. As tar can go through thermal cracking to generate volatiles, recycling of the tar might be

beneficial for the syngas compositions. The only related research is presented by Rabou [31], this paper only introduced one run, with unstable tar feeds during the total running procedure. The author concluded the tar recycle would increase 50% tar amount in producer gas, and the main advantage is the reduction of the disposal costs. Obviously, plentiful improvements regarding on the experiment design can be considered to further discuss this issue. For example, the feed of the tar should be known and fixed while taking syngas samples, and more runs should be taken to justify the results.

Suffering from all the abnormal running status of the gasifier, our research group found there are seldom research papers deliberating the problems in startups, stabilization, and the shutdown process of the bed. Failure in bed maintenance will cause uncontrollable temperature increase or reduction, which can further develop to bed turbulence or shutdown. A report regarding the process control and safety issues is necessary to be addressed.

1.2. RESEARCH OBJECTIVES

The current study aims to numerically and experimentally investigate the formation and recycling of tar. Aspen Plus software is used to fully understand the gasification process. For the experimental part, a full gasification setup equipped with gas cleaning apparatus is built to study the influence of tar recycling. The general objectives of the current study can be summarized as follows:

(1) Develop and validate kinetic models for biomass gasification to substitute the equilibrium-based model. The kinetic models should be able to correctly predict syngas

composition as well as tar formation and cracking. This dissertation presents models regarding updraft and downdraft gasifiers, respectively.

(2) Collected tar is mixed with the plain biomass and fed into the gasifier. The controlled parameters include equivalence ratio, three types of biomass feedstocks and three different gasifier sizes. Syngas compositions are analyzed using gas chromatography. The prospect of tar recycling is assessed.

(3) The experienced problems during the experimental runs are elaborated, the possible reasons are discussed, and, the solutions to our best knowledge is provided.

PAPER

**I. VALIDATION AND APPLICATION OF A KINETIC MODEL FOR BIOMASS
GASIFICATION SIMULATION AND OPTIMIZATION IN UPDRAFT
GASIFIERS**

*Jia Yu and Joseph D. Smith**

Department of Chemical and Biochemical Engineering, Missouri University of Science
and Technology, Rolla, MO 65401, United States

*Corresponding authors: smithjose@mst.edu (Dr. J. D. Smith), 1101 North State Street,

110 Bertelsmeyer Hall, Rolla, MO 65401, United States

Tel.: +1 (573) 341-4294

ABSTRACT

Biomass gasification has attracted great interest recently for its great potential as a thermal degradation method that converts biomass or carbonaceous solids into combustible gases with a usable heating value. However, accurate simulation of biomass gasification faces significant challenges as it has a complicated dependence on reaction kinetics, reactor geometry, processing methodology and operating condition. In this paper, a reaction model (RXN model) based on comprehensive biomass gasification kinetics is introduced and validated to predict the syngas and tar compositions. By comparing the simulating predictions with data from two updraft gasification experiment findings available in the literature, it is demonstrated that the RXN model is able to provide a more accurate description for updraft biomass gasification than the minimizing Gibbs free energy model (MGFE model), which can substitute for the widely used yet not accurate MGFE model. Parametric optimization studies were conducted to investigate the impacts of equivalence ratio (ER), gasifier temperature, biomass feed types on syngas and unreacted tar compositions. The results of this work provide vital information for large-scale gasifier design, operating decisions, and optimization.

Keywords: Biomass gasification; Process simulation; Updraft gasifier; Tar prediction

1. INTRODUCTION

Biomass energy has gathered attention in recent years as it has great potential to contribute to sustainable energy development and security [1-4]. Biomass gasification is one of the key technologies to convert waste biomass or carbonaceous materials to syngas efficiently and economically. Syngas is the source for high-value chemicals (such as methanol, DME [5-7] and liquid carbohydrates [2, 8-10]). Syngas can also be used by some other devices, such as gas turbines, internal combustion engines, and fuel cells, to produce electricity or heat [11-13]. Biomass gasification is also considered as a greener alternative as it does not produce extra carbon dioxide during the process [14].

Gasifiers are the main devices used in the gasification process, in which biomass is converted to syngas, consisting mainly of CO, H₂, CO₂, N₂, tar, ashes and small particulates [15]. Several types of gasifiers have been developed, which includes entrained flow gasifiers [16-18], fluidized bed gasifiers [19-23], and fixed bed gasifiers [24, 25]. Entrained flow gasifiers produce syngas with a lower tar content, but about 20% more oxygen is required [26]. In fluidized bed gasifiers, high amounts of oxygen bypass the reactor bed due to the low level of oxygen dissemination from the gas bubbles, which reduces the efficiency of the gasifier. Fixed bed gasifiers can be further divided into downdraft [27-33] or updraft [34-38] based on the gas flow direction. In downdraft bed gasifiers, tar content is much lower compared to that in an updraft gasifier, but the syngas has less calorific value [26].

The updraft gasifier is one of the oldest types of gasifiers due to its design simplicity and tractability. Biomass is normally fed from the top of the reactor and moves downwards,

while the gasifying agents are injected from the bottom of the gasifier and move upwards. Most chemical reactions take place at the bottom of the bed, where the temperature is the highest in the gasifier. The produced syngas exits from the top of the gasifier at a relatively low temperature (420K-570K) [39]. Updraft gasifiers have the ability to gasify high moisture content biomass as there is a high heat exchange rate between the combustion zone and the drying zone. Also, it could achieve relatively high carbon conversion rate due to the long residence time of biomass [40]. For all the gasifier types, the economical tar removal process is still considered to be the main technological barrier [35], thus it is necessary for process models to predict tar residue production.

Table 1 summarised the experimental and numerical studies on updraft gasifiers in past decades. Notice that in the experiment section, the effects of different conditions on gasifier performance have been studied, including gasifier temperature, equivalence ratio (ER), mixed gasification agents, and biomass types. Compositions of syngas were analyzed in most cases to evaluate the processing conditions, gasifying temperatures were usually around 1000K, ER was usually controlled between 0-0.4, air and steam were the popular gasifying agents, and both hard and soft woods were fed into the gasifiers.

Even fewer numerical studies on updraft gasifier have been reported. Some researchers were using the equilibrium-based model to approximate the syngas compositions [41, 42]. Although equilibrium-based models were widely used, not only for updraft gasifiers but also for fluidized gasifiers [43-46], entrained flow gasifiers [47, 48] and downdraft gasifiers [49-53], it is known that equilibrium base model is not reliable, especially when the equivalence ratio lays between 0.10-0.30. A few finite-rate kinetics models were developed for updraft gasifiers, while some models [54, 55] approximated

char conversion and tar formation were not discussed. Thus, developing and validation a kinetic model based on comprehensive and reliable reaction kinetics is needed. Also, a comparative study of equilibrium based model versus kinetic model is needed.

The objective of this work is to develop and validate a kinetic model for biomass gasification in updraft gasifiers using Aspen Plus to substitute the equilibrium-based model. The proposed kinetic model is able to correctly predict syngas composition and approximate tar formation and cracking. The paper is organized as follows. In the following section, methods and simulations settings are presented. Then, the kinetic model (is also called RXN model in this work) was validated by comparing with the experimental data available in literature and the MGFE model. At last, the validated RXN model was applied to investigate the effects of equivalence ratio (ER), gasification temperature, biomass mixture, biomass moisture and compositions on syngas and tar products.

Table 1. Experiments and simulations for the updraft gasifiers in past decades

Experiments				
Authors	Gasification agent	Biomass type	Equivalence ratio or air/fuel ratio range	Comments
Aljbour and Kawamoto, 2013 [56, 57]	Air and steam	Japanese cedar wood	0-0.3	Temperatures vary between 932K and 1223K, steam to carbon ratios vary between 0-2.0.
Kayal and Chakravarty, 1994 [58]	Air	Jute-stick	Not documented	Tested the influence of air inlet velocities on gas components, as well as the temperature along the bed.
Chen et al., 2012 [34]	Air	Mesquite and redberry juniper	0.25-0.37	CO: 13-21%, H ₂ : 1.6-3%, CH ₄ : 1-1.5%, C ₂ H ₆ : 0.4-0.6%, N ₂ : 60-64%, CO ₂ : 11-25%, and O ₂ : 1-2%.
Kihedu et al., 2016 [59]	Air and steam	Black pine pellets	Biomass feed 9g/min, gasified with 16L/min air or 11.3L/min air+1.5g/min steam	Tested the bed height, temperature, gas and tar compositions inside the reactor.
Pedroso et al., 2013 [35]	Air	Japanese Poplar woodchip	Not documented	Presented a modified reactor design with two air inlets to decrease the tar production. The gasifier was run for 19 times, for 6h periods.

Table 1. Experiments and simulations for the updraft gasifiers in past decades (cont.)

Saravanakumar et al., 2004 [60]	Air	long stick wood (leucaena species)	varied ERs between 0.19-0.95 in the same run	In the top lit updraft configuration, the gasifier was a top lit updraft system, was run 27 times, and 5 h and 15 min periods. This new design produced significant lower tar content than the conventional updraft gasifiers.
Saravanakumar et al., 2007 [37]	Air	long stick wood (prosopis species)	Wood varies from 45-50kg, air feed was 24.11-24.45m ³ /h in selected runs	In the bottom lit updraft configuration, the gasifier system was run ten times under various airflow rate operating conditions, each for a period of 5 h and 15 min.
Kurkela et al., 1989 [61]	Air and steam	Peat and wood chips	Not documented	Peat gasification: CO: 16.1%-24.2%, H ₂ : 16.7%-18.8, CH ₄ 2.0%-3.0%, CO ₂ : 10.3%-14.3%. For biomass: CO: 28.9%-20.6%, H ₂ 14.0%-17.6%, CH ₄ : 1.6%-2.5%, CO ₂ : 6.8%-13.8%.
Mandl et al. 2011 [39]	Air	Softwood pellets	Air/fuel ratio 1.0-1.6 kg/kg	CO: 24.4%-26.6%, CO ₂ : 4.7%-6.2%, CH ₄ : 1.6%-1.7%, H ₂ : 3.9%-6.3%, H ₂ O: 14.6%-18.4%.

Table 1. Experiments and simulations for the updraft gasifiers in past decades (cont.)

Lucas, 2005 [62]	Air/steam	Wood pellets, wood chips, bark and charcoal	20kg wood pellets feed with 50m ³ /h air	Batch gasification with preheated agents at different temperatures. All the gas composition data were collected along with operating time.
Gao et al., 2008 [63]	Air/steam	pine sawdust	0, 0.05, 0.1, 0.3	The effects of temperature, ER, steam/biomass ratio, and porous ceramic reforming on the gas characteristic parameters were investigated. A steam/biomass ratio of 2.05 was found to be optimum in all runs.
Chen et al., 2013 [64]	Air, air/steam, carbon dioxide/oxygen	Mesquite	2.7-4.3	Compared to air gasification, both the peak and average bed temperatures decreased for using air/steam mixtures as an oxidizing agent. Using a CO ₂ /O ₂ mixture for gasification produced a much higher HHV syngas.

Table 1. Experiments and simulations for the updraft gasifiers in past decades (cont.)

Simulations				
<i>Authors and Year</i>	<i>Bed type</i>	<i>Codes</i>	<i>Zone</i>	<i>Comments</i>
Kayal and Chakravart y, 1994 [58]	Updraft	Matlab	Entire bed	Mathematical model predicts the biomass conversion, gas production rate, gas composition and stream temperatures along the gasifier as well as the final syngas, as a function of air-input rate using jute-stick as the feedstock.
Yang et al., 2003 [65]	Fixed bed	Matlab	Entire bed	Effects of devolatilization rate and fuel moisture were assessed.
Di Blasi, 2004 [55]	Updraft	Matlab	Entire bed	A one-dimensional, unsteady mathematical model was presented, energy and mass transport, drying and devolatilization, char gasification, and combustion zone were coupled.

Table 1. Experiments and simulations for the updraft gasifiers in past decades (cont.)

Mandl et al., 2010 [54]	Updraft	CFD	Entire bed	The model considered one-step global pyrolysis kinetics. Drying, heat and mass transfer in the solid, gas and solid-gas phases, heat loss, particle movement and shrinkage were considered.
Ramzan et al., 2011[41]	Updraft	Matlab	Entire bed	Equilibrium method was used.
Ueki et al., 2012 [66]	Updraft	CFD	Entire bed	A Euler–Euler model was used to simulate the gasification process with superheated steam. The calculation showed there was a 150K–300 K temperature difference between gas phase and solid phase.
Chen et al., 2013 [42]	Updraft	Aspen Plus	Entire bed	Simulated two types of updraft bed based on a minimization of the Gibbs free energy at equilibrium.

2. MODEL DEVELOPMENT

2.1. MINIMIZING GIBBS FREE ENERGY MODEL (MGFE MODEL)

In the MGFE model, an RGIBBS operation block is used to convert biomass to syngas. Its mathematical theory is explained below. All reactions in the gasification process are assumed to reach chemical equilibrium before the syngas leaves the reactor. Thermodynamically, the total Gibbs free energy of a closed system at a constant temperature and pressure must decrease during an irreversible process. When the equilibrium state is reached, G_t attains its minimum value [67],

$$(dG_t)_{T,P} = 0 \quad (1)$$

When applying Eq. (1), each component involved in the process also follows mass balance law, namely, the mass of each element in the biomass and provided air equals the mass of each element in the syngas mixture, char, tar and ash:

$$\sum_{i=0}^N a_{i,j} n_i = A_j \quad (2)$$

Based on the assumption that all reactions reach equilibrium, the MGFE cannot be used to approximate the char and tar residues because tar is an intermediate byproduct. Thus, the development of reaction model is needed.

2.2. REACTION MODEL (RXN MODEL)

In this work, an RXN model based on detailed kinetic parameters of each reaction has been developed. The RXN model is fundamentally more accurate than the MGFE model because reaction kinetics are used instead of chemical equilibrium assumption. The kinetic reaction rate of species i of reaction r is expressed as follows:

$$r_{i,r} = k_r \prod_{i=1}^N [C_{i,r}]^{\alpha_{i,r}} \quad (3)$$

where k_r is computed using the Arrhenius expression:

$$k_r = A_r T^\beta e^{-\frac{E_a}{RT}} \quad (4)$$

To approximate and formulate the whole gasification process, H_2 , O_2 , N_2 , CO , CO_2 , CH_4 , H_2S , H_2O , char, tar and ash were considered, and all the other possible components are neglected. The RXN model is validated by comparison with both experimental data and the MGFE model.

2.2.1. Schematic of the Kinetic Model. Figure 1(a) shows the structural diagram of a typical updraft gasifier. The simulation procedure, Figure 1(b), corresponds with the structural diagram. The bed in an updraft gasifier is usually divided into four zones. Biomass stream passes through four zones sequentially from the top to the bottom while the air stream goes upwards. Biomass is progressively decomposed when passing through each zone and reacts with air to produce syngas. The reaction path was inspired by previously published articles on biomass gasification stages and steps by considering more reactions details. Ahmed et al. [68] illustrated that gasification process consists of many steps and these steps overlap each other. Although there are no clear boundaries between each step, these steps were divided into several groups or zones for modeling purposes. The top layer is the drying zone in which moisture separates from the feedstock due to the heat coming from the reactor core, generating steam and dried biomass. Pyrolysis zone would decompose the biomass into gasses (CO , H_2 etc.), liquids (tars and oils) and solid (char). Most Aspen Plus models only decompose biomass into basic elements and then used an RGIBBS block to optimize the final products, which allowed

no tar formation during the process. This has also been a common defect in previous biomass gasification models [49, 69]. In this paper, a series of physical and chemical processes take place and dried biomass is decomposed to primary tar, volatiles, charcoal and ash [70]. Primary tar goes under thermal cracking to achieve light gases and secondary tar. Gasification zone (also called reduction zone) is where Water-Gas shift and Boudouard reactions are the dominant reactions taking place due to limited oxygen. The combustion zone lies at the very bottom of the reactor, in which light gases, volatiles and charcoal are partially burnt by the incoming air and generates CO_2 and H_2O . Ash is considered inert for all reactions. Temperatures may rise to around 1200°C due to the oxidation reactions, which provides the heat for the whole gasification process. All processes follow mass balance and energy conservation in the RXN model. As the model works primarily with mixtures of hydrocarbons up to their critical points, Peng–Robinson equation of state was to approximate physical properties of the conventional components in the gasification process. The enthalpy and density model selected for both non-conventional components biomass and ash were HCOALGEN and DCOALIGT. Char is defined as pure carbon.

2.2.2. Drying and Devolatilization. Figure 2 shows the Aspen Plus simulation flowsheet of the RXN model. Biomass was specified as a non-conventional component and is defined by its ultimate analysis (UA) and proximate analysis (PA). The temperatures of the drying, pyrolysis and combustion zones were set based on experimentally measured values, the temperature of the gasification zone was

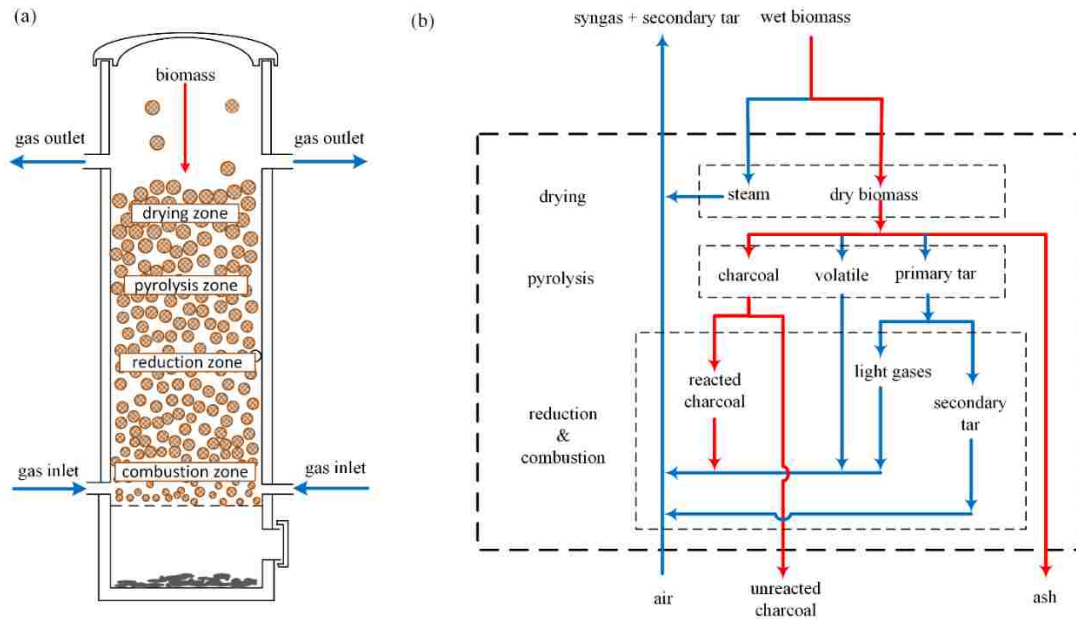


Figure 1. (a) Structural diagram of an updraft gasifier, (b) simulator schematic for the RXN model

calculated that the temperatures in the drying zone were between 100°C-200°C, 70°C - 200°C, 150°C-300°C, respectively. Thus, the temperature of the drying zone was set at 127°C in this work. Pyrolysis zone temperature was set at 330°C according to Reed [71], who estimated the pyrolysis temperatures to be 250°C-450°C, but mostly at 330°C. For drying and pyrolysis stages, see Figure 2(a) and 2(b). an RYIELD block was used to break down the biomass into basic chemical elements (carbon, hydrogen, oxygen, and sulfur etc.), ash, water and primary tar. The primary tar included acetone, toluene and phenol, and the compositions of which were defined under the assumption that tar takes 20% of the total biomass weight [66]. The secondary tar included naphthalene and benzene only for this model. A SEP block separated the primary tar and water from the ash and basic elements. Then, an SSPLIT block was used to separate fixed carbon from rest of the volatile elements,

the ratio if separation equaled to fixed carbon/total remained carbon. The volatile elements contain basic elements to form volatiles, an RGIBBS block was used to convert these chemical elements to light gases (CO, H₂, CO₂, N₂ etc.). The mixture stream of fixed carbon, light gases, primary tar, steam and ash was considered as a pyrolysis product.

2.2.3. Gasification and Combustion. Char, secondary tar and volatiles reacted with abundant air in the combustion zone, and limited air in the gasification zone. In an updraft gasifier, the gas phase goes in from the bottom and flows to the top, while the solid phase flows in the opposite direction. Figure 2(c) shows how the streams and operation blocks corresponded to these reactor facts. The stream “Gas*” was not a recycle stream, but it was circulated since this gas phase stream comes out of the combustion zone and goes into the gasification zone. This flowsheet became complex when Aspen Plus blocks involved in it, see Figure 2(d). The returned stream “Gas*” was also labeled in this figure.

The model divided char gasification into heterogeneous reactions and homogeneous reactions. Kaushal and Tyagi [46] used this thought and developed a kinetic simulation for a fluidized bed gasifier, but they did not specify any details regarding residence time. As is well-known, gas usually goes through the reactor much faster than the biomass: the residence time of the biomass is in the order of several hundred to several thousand times larger than that of the gas. Thus, the residence times for gas-solid phase reaction set and gas phase reaction set should be set separately. To cater this phenomenon, as shown in Figure 2(d), two RCSTR blocks were used for gasification zone considering different residence times, the same settings were applied to the combustion zone. Since the void ratio of the bed is around 0.5, the gas phase would have back flows and diverse velocities [72]. The gasifier was considered to have the hybrid nature of both PFR and

CSTR. To approximate this flow, one CSTR was used in each zone for each homogeneous or heterogeneous reaction set, but CSTRs in series were used to mimic the plug flow nature. Fogler [73] drew a conclusion that we can model a PFR with a large number of CSTRs, justifying that a number of CSTRs in series could be used to mimic a PFR. Nikoo and Mahinpey [74], Abdelouahed et al.[75] also used two RCSTR blocks in series to optimize fluidized gasifier. Due to these reasons, the use of CSTR blocks is appropriate. Notice that adding sets of heterogeneous and homogeneous blocks could benefit the model accuracy, it is also necessary when this model is used in industry scale gasifiers.

Heterogeneous reactions were activated in “HETERO1” and “HETERO2”, and homogeneous reactions were activated in blocks “HOMO1” and “HOMO2”. All the reactions and their rates considered in this work are shown in Table 3. In this paper, the volume of gasification zone and combustion zone were assumed to be $\frac{1}{4}$ of the total bed height. Chen et al. [34] conducted an experiment for updraft gasifier, in which he provided temperature profile along the bed height. The total length of the bed was 22cm, and each zone occupied approximately $\frac{1}{4}$ of the total length (around 6cm). Hihedu et al. [59] and Ueki et al. [38] also reported bed temperature profiles, indicating the combustion and gasification zones were almost the same length, and they in total took half of the reactor length. The residence time of each block was calculated by a quarter of the total residence time of gas phase and solid phase.

As CSTRs were used to mimic the gasification and combustion processes, the total residence time could be calculated by the feed, void ratio and zone volume. The total residence time of solid phase was estimated by Eq. (8), for gas phase was estimated by Eq. (9). For the approximation of heterogeneous reaction CSTR block, the simulated

reactor diameters were the same as those used in experiments, the reactor length could be calculated by Eq. (10).

$$V_{rt} = \pi D^2 L / 4 \quad (5)$$

$$t_{ht,total} = \rho_{bio} V_{rt} / F_{bio} \quad (6)$$

$$t_{homo,total} = (1 - \phi) V_{rt} / F_{air} \quad (7)$$

$$t_{ht,zone} = 1 / 4 t_{ht,total} \quad (8)$$

$$t_{hm,zone} = 1 / 4 t_{hm,total} \quad (9)$$

$$L_{hm} = L_{ht} \times t_{hm,total} / t_{ht,total} \quad (10)$$

A “COOLDOWN” block was used to simulate gas transformations and temperature change after it leaves the high-temperature zones and “syngas” stream was the final syngas product.

Zainal et al. [33] reported that the combustion zone temperature was 1000°C. Dogru et al. [28] and Sheth and Babu [76] reported the combustion zone temperature for downdraft gasifiers were 1000°C- 1200°C and 900°C-1050°C, respectively. So, combustion zone temperature was set at 1000°C in this work. The gasification zone temperature was calculated by overall energy balance. The calculated temperature was around 570°C-670°C in this work, which was consistent with the values reports by Ueki [38] and Zainal [33] (approximately 450°C -800°C). The temperatures of “HOMO1” and “HETERO1” were the same, and were calculated by a “DESIGN SPEC” block. To maintain energy conservation, the net released energy were calculated by:

$$Q_{hm1} + Q_{ht1} = -Q_{hm2} - Q_{ht2} \quad (11)$$

$$T_{hm1} = T_{ht1} \quad (12)$$

Development and validation of a reliable model for large-scale gasifier is definitely needed. However, the experimental data of industrial-scale gasifier that can be used for comparing with models is still insufficient. For example, as the gasification goes, the biomass shrinkage and breakup theory were not well developed yet, the void ratio along the bed length would not be as uniform as a pilot scale reactor. Furthermore, the heat loss to the surroundings, heat exchange between each zone and zone volumes would change vigorously due to the scaling up. For a large-scale reactor, a large number of CSTRs will be needed, which will also make this model harder to converge as the number of CSTR increases.

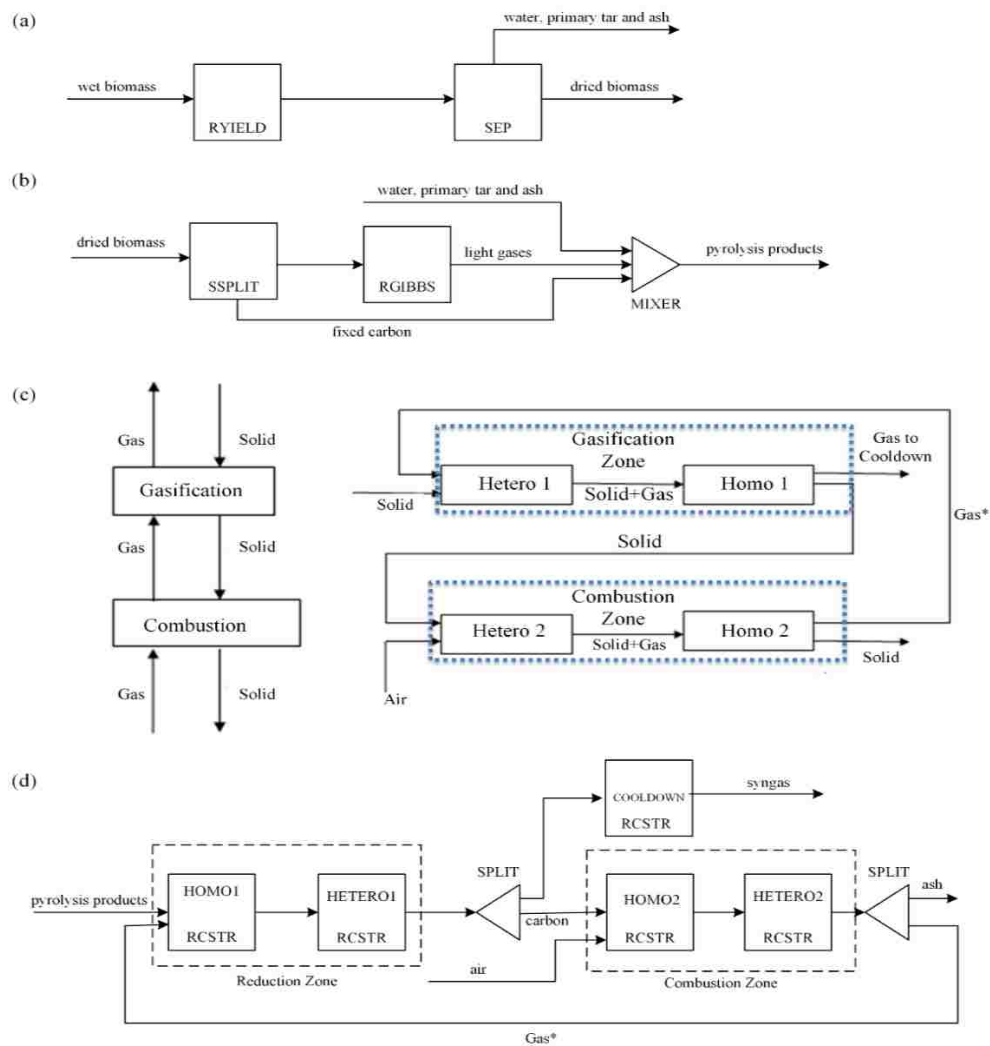


Figure 2. (a) Flowsheet for drying and breaking down; (b) flowsheet for pyrolysis; (c) streams and operation blocks corresponded to reactor facts; and (d) Aspen flowsheet for gasification and oxidation zones

Table 2. Reactions involved in biomass gasification and their kinetic parameters

Reactions		Kinetic Parameters		
Heterogeneous Reactions		$ArT^{\beta} (\text{mol}^{(1-\alpha)}\text{m}^{(3\alpha-3)}\text{s}^{-1})$		Ea (kJ/kmol)
Boudouard [77]	$\text{C}+\text{CO}_2\rightarrow 2\text{CO}$	589T		222829
Carbon shift [78]	$\text{C}+\text{H}_2\text{O}\rightarrow\text{CO}+\text{H}_2$	5.714T		129706
Combustion I [48]	$\text{C}+0.5\text{O}_2\rightarrow \text{CO}$	0.002		79000
Combustion II [79]	$\text{C}+\text{O}_2\rightarrow\text{CO}_2$	7.96×10^{-7}		27118
Methanation [80]	$\text{C}+2\text{H}_2\rightarrow\text{CH}_4$	0.0342T		129706
Homogeneous Reactions		$ArT^{\beta} (\text{mol}^{(1-\alpha)}\text{m}^{(3\alpha-3)}\text{s}^{-1})$		Ea (kJ/kmol)
Combustion III [81]	$\text{CO}+0.5\text{O}_2\rightarrow\text{CO}_2$	$1.3\times 10^{11}\text{C}_{\text{H}_2\text{O}}^{0.5}$		125600
Water-gas shift [77]	$\text{CO}+\text{H}_2\text{O}\leftrightarrow\text{CO}_2+\text{H}_2$	Fr	2.78	12560
		Rr	104.830	78364
Steam methane reform [82]	$\text{CO}+3\text{H}_2\leftrightarrow\text{CH}_4+\text{H}_2\text{O}$	Fr	312	30000
		Rr	6.09×10^{14}	257000
Combustion IV [77]	$\text{H}_2+0.5\text{O}_2\rightarrow\text{H}_2\text{O}$	$3.53\times 10^{8.4}$		30514
Acetone cracking [66]	$\text{C}_3\text{H}_6\text{O}_2\rightarrow 0.5\text{C}_6\text{H}_6\text{O}+1.5\text{H}_2\text{O}$	10^4		136000
Phenol cracking [66]	$\text{C}_6\text{H}_6\text{O}\rightarrow 0.5\text{C}_{10}\text{H}_8+\text{CO}+\text{H}_2$	10^7		100000
Toluene cracking [66]	$\text{C}_7\text{H}_8+\text{H}_2\rightarrow\text{C}_6\text{H}_6+\text{CH}_4$	3.3×10^{10}		247000

3. MODEL VALIDATION

To validate the RXN model, the predicted syngas compositions at different equivalence ratios (ERs) were compared with the corresponding experimental data. ER is an essential parameter influencing gasification temperatures and syngas compositions. It is defined as the ratio of provided oxygen to oxygen required for full combustion:

$$ER = \frac{\text{the actual air/fuel ratio}}{\text{air/fuel ratio for stoichiometric combustion}} \quad (13)$$

3.1. SIMULATION OBJECTS

Two representative experiments were selected to test and validate the RXN-model. Test Case I was conducted by Yasuaki Ueki et al [38]. The gasifier had a height of 1m and an inner diameter of 0.102 m, and the biomass bed height was 0.6m. The steady state biomass feeding rate was 0.75 kg/h with 20min internals, air flow rate was set at 20 L/min. Test Case II was reported by Seggiani et al. [83], who adopted a gasifier of 2 m height and 0.165 m internal diameter with a bed height 1 m. Experimental tests were conducted at different mixing ratios of blending sewage sludge (SS) and wood pellets (WP) mixtures to analyze the effects on gasification behaviors. ER ratios at 0.15, 0.20, and 0.25 were operated for all mixtures. In our simulation, the ERs vary from 0.10-0.30, with a 0.025 interval to achieve a better understanding of the compositions changes against ER. Table 3 shows the results of the proximate analysis and ultimate analysis of biomass species used in these cases.

3.2. VALIDATION

In Figure 3, the RXN simulation results and the MGFE model predictions were compared with experimental data at air/fuel ratio equals to $1.6\text{m}^3/\text{kg}$ for Case I. It can be seen that the predictions of the RXN model corresponded closely to the experimental data, while MGFE model results failed to correctly predict the syngas compositions. For CO, the prediction error of the RXN model was about 11%, while the error of MGFE model was approximately 36%. For CO₂ and H₂, the values predicted by the RXN model were very close to experimental data, while the MGFE model gave a value twice bigger than the experimental data. Both the RXN and the MGFE models overpredicted CH₄. As described in Case I, the woody biomass pellets were pre-dried for 24 hours prior to each

Table 3. Proximate and ultimate analysis of biomass in the two experiments

	Case I	Case II	
	Wood pellets	Wood pellets	Sewage sludge
Proximate Analysis (wt.%)			
Volatile matter	79.70	74.1	44.0
Fixed carbon	15.09	17.2	5.1
Ash	0.57	0.7	30.9
Moisture	4.64	8.0	20.0
Ultimate Analysis (wt.% dry, ash-free basis)			
Carbon	49.58	49.3	51.2
Hydrogen	6.65	6.2	8.2
Oxygen	43.59	44.5	31.8
Nitrogen	0.19	<0.1	7.1
Sulfur		<0.1	1.7

run, yet the original analysis was used in the simulations. This also resulted in bigger errors.

Figure 4 shows the comparison of the RXN and the MGFE models predictions with experimental data at ER 0.10 to 0.30 for Case II. In Figure 4a, the volume fractions of CO at ER= 0.15, 0.20, 0.25 obtained from the experiment were about 0.3. The RXN model reasonably underpredicted the CO mole fraction, while the MGFE model significantly misestimated it. In Figure 4(b), the experimental measurement of CO₂ volume fraction slightly increases with the increasing ER from 0.15 to 0.25. The RXN model prediction gives a similar trend with the experimental data, while MGFE model gives an opposite trend. For CH₄ and H₂, the RXN model correctly predicted their value, while MGFE model gave more than 100% errors in CO₂ predictions and more than 200% in CH₄ predictions, both of which are not acceptable.

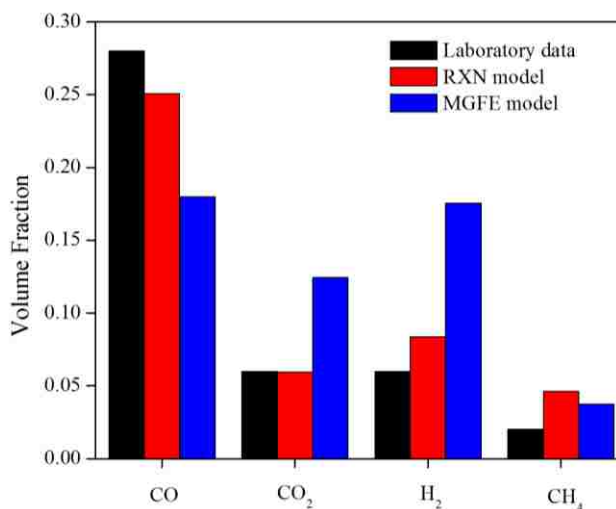


Figure 3. Case I syngas compositions for CO, CO₂, H₂ and CH₄

According to the comparisons above, the RXN model is more accurate than the MGFE model. The RXN model benefits from the theoretical fundamentals of using reaction kinetics as it takes the time scale into account, it. The application of different residence times for heterogeneous and homogeneous reactions are also considered the main parameter for a more precise model.

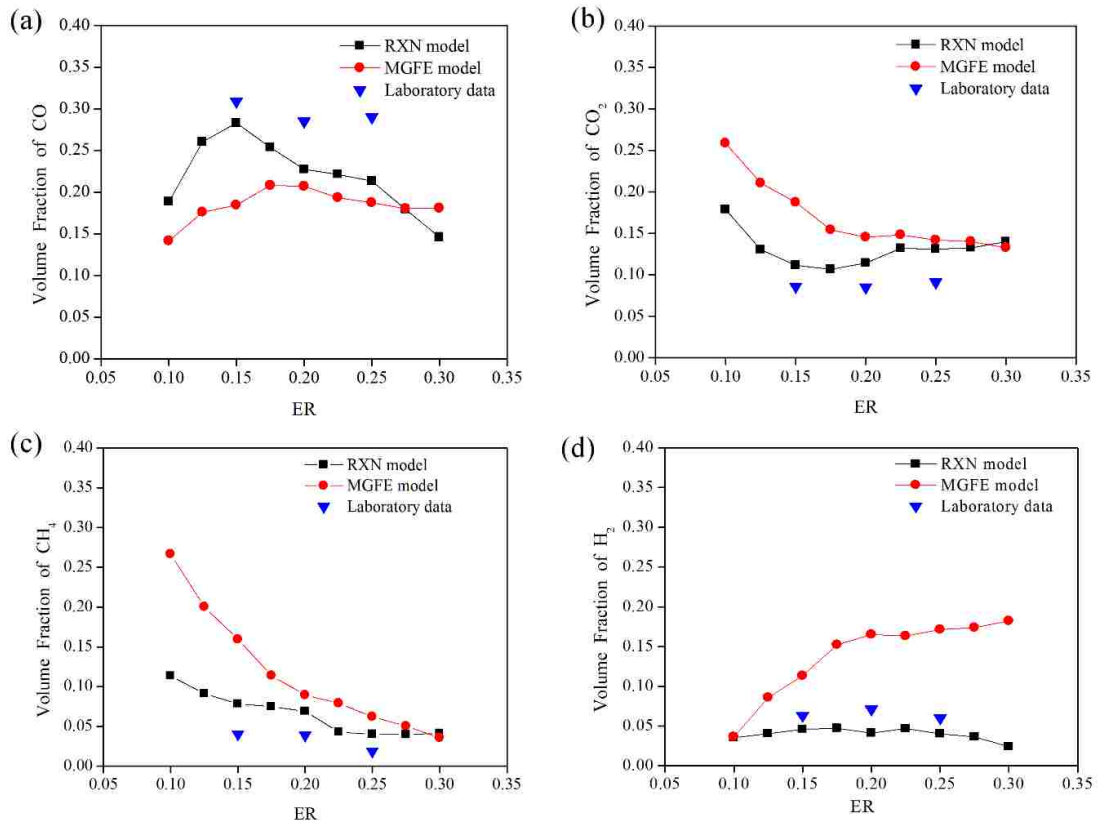


Figure 4. Case II syngas compositions for (a) CO; (b) CO₂; (c) CH₄; (d) H₂

4. MODEL APPLICATION AND OPTIMIZATION

4.1. EQUIVALENCE RATIO INFLUENCES

In updraft gasifiers, the ERs are usually controlled between 0.10-0.30 depending on diverse types of feed. Generally, a higher value of ER means more oxygen is provided, resulting in better combustion as well as a higher reactor temperature. For RXN simulation of Case II, it can be seen that CO volume fraction first increases as ER increases to peak values and then decreases. This trend is not obvious in Case II experimental data, but it can be clearly seen in the experiment of Chen et al. [34] and Blasi et al. [84] in the updraft gasifiers. Chen et al. reported that the CO volume fraction peak is at ER=0.3 for juniper gasification and 0.27-0.37 for Mesquite gasification. This difference of ER peaks may due several reasons, such as differences in bed void ratios, gasifier sizes, and chemical and physical properties of the biomass. For example, beds filled up by biomass of difference shapes have different void ratios, which influence gas phase flow pattern significantly. Picks usually suffer from a worse bridging phenomena than pellets [85], bridging and the resulted flow pattern would cause more air bypassing the bed, and therefore requires a higher optimized ER. Blasi et al. found that the CO volume fraction increases with the increasing ER (air/fuel ratio 0.80-1.50kg/kg), which matches the trendline before reaching the CO peak. This phenomenon is also observed in some downdraft gasification experiments [21, 36, 86].

A slight discrepancy can be observed between the RXN prediction and the experiment. For example, the RXN model gives CO values lower than the experimental data. Possible reasons are as follows. First, the gasification reaction kinetics are very

complex and highly coupled as reported frequently in the literature. Therefore, the final predictions would divert from the experimental data, even if one of the reaction kinetics is not accurate. Moreover, as Aspen Plus restrains the RXN model to consider the detailed temperature and component concentration distributions inside the gasifier, uniform distributions were assumed for each zone. This also explains why there is a 1% oxygen in the experimental data, while oxygen concentrations are always calculated to be zero in simulation cases.

To better understand the quality and calorific value of the syngas product, the lower heating value (LHV) of syngas is introduced and defined as follows:

$$\text{LHV} = \text{CO} \times 12.636 + \text{H}_2 \times 10.798 + \text{CH}_4 \times 35.818 + \text{C}_2\text{H}_4 \times 59.036 + \text{C}_2\text{H}_6 \times 63.772 \quad (14)$$

where, CO, H₂, CH₄, C₂H₄ and C₂H₆ are the molar percentages of components in the syngas.

The η , LHV per kg biomass, represents the energy extracts from 1kg of biomass, which is calculated by

$$\eta = \text{LHV} \times \text{dgp} / F_{\text{bio}} \quad (15)$$

Figure 5(a) and 5(b) show the LHV and η as functions of ER, respectively. It can be seen that LHV increases from ER=0.10 to ER=0.125, and then decreases, with the maximum value (7.0MJ/m³) occurring at ER=0.125. It has the same pattern with CO volume fraction as the function of ER as shown Figure 4(a). The maximum value of η exists at ER=0.15, which means the maximum energy of 15.5MJ can be obtained from 1kg of biomass. The η peak and CO volume fraction peak exist at the same ER, both are close to the LHV peak at ER=0.125. From the aspect of energy conversion, ER=0.15 is the optimum operation condition for gasification of the biomass we used in our simulation (wood pellets). The optimal ER may be adjusted according to the following chemical

processes. For example, if the syngas will be fed into a Fischer–Tropsch reactor to produce hydrocarbons, the ER should be set to 0.30 in order to cater the ideal feeding ratio $H_2/CO=2$ [87, 88].

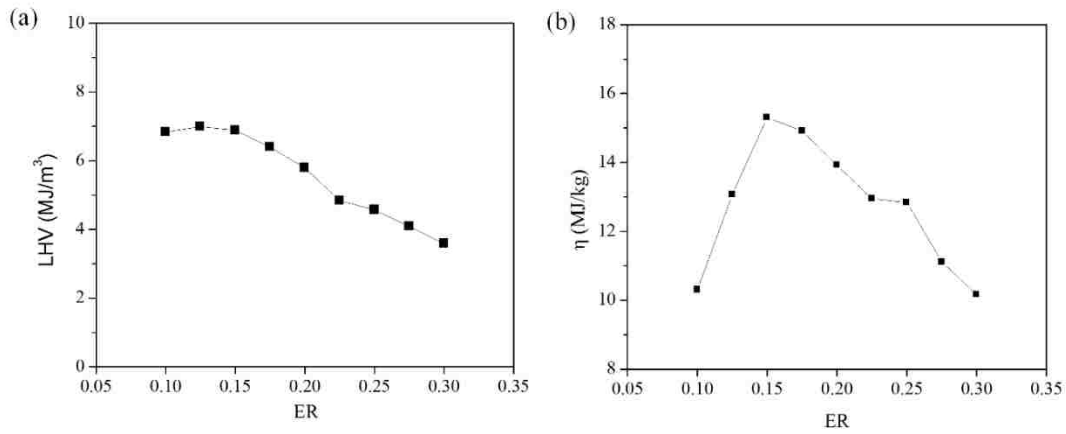


Figure 5. The RXN simulations for Case II (a) LHV and (b) η at different ERs

4.2. GASIFICATION TEMPERATURE INFLUENCE

The biomass gasifiers are preferred to be energy self-sustainable, as the heat produced from the combustion zone transfers to other areas of the bed and fully support all reactions. Additional heat can be provided by adding water steam as a co-gasification agent or applying hot wire to raise the bed temperature. The syngas compositions would be reformed at a higher gasification temperature and thus preserve more energy. Figure 6(a) gives the syngas compositions at ER=0.25, +0°C represents the calculated temperature with no extra heat funneled, gas compositions are also given for raised temperatures to evaluate the effect of gasification temperatures. The figure clarifies the CO and H_2 mole

fractions increase with the increase of temperature, while the H₂O mole fraction decreases. This prediction matches the experiment facts in the review paper [89]. The mole fraction of syngas compositions after the water condensed are given in Figure 6(b). CO compositions are comparable at low temperatures (+0°C-+90°C) due to increased steam composition, but it increases to 0.24 at +120°C, H₂ increases with increasing temperature. CH₄ mole fraction remains fairly steady, CO₂ fraction increases to a peak value at +60°C and then decrease on both wet and dry basis. This same trend can be found in experiments conducted by Lapuerta et al. [90] and Peng et al. [91]. The extra energy needed and produced are shown in Figure 6(c), this illustrates that the syngas has bigger heating values if the gasifier is operated at higher temperatures, but this needs a lot more energy to be put into the system. According to this prediction, it is not wise to use commercial energy resources (such as electricity or natural gas) to increase the bed temperature, but the hybrid of gasification and exothermic chemical processes could be a better solution.

4.3. BIOMASS MIXTURE INFLUENCE

Several authors have investigated the co-gasification of biomass-coal [92-97] as well as co-gasification of biomass mixtures [91, 98, 99]. It is very important for gasification plants to have different biomass feeds at the different times of the year because of the particular biomass harvest times. Feed type with a higher heating value (i.e., lower moisture, lower ash, and higher carbon content) will produce syngas with more combustible components, which means higher syngas quality. This phenomenon could be found in the experiments by Ong et al. [98] and Seggiani etc. [83], Ong et al. gasified sewage sludge and

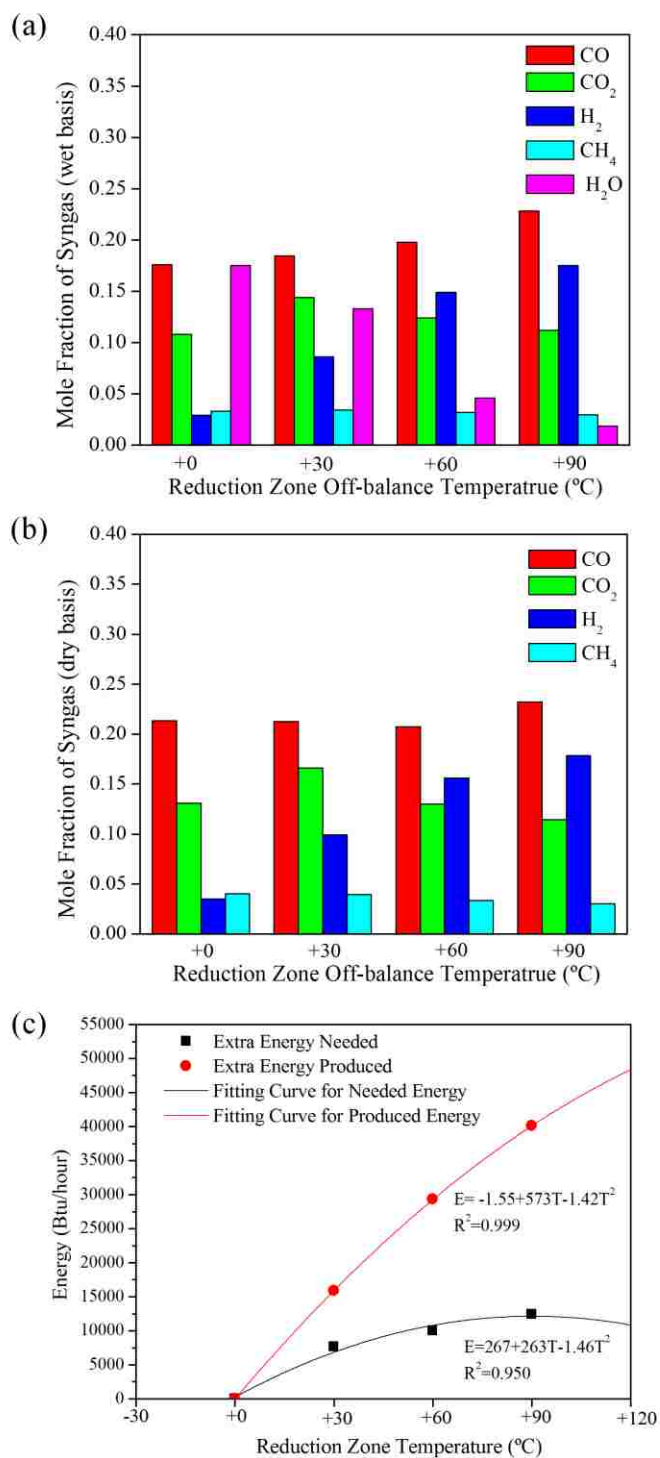


Figure 6. Reduction zone temperature influence on (a) syngas composition (wet basis); (b) syngas composition (dry basis); (c) extra energy needed and extra energy produced

wood chips mixture, while Seggiani et al. used sewage sludge with wood pellets to test the compositions in syngas products. The wood pellets/chips have higher heating values than the sewage sludge, higher CO compositions are also found as a higher ratio of wood chip/pellets were mixed. Figure 7 shows the gasification products and their LHV's using different mixtures of sewage sludge and wood pellets, their UA and PA are provided by Seggiani et al. [83]. As it can be seen, the RXN simulation gave a similar prediction as experiments mentioned above. CO decreases significantly due to higher mixed sewage sludge, both H₂ and CO₂ composition first increase to a maximum and then decrease, while CH₄ stays fairly constant. LHV decreases significantly as more sewage sludge was fed, this verifies the fact that it is favorable to add higher heating value biomass into the lower heating value biomass to reform the syngas composition. This operation also stabilizes the bed temperature and prevents the bed from a shutdown.

Because of degradation on heating values, coal is a better fuel than hardwood, while softwood is the worst among these three. Traditionally, hardwood has been the preferred fuel in wood stoves and fireplaces, and also gasifiers due to its low moisture content and higher energy density. Softwood is easy to ignite so it is convenient for startups. Thus, experimentalists should be careful on what kind of biomass to use due to the different scenario, and these choices are also limited by the accessible kinds of biomass over different seasons at different locations. However, if both hardwood and softwood are dried and compressed to the same density, their BTUs are very similar, which means they will have the almost the same performance on gasification. Drying and compressing also benefit the bed performances, as these processes can reduce bed shutdowns and bridging phenomena.

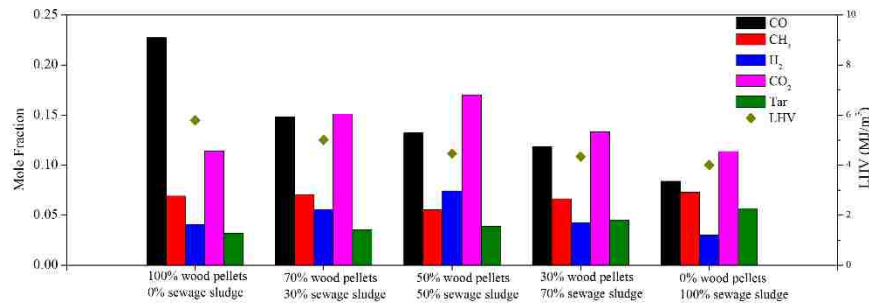


Figure 7. Syngas compositions and lower heating value for different ratio of wood pellets and sewage sludge mixtures

4.4. MOISTURE CONTENT INFLUENCE

Moisture content has a significant impact on the outcome of the gasification process. Some type of biomass needs to be preheated and control the moisture content less than 15% for most gasifiers [100], yet some updraft reactors may process biomass with a moisture content as high as 50% [101]. Moisture content above 30% usually results in ignition difficulty and is more likely to cause bed failures. Higher moisture content means more energy is required for water evaporation in the drying zone, which lowers the bed temperature. Decreased bed temperature results in incomplete tar cracking and degrade syngas formation. Figure 8 gives the syngas compositions with different moisture contents at ER=0.15. The biomass UA and PA are exactly the same as wood pellets [83], except for the moisture contents are set at 4%, 8%, 12% and 16%. Figure 8(a) CO and CH₄ compositions illustrate syngas compositions are almost the same, yet the H₂ composition decreases significantly as moisture content increases, thus resulting in a lower LHV value, as shown in Figure 8(b). At the same time, the dry gas production also decreases, so the

energy produced per kilogram of biomass (η) also decreases as moisture content gets higher. This verifies the increasing moisture impairs the syngas quality.

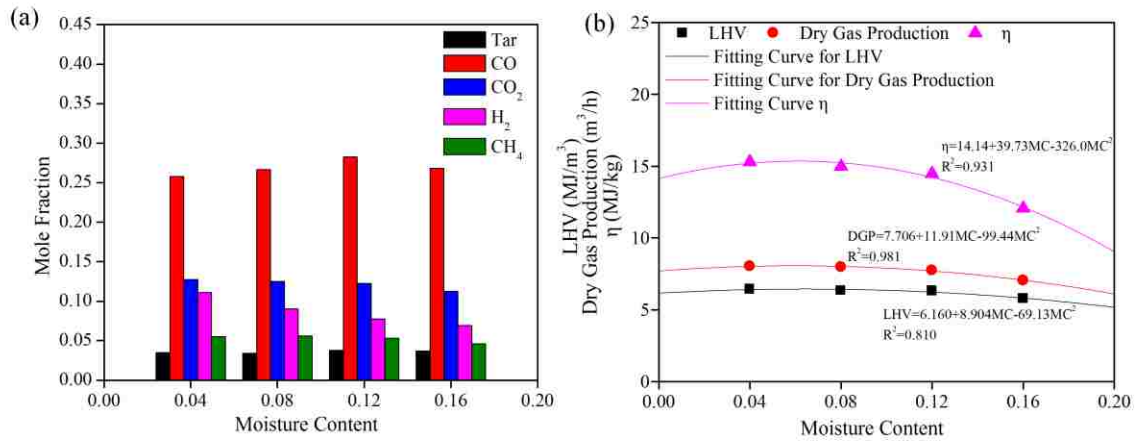


Figure 8. Moisture content influence on (a) syngas compositions of wood pellets gasification; (b) LHV, dry gas production and η

4.5. GASIFICATION CONDITIONS INFLUENCES ON TAR YIELD

In the downstream of the gasification process, high molecular weight compounds are condensed to form tar if the temperature drops below 450°C. Most tar is deposited in the pipe line and the rest remains as an aerosol in the syngas. Two strategies are developed to remove the tar: (1) apply removal apparatus to clean the syngas [102], and (2) improve the gasification technology to reduce the tar formation[103]. Mechanical/physical methods for tar removal face serious problems such as high operation cost and environmental discomfort [104], thus it became essential to enhance tar cracking (i.e. thermal and catalyst cracking) in the gasification process. Brandt et al. [105] claimed that it is necessary for the

gas to stay at 1250 °C for more than 0.5 seconds in order to achieve efficient tar thermal cracking. Updraft gasifiers produce at least 10 times more tar than the downdraft gasifiers [26] due to the limited residence time. Since tar formation will cause harm to the engine system, it is beneficial to predict how much tar will be in the final syngas product.

It is impossible for MGFE model to achieve tar compositions, due to the fact that tar is an intermediate product. Some researchers have developed models shows tar formation. Gagliano et al. [106] developed a numerical model for downdraft gasifiers. In Gagliano's model to approximate downdraft gasification process, tar yield was fixed to 4.5% w/w independent of the operating conditions, and the chemical formula $C_6H_6O_{0.2}$ was used to represent the tar, and the thermochemical properties were assumed to be the same as benzene. An obvious disadvantage arises due to the tar yield ratio assumption that the tar yields and compositions do not change due to different operating conditions (such as ERs and bed temperatures). While in this model, the RXN model defined specific chemicals for primary and secondary tar, the amount of each chemical could be viewed in the final "syngas" stream.

Downdraft gasifiers usually produce 4.5% w/w tar [26, 40]. Since the updraft gasifiers produce more tar than downdraft gasifiers [107], the calculated tar yield 6-8% w/w could be trusted. This model predicted a complete char conversion, means that all the char reacts inside of the gasifier to support the gasification process. Experimentalists regularly report syngas compositions as they consider syngas as the mean product. Some researchers consider tar, the mean contaminant, but its composition is hard to analyze. Char is neither important nor hazardous so it seldom draws any attention. Although this model

predicts char amount, the predictions are not justified due to the lack of char information in the experimental findings.

Figure 9(a) shows the simulated tar composition of wood pellets gasification by the RXN model, it can be seen that tar composition decreases drastically with increasing ER due to increasing gasification temperature. Figure 9(b) also gives the same trend that tar composition decreases with increasing gasification zone temperatures at ER=0.2. It can be concluded that higher gasification temperature is helpful for tar cracking to increase the combustible compositions. Figure 9(c) illustrates there is very little benzene presence in tar, toluene and acetone occupy more than 50% mole fraction of tar and they escalate a little, while the naphthalene and phenol vary as ER increases.

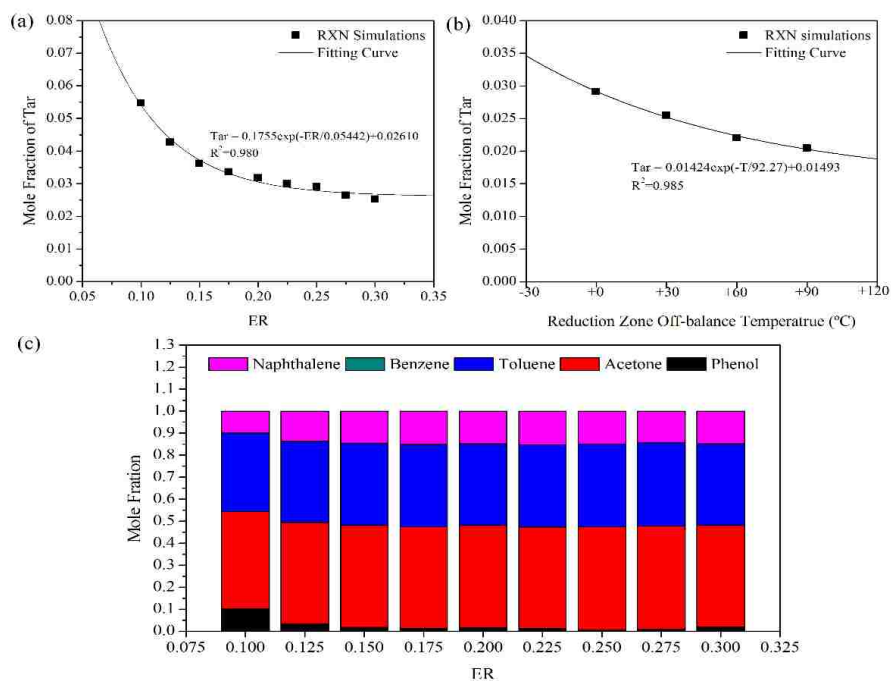


Figure 9. Impact on tar amounts due to: (a) ER value, (b) reduction zone temperatures, (c) tar compositions

5. CONCLUSIONS

A kinetic model of biomass gasification was developed to simulate and optimize reactor performance in updraft gasifiers. The kinetic model was validated by comparison with two experimental findings available in the literature. It is found that the kinetic model could correctly predict the syngas and tar compositions, which is more accurate than the equilibrium model. Systematic parametric studies were conducted to investigate the effect of ER, gasification temperature, biomass mixture and moisture content on syngas and tar compositions. This study reveals that: 1) The optimal ER depends on the specific application of syngas, 2) Recovering waste heat to achieve a higher gasification temperature is favorable, 3) Lower heating value biomass could be mixed with higher heating value biomass to improve syngas quality, 4) The gasification temperature has a significant effect on tar production amount and compositions.

ACKNOWLEDGEMENTS

The authors gratefully acknowledge financial support from the Wayne and Gayle Laufer Endowment.

NOTATION

a	number for atoms
A	total number of atoms entering the reactor
A_r	frequency factor ($\text{mol}^{(1-\alpha)}\text{m}^{(3\alpha-3)}\text{s}^{-1}$)
C	concentration (mol/m^3)
D	diameter of the gasifier (m)
d_{gp}	dry gas production (m^3/h)
E_a	activation energy (kJ/kmol)
ER	equivalence ratio
F_{bio}	feed rate of biomass (kg/h)
F_{air}	feed rate of air (m^3/h)
G_t	total Gibbs energy of system (kJ/mol)
k_r	reaction rate coefficient ($\text{mol}^{(1-\alpha)}\text{m}^{(3\alpha-3)}\text{s}^{-1}$)
L	total length of combustion and gasification zones (m)
L_{hm}	reactor length of homogeneous reactor (m)
L_{ht}	reactor length of homogeneous reactor (m)
LHV	lower heating value (MJ/m^3)
n	moles (mol)
Q_{hm1}	heat generated by block “HOMO1” (J/sec)
Q_{ht1}	heat generated by block “HETERO1” (J/sec)
Q_{hm2}	heat generated by block “HOMO2” (J/sec)
Q_{ht2}	heat generated by block “HETERO2” (J/sec)

R	gas constant (kJ/kmol K)
r	rate of reaction (mol/sec•m ³)
$t_{hm,total}$	total residence time of combustion and gasification zones for homogeneous reactor (h)
$t_{hm,zone}$	total residence time of combustion or gasification zone for homogeneous reactor (h)
$t_{ht,total}$	total residence time of combustion and gasification zones for heterogeneous reactor (h)
$t_{ht,zone}$	total residence time of combustion or gasification zone for heterogeneous reactor (h)
T	reaction temperature
T_{hm1}	temperature (K)
T_{ht1}	temperature (K)
V_{rt}	volume (m ³)

Greek letters

α	reaction order
ρ_{bio}	bulk density of biomass (kg/m ³)
β	temperature exponent
η	lower heating value of syngas out of 1kg biomass (MJ/kg)
ϕ	void ratio

Subscripts

i	species index
j	element index
r	reaction index

REFERENCES

1. World Energy Council, World Energy Resources, Bioenergy, 2016. 2016.
2. Tilman, D., et al., Beneficial biofuels—the food, energy, and environment trilemma. *Science*, 2009. 325(5938): p. 270-271.
3. Chum, H.L. and R.P. Overend, Biomass and renewable fuels. *Fuel processing technology*, 2001. 71(1-3): p. 187-195.
4. Higman, C. and M. Van Der Burgt, *Gasification*. 2003: Gulf Professional Publishing.
5. Zhao, Y., et al., Characteristics of rice husk gasification in an entrained flow reactor. *Bioresource technology*, 2009. 100(23): p. 6040-6044.
6. Zhou, J., et al., Biomass–oxygen gasification in a high-temperature entrained-flow gasifier. *Biotechnology advances*, 2009. 27(5): p. 606-611.
7. Hernández, J.J., G. Aranda-Almansa, and A. Bula, Gasification of biomass wastes in an entrained flow gasifier: Effect of the particle size and the residence time. *Fuel Processing Technology*, 2010. 91(6): p. 681-692.
8. Turn, S., et al., An experimental investigation of hydrogen production from biomass gasification. *International Journal of Hydrogen Energy*, 1998. 23(8): p. 641-648.
9. Lv, P., et al., An experimental study on biomass air–steam gasification in a fluidized bed. *Bioresource technology*, 2004. 95(1): p. 95-101.
10. Li, X., et al., Biomass gasification in a circulating fluidized bed. *Biomass and bioenergy*, 2004. 26(2): p. 171-193.
11. Breault, R.W., T. Li, and P. Nicoletti, Mass transfer effects in a gasification riser. *Powder technology*, 2013. 242: p. 108-116.
12. Xiong, Q., S.-C. Kong, and A. Passalacqua, Development of a generalized numerical framework for simulating biomass fast pyrolysis in fluidized-bed reactors. *Chemical Engineering Science*, 2013. 99: p. 305-313.
13. Collot, A., et al., Co-pyrolysis and co-gasification of coal and biomass in bench-scale fixed-bed and fluidised bed reactors. *Fuel*, 1999. 78(6): p. 667-679.
14. Chopra, S. and A. Jain, A review of fixed bed gasification systems for biomass. 2007.
15. Atnaw, S.M., S.A. Sulaiman, and S. Yusup, Syngas production from downdraft gasification of oil palm fronds. *Energy*, 2013. 61: p. 491-501.

16. Dogru, M., et al., Gasification of hazelnut shells in a downdraft gasifier. *Energy*, 2002. 27(5): p. 415-427.
17. Gai, C. and Y. Dong, Experimental study on non-woody biomass gasification in a downdraft gasifier. *International Journal of hydrogen energy*, 2012. 37(6): p. 4935-4944.
18. Janajreh, I. and M. Al Shrah, Numerical and experimental investigation of downdraft gasification of wood chips. *Energy Conversion and Management*, 2013. 65: p. 783-792.
19. Lv, P., et al., Hydrogen-rich gas production from biomass air and oxygen/steam gasification in a downdraft gasifier. *Renewable Energy*, 2007. 32(13): p. 2173-2185.
20. Pérez, J.F., A. Melgar, and P.N. Benjumea, Effect of operating and design parameters on the gasification/combustion process of waste biomass in fixed bed downdraft reactors: An experimental study. *Fuel*, 2012. 96: p. 487-496.
21. Zainal, Z., et al., Experimental investigation of a downdraft biomass gasifier. *Biomass and bioenergy*, 2002. 23(4): p. 283-289.
22. Chen, W., et al., Updraft fixed bed gasification of mesquite and juniper wood samples. *Energy*, 2012. 41(1): p. 454-461.
23. Pedroso, D.T., et al., Experimental study of bottom feed updraft gasifier. *Renewable energy*, 2013. 57: p. 311-316.
24. Plis, P. and R. Wilk, Theoretical and experimental investigation of biomass gasification process in a fixed bed gasifier. *Energy*, 2011. 36(6): p. 3838-3845.
25. Saravanakumar, A., et al., Experimental investigations of long stick wood gasification in a bottom lit updraft fixed bed gasifier. *Fuel processing technology*, 2007. 88(6): p. 617-622.
26. Ueki, Y., et al., Gasification characteristics of woody biomass in the packed bed reactor. *Proceedings of the Combustion Institute*, 2011. 33(2): p. 1795-1800.
27. Reed, T. and A. Das, *Handbook of biomass downdraft gasifier engine systems*. 1988: Biomass Energy Foundation.
28. Higman, C., *Gasification, in Combustion Engineering Issues for Solid Fuel Systems*. 2008, Elsevier. p. 423-468.
29. McKendry, P., *Energy production from biomass (part 3): gasification technologies*. *Bioresource technology*, 2002. 83(1): p. 55-63.

30. Corton, J., et al., The Impact of Biomass Feedstock Composition and Pre-treatments on Tar Formation during Biomass Gasification. *Advances in Biofeedstocks and Biofuels: Biofeedstocks and Their Processing*, 2017: p. 33-53.
31. Rabou, L., Biomass tar recycling and destruction in a CFB gasifier. *Fuel*, 2005. 84(5): p. 577-581.
32. Rapagna, S., et al., Steam-gasification of biomass in a fluidised-bed of olivine particles. *Biomass and Bioenergy*, 2000. 19(3): p. 187-197.
33. Dogru, M., et al., Gasification of hazelnut shells in a downdraft gasifier. *Energy*. 27(5): p. 415-427.
34. Papadikis, K., A. Bridgwater, and S. Gu, CFD modelling of the fast pyrolysis of biomass in fluidised bed reactors, Part A: Eulerian computation of momentum transport in bubbling fluidised beds. *Chemical Engineering Science*, 2008. 63(16): p. 4218-4227.
35. Ruiz, J., et al., Biomass gasification for electricity generation: review of current technology barriers. *Renewable and Sustainable Energy Reviews*, 2013. 18: p. 174-183.
36. Bridgwater, A., The technical and economic feasibility of biomass gasification for power generation. *Fuel*, 1995. 74(5): p. 631-653.
37. Basu, P., *Combustion and gasification in fluidized beds*. 2006: CRC press.
38. Doherty, W., A. Reynolds, and D. Kennedy, The effect of air preheating in a biomass CFB gasifier using ASPEN Plus simulation. *Biomass and Bioenergy*, 2009. 33(9): p. 1158-1167.
39. Corella, J., J.M. Toledo, and G. Molina, A review on dual fluidized-bed biomass gasifiers. *Industrial & Engineering Chemistry Research*, 2007. 46(21): p. 6831-6839.
40. Lucas, J., C. Lim, and A. Watkinson, A nonisothermal model of a spouted bed gasifier. *Fuel*, 1998. 77(7): p. 683-694.
41. Hosseini, M., I. Dincer, and M.A. Rosen, Steam and air fed biomass gasification: comparisons based on energy and exergy. *International journal of hydrogen energy*, 2012. 37(21): p. 16446-16452.
42. Inayat, A., M.M. Ahmad, and M.A. Mutalib. Effect of process parameters on hydrogen production and efficiency in biomass steam gasification with in-situ CO₂ capture. in *Proceedings of International Conference on Process Engineering and Advanced Materials*. 2010.

43. Jaojaruek, K. and S. Kumar, Numerical simulation of the pyrolysis zone in a downdraft gasification process. *Bioresource technology*, 2009. 100(23): p. 6052-6058.
44. Nikoo, M.B. and N. Mahinpey, Simulation of biomass gasification in fluidized bed reactor using ASPEN PLUS. *Biomass and Bioenergy*, 2008. 32(12): p. 1245-1254.
45. Abstracts of Papers, s.A.N.M., San Diego, CA, United States, April 1-5, 2001 Abdelouahed, Lokmane, et al., Detailed modeling of biomass gasification in dual fluidized bed reactors under Aspen Plus. *Energy & Fuels*, 2012. 26(6): p. 3840-3855.
46. Kaushal, P. and R. Tyagi, Advanced simulation of biomass gasification in a fluidized bed reactor using ASPEN PLUS. *Renewable Energy*, 2017. 101: p. 629-636.
47. Gómez-Barea, A. and B. Leckner, Modeling of biomass gasification in fluidized bed. *Progress in Energy and Combustion Science*, 2010. 36(4): p. 444-509.
48. Xue, Q., T. Heindel, and R. Fox, A CFD model for biomass fast pyrolysis in fluidized-bed reactors. *Chemical Engineering Science*, 2011. 66(11): p. 2440-2452.
49. Fletcher, D., et al., A CFD based combustion model of an entrained flow biomass gasifier. *Applied mathematical modelling*, 2000. 24(3): p. 165-182.
50. Gentile, G., et al., A comprehensive CFD model for the biomass pyrolysis. *Chemical Engineering Transactions*, 2015. 43.
51. Guo, B., et al., Simulation of biomass gasification with a hybrid neural network model. *Bioresource Technology*, 2001. 76(2): p. 77-83.
52. Hornik, K., Approximation capabilities of multilayer feedforward networks. *Neural networks*, 1991. 4(2): p. 251-257.
53. Psychogios, D.C. and L.H. Ungar, A hybrid neural network-first principles approach to process modeling. *AIChE Journal*, 1992. 38(10): p. 1499-1511.
54. Barker, R., et al., ASPEN modeling of the tri-state indirect-liquefaction process. 1983, Oak Ridge National Lab., TN (USA).
55. Jiang, Y. and D. Bhattacharyya, Plant-wide modeling of an indirect coal-biomass to liquids (CBTL) plant with CO₂ capture and storage (CCS). *International Journal of Greenhouse Gas Control*, 2014. 31: p. 1-15.
56. Xiangdong, K., et al., Three stage equilibrium model for coal gasification in entrained flow gasifiers based on Aspen Plus. *Chinese Journal of Chemical Engineering*, 2013. 21(1): p. 79-84.
57. Phillips, J.N., Study of the off-design performance of integrated coal gasification combined-cycle power plants. 1986, Stanford Univ., CA (USA).

58. Shen, L., Y. Gao, and J. Xiao, Simulation of hydrogen production from biomass gasification in interconnected fluidized beds. *Biomass and Bioenergy*, 2008. 32(2): p. 120-127.
59. Ramzan, N., et al., Simulation of hybrid biomass gasification using Aspen plus: A comparative performance analysis for food, municipal solid and poultry waste. *Biomass and Bioenergy*, 2011. 35(9): p. 3962-3969.
60. Keche, A.J., A.P.R. Gaddale, and R.G. Tated, Simulation of biomass gasification in downdraft gasifier for different biomass fuels using ASPEN PLUS. *Clean Technologies and Environmental Policy*, 2015. 17(2): p. 465-473.
61. Kuo, P.-C., W. Wu, and W.-H. Chen, Gasification performances of raw and torrefied biomass in a downdraft fixed bed gasifier using thermodynamic analysis. *Fuel*, 2014. 117: p. 1231-1241.
62. De Kam, M.J., R.V. Morey, and D.G. Tiffany, Integrating biomass to produce heat and power at ethanol plants. *Applied engineering in agriculture*, 2009. 25(2): p. 227-244.
63. Chen, J.-s., Kinetic engineering modeling of co-current moving bed gasification reactors for carbonaceous materials. 1986, Cornell Univ., Ithaca, NY (USA).
64. Wang, Y. and C. Kinoshita, Kinetic model of biomass gasification. *Solar Energy*, 1993. 51(1): p. 19-25.
65. Milligan, J., Downdraft gasification of biomass. 1994, Aston University, Birmingham, UK.
66. Giltrap, D., R. McKibbin, and G. Barnes, A steady state model of gas-char reactions in a downdraft biomass gasifier. *Solar Energy*, 2003. 74(1): p. 85-91.
67. Yang, Y., et al., Effects of fuel devolatilisation on the combustion of wood chips and incineration of simulated municipal solid wastes in a packed bed☆. *Fuel*, 2003. 82(18): p. 2205-2221.
68. Di Blasi, C., Modeling wood gasification in a countercurrent fixed-bed reactor. *AIChE Journal*, 2004. 50(9): p. 2306-2319.
69. Dennis, J., et al., The kinetics of combustion of chars derived from sewage sludge. *Fuel*, 2005. 84(2): p. 117-126.
70. Gøbel, B., et al., The development of a computer model for a fixed bed gasifier and its use for optimization and control. *Bioresource Technology*, 2007. 98(10): p. 2043-2052.
71. Sharma, A.K., Equilibrium and kinetic modeling of char reduction reactions in a downdraft biomass gasifier: A comparison. *Solar Energy*, 2008. 82(10): p. 918-928.

72. Zhong, L.-D. and W.-H. Mei. Kinetic model establishment and verification of the biomass gasification on fluidized bed. in Machine Learning and Cybernetics, 2009 International Conference on. 2009. IEEE.
73. Roy, P.C., A. Datta, and N. Chakraborty, Modelling of a downdraft biomass gasifier with finite rate kinetics in the reduction zone. International Journal of Energy Research, 2009. 33(9): p. 833-851.
74. Abdelouahed, L., et al., Detailed modeling of biomass gasification in dual fluidized bed reactors under Aspen Plus. Energy & Fuels, 2012. 26(6): p. 3840-3855.
75. Mendiburu, A.Z., et al., Thermochemical equilibrium modeling of a biomass downdraft gasifier: Constrained and unconstrained non-stoichiometric models. Energy, 2014. 71: p. 624-637.
76. Jangsawang, W., K. Laohalidanond, and S. Kerdsuwan, Optimum equivalence ratio of biomass gasification process based on thermodynamic equilibrium model. Energy Procedia, 2015. 79: p. 520-527.
77. Smith, J., H. Van Ness, and M. Abbott, Introduction to Chemical Engineering Thermodynamics, (2001) and 7th ed.(2005). McGraw-Hill, New York.
78. Inc., A.T., Aspen Plus User's Guide. 2000.
79. Fogler, H.S., in Elements of Chemical Reaction Engineering. 2005, Prentice Hall.
80. Wu, Y., et al., Two-dimensional computational fluid dynamics simulation of biomass gasification in a downdraft fixed-bed gasifier with highly preheated air and steam. Energy & Fuels, 2013. 27(6): p. 3274-3282.
81. Hobbs, M., P. Radulovic, and L. Smoot, Combustion and gasification of coals in fixed-beds. Progress in Energy and Combustion Science, 1993. 19(6): p. 505-586.
82. Yoon, H., J. Wei, and M.M. Denn, A model for moving-bed coal gasification reactors. AIChE Journal, 1978. 24(5): p. 885-903.
83. Chen, W.-H., et al., A comparison of gasification phenomena among raw biomass, torrefied biomass and coal in an entrained-flow reactor. Applied energy, 2013. 112: p. 421-430.
84. Du, S.-W. and W.-H. Chen, Numerical prediction and practical improvement of pulverized coal combustion in blast furnace. International Communications in Heat and Mass Transfer, 2006. 33(3): p. 327-334.
85. Arthur, J., Reactions between carbon and oxygen. Transactions of the Faraday Society, 1951. 47: p. 164-178.

86. Gerber, S., F. Behrendt, and M. Oevermann, An Eulerian modeling approach of wood gasification in a bubbling fluidized bed reactor using char as bed material. *Fuel*, 2010. 89(10): p. 2903-2917.
87. Umeki, K., T. Namioka, and K. Yoshikawa, Analysis of an updraft biomass gasifier with high temperature steam using a numerical model. *Applied energy*, 2012. 90(1): p. 38-45.
88. Howard, J., G. Williams, and D. Fine. Kinetics of carbon monoxide oxidation in postflame gases. in *Symposium (International) on Combustion*. 1973. Elsevier.
89. Macak, J. and J. Malecha, Mathematical model for the gasification of coal under pressure. *Industrial & Engineering Chemistry Process Design and Development*, 1978. 17(1): p. 92-98.
90. Robinson, P.J. and W.L. Luyben, Simple dynamic gasifier model that runs in Aspen Dynamics. *Industrial & engineering chemistry research*, 2008. 47(20): p. 7784-7792.
91. Varma, A.K., A.U. Chatwani, and F.V. Bracco, Studies of premixed laminar hydrogen air flames using elementary and global kinetics models. *Combustion and flame*, 1986. 64(2): p. 233-236.
92. Dryer, F. and I. Glassman. High-temperature oxidation of CO and CH₄. in *Symposium (International) on Combustion*. 1973. Elsevier.
93. Morf, P., P. Hasler, and T. Nussbaumer, Mechanisms and kinetics of homogeneous secondary reactions of tar from continuous pyrolysis of wood chips. *Fuel*, 2002. 81(7): p. 843-853.
94. Milne, T.A., R.J. Evans, and N. Abatzoglou, Biomass Gasifier "Tars": Their Nature, Formation, and Conversion. 1998, National Renewable Energy Laboratory, Golden, CO (US).
95. Devi, L., K.J. Ptasinski, and F.J. Janssen, A review of the primary measures for tar elimination in biomass gasification processes. *Biomass and bioenergy*, 2003. 24(2): p. 125-140.
96. Asadullah, M., Barriers of commercial power generation using biomass gasification gas: a review. *Renewable and Sustainable Energy Reviews*, 2014. 29: p. 201-215.
97. Fagbemi, L., L. Khezami, and R. Capart, Pyrolysis products from different biomasses: application to the thermal cracking of tar. *Applied energy*, 2001. 69(4): p. 293-306.
98. El-Rub, Z.A., E.A. Bramer, and G. Brem, Experimental comparison of biomass chars with other catalysts for tar reduction. *Fuel*, 2008. 87(10-11): p. 2243-2252.

99. Anis, S. and Z. Zainal, Tar reduction in biomass producer gas via mechanical, catalytic and thermal methods: A review. *Renewable and Sustainable Energy Reviews*, 2011. 15(5): p. 2355-2377.
100. Han, J. and H. Kim, The reduction and control technology of tar during biomass gasification/pyrolysis: an overview. *Renewable and Sustainable Energy Reviews*, 2008. 12(2): p. 397-416.
101. Yu, J. and J. Smith, Validation and application of a kinetic model for biomass gasification simulation and optimization in updraft gasifiers. *Chemical Engineering and Processing - Process Intensification*, 2018. 125: p. 214-226.
102. Nakamura, S., S. Kitano, and K. Yoshikawa, Biomass gasification process with the tar removal technologies utilizing bio-oil scrubber and char bed. *Applied Energy*, 2016. 170: p. 186-192.
103. Bui, T., R. Loof, and S. Bhattacharya, Multi-stage reactor for thermal gasification of wood. *Energy*, 1994. 19(4): p. 397-404.
104. Woolcock, P.J. and R.C. Brown, A review of cleaning technologies for biomass-derived syngas. *Biomass and bioenergy*, 2013. 52: p. 54-84.
105. Cao, Y., et al., A novel biomass air gasification process for producing tar-free higher heating value fuel gas. *Fuel Processing Technology*, 2006. 87(4): p. 343-353.
106. Pan, Y., et al., Removal of tar by secondary air in fluidised bed gasification of residual biomass and coal. *Fuel*, 1999. 78(14): p. 1703-1709.
107. Narvaez, I., et al., Biomass gasification with air in an atmospheric bubbling fluidized bed. Effect of six operational variables on the quality of the produced raw gas. *Industrial & Engineering Chemistry Research*, 1996. 35(7): p. 2110-2120.
108. Yu, H., et al., Characteristics of tar formation during cellulose, hemicellulose and lignin gasification. *Fuel*, 2014. 118: p. 250-256.
109. Edwards, N.T., Polycyclic aromatic hydrocarbons (PAH's) in the terrestrial environment—a review. *Journal of Environmental Quality*, 1983. 12(4): p. 427-441.
110. Laflamme, R.E. and R.A. Hites, The global distribution of polycyclic aromatic hydrocarbons in recent sediments. *Geochimica et cosmochimica Acta*, 1978. 42(3): p. 289-303.
111. Samanta, S.K., O.V. Singh, and R.K. Jain, Polycyclic aromatic hydrocarbons: environmental pollution and bioremediation. *TRENDS in Biotechnology*, 2002. 20(6): p. 243-248.

112. Falahatpisheh, M., K. Donnelly, and K. Ramos, Antagonistic interactions among nephrotoxic polycyclic aromatic hydrocarbons. *Journal of Toxicology and Environmental Health Part A*, 2001. 62(7): p. 543-560.
113. Unwin, J., et al., An assessment of occupational exposure to polycyclic aromatic hydrocarbons in the UK. *Annals of Occupational Hygiene*, 2006. 50(4): p. 395-403.
114. Abdel-Shafy, H.I. and M.S. Mansour, A review on polycyclic aromatic hydrocarbons: source, environmental impact, effect on human health and remediation. *Egyptian Journal of Petroleum*, 2016. 25(1): p. 107-123.

II. KINETIC MODELING AND SIMULATION OF BIOMASS GASIFICATION IN DOWNDRAFT FIXED BED GASIFIERS

Jia Yu¹, Joseph D. Smith^{1}, Hassan Golpour², Anand Alembath¹, Haider Al-Rubaye¹, Xi Gao³*

¹Department of Chemical and Biochemical Engineering, Missouri University of Science
and Technology.

1101 North State Street, 110 Bertelsmeyer Hall, Rolla, MO 65401-09, United States

²Hassan Golpour

Department of Chemical & Bio-molecular Engineering, North Carolina State University.

2094 EB1 Centennial Campus, 911 Partners Way, Raleigh, NC 27695-7905, United
States

³Xi Gao

National Energy Technology Laboratory, Morgantown, WV, 26507, United States

*** Corresponding Author**

E-mail address: smithjose@mst.edu (*Dr. J. D. Smith*)

ABSTRACT

Biomass gasification is widely recognized as an effective method to obtain renewable energy. To predict the syngas composition, a kinetic model considering the reaction kinetics of biomass gasification inside downdraft fixed bed gasifiers was developed and implemented in Aspen Plus V8.6. The model considered different residence times for the homogeneous and heterogeneous reaction blocks. This model has been applied to a broad range of equivalence ratios (ER) more than commonly considered in the standard Gibbs Energy-Minimizing model (GEM model). The Kinetic Model has been validated by direct comparison to experimental results available in the literature. The Kinetic Model has been used to identify the optimal ER to maximize syngas production and to simulate the gasification process for different operating conditions to investigate how ER, gasification temperature, biomass moisture content and biomass composition affect final syngas composition. Accurate water gas shift reaction kinetics were found to be critical to achieving good comparison to experimental results.

Keywords: Biofuel; gasification; biomass; downdraft gasifier; Aspen Plus; reaction kinetics

1. INTRODUCTION

Biomass energy has been widely recognized and applied for hundreds of years as a renewable energy and is currently considered a good replacement to fossil fuels. Gasification is one of the most efficient methods of converting biomass to useful products. Biomass gasification is considered environmentally friendly because it does not generate additional greenhouse gases when producing energy therefore it is considered carbon neutral.

Several types of gasifiers are currently available, including entrained flow gasifiers [5-7], fluidized bed gasifiers[8, 9, 32], updraft gasifiers[22, 24, 25] and downdraft gasifiers[17-21, 33]. The Entrained flow gasifiers produce a low amount of tar in the final product, but, with this process, a high percentage of energy is lost as sensible heat. The fluidized bed gasifier achieves efficient mixing and long residence time, offers high intra-particle heat transfer rate, yet the product is contaminated with excessive particulates[34]. An updraft gasifier is flexible in design and allows a large range of biomass moisture content, and the heating value of its syngas product including tar composition is usually higher than the downdraft gasifiers[35]. But the syngas contains a high amount of ash and tar which needs extensive gas cleanup[36]. The downdraft gasifier is commonly selected since it produces syngas with low tar content, and is suitable for engine applications[27]. It has higher thermal efficiency because it efficiently transfers heat from the combustion

zone to the gasification zone. Air and steam are two common gasification agents in the gasification process. When air is the gasifying agent, the prominent product is carbon monoxide. When steam is used, carbon monoxide, hydrogen and methane are favorable. In a downdraft gasifier, biomass and air/steam are introduced into the reactor together and flow downwards simultaneously, where biomass is decomposed and gasified to syngas. Air gasification produces syngas within a range of 4-7 MJ/m³ higher heating value (HHV)[37], however, a range of 10-18MJ/m³ HHV could be achieved for oxygen fed gasification[37, 38]. Some other types of gasifiers (E.g., cross-flow gasifiers[29], dual fluidized gasifiers[39], circulating fluidized gasifiers[10], spouted bed gasifiers[40])were developed to search for better syngas compositions and operational feasibility.

Various methods have been used for downdraft biomass gasifiers, which includes process models[38, 41-46] , computational fluid dynamics (CFD) models (i.e. Fluent[18, 34, 47, 48], CFX[49] and OpenFOAM[50]),and artificial neural networks models[51-53]. Process simulators were used because of their user-friendly interface and lower CPU requirement. Aspen has been adopted to simulate coal-related processes, including coal liquefaction[54, 55], coal gasification[56], and integrated coal gasification combined cycle (IGCC)[57], and to optimize the species composition from biomass gasifiers and their performance. Table 1 summarized the experiments performed on downdraft gasifiers and the process simulations developed on all kinds of gasifiers for the last several decades.

Most Aspen-based gasification simulations were performed for fluidized bed reactors[38, 44, 45, 58], some of them were used to simulate updraft beds[59] and downdraft gasifiers[60, 61]. For the Aspen simulations of gasifiers, researchers started with applying chemical equilibrium by minimizing Gibbs Free energy for gasification and combustion zones, which is performed by an RGIBBS block[59-62]. There are plenty of gasification models developed based on the equilibrium method, yet the kinetic models were limited to specific reaction steps or reaction zones. Kaushal and Tyagi[46] used the kinetic information to simulate each zone in a fluidized bed, but the reaction rates were not used in the devolatilization zone directly, instead, the composition ratios were defined by the ratios of corresponding reaction kinetics. The gasification zone composition was calculated by stoichiometric information. Nikko and Mahinpey[44] assumed biomass decomposition and volatile process reacted instantaneously, an RCSTR was used to perform char gasification by using reaction kinetics with an external FORTRAN code. They also divided the simulation zone into bed and freeboard regions and employed different hydrodynamic parameters, each region was simulated by one RCSTR. Few kinetic Aspen models were developed for downdraft gasifier to simulate the entire gasifier.

The objective of this work is to develop an explicit steady-state model with chemical kinetics of the downdraft biomass gasification process, using Aspen Plus. This paper first discusses the Gibbs Energy minimization model, and then introduces the

proposed kinetic model. Next, simulation predictions are compared with previously published experimental data to validate the Aspen Plus model. Finally, the effect of Equivalence Ratio (ER), gasification temperature, moisture content and biomass composition on product composition are analyzed and discussed.

Table 1. Summary of experimental investigations on downdraft gasifier and process simulations on all bed types in the past decades

Experiments				
Authors	Gasification Agent	Reactor Scale	Biomass Type	Comments
Dugru et al. 2002[33]	Air	Pilot-scale	Hazelnut	11 runs among air/fuel ranged 1.37-1.64m ³ /kg
Zainal et al., 2002[21]	Air	Lab scale	Furniture wood and wood chips	7 runs among ER 0.25-0.47, another 7 runs to test the performance of the gasifier
Lv et al. 2007[19]	Air and oxygen/steam	Pilot-scale	Pinewood	Ran temperature distribution tests, tested the biomass gasification with oxygen gas, air and oxygen/steam
Janajreh and Shrah, 2012[18]	Air	Lab scale	Wood pellets	Got temperature profile along the reactor length and with time
Gai and Dong, 2012[17]	Air	Pilot-scale	Non-woody biomass	Temperature profile on varied ERs, syngas compositions of 7 runs among air/fuel 1.29-2.88m ³ /kg

Table 1. Summary of experimental investigations on downdraft gasifier and process simulations on all bed types in the past decades (cont.)

Simulations				
Authors and Year	Bed Type	Codes	Zone	Comments
Chen,1986[63]	Downdraft	Matlab	Entire bed	Non-isothermal particle model, with intra-particle temperature and gas concentration gradients, developed a “lumped” zone for drying pyrolysis and combustion zones
Wang and Kinnoshita, 1993[64]	Fluidized	Matlab	Entire bed	A kinetic model was developed based on the mechanism of surface reactions
Milligan, 1994[65]	Downdraft	Matlab	Entire bed	Developed Milligan's flaming pyrolysis zone model to calculate the gas compositions
Giltrap et al., 2003[66]	Downdraft	Matlab	Reduction	Kinetic rates for reduction zone, methane was overpredicted
Yang et al., 2003[67]	Fixed	Matlab	Entire bed	Effects of devolatilization rate and moisture level in the fuel were assessed

Table 1. Summary of experimental investigations on downdraft gasifier and process simulations on all bed types in the past decades (cont.)

Blasi, 2004[68]	Updraft	Matlab	Entire bed	Finite-rate kinetics with mass and heat transfer across the bed, but only water-gas shift reaction is considered for homogeneous gas-phase reaction
Dennis et al., 2005[69]	Fluidized	Matlab	Combustion zone	Derived the kinetics for char combustion
Gobel et al. 2007[70]	Downdraft, two-stage	Matlab	Entire bed	Developed a Langmuir-Hinshelwood kinetics from char conversion
Shen et al., 2008[58]	Interconnecte d fluidized	Aspen Plus	Entire bed	Combustor and gasifier are separated, both of them reached chemical equilibrium
Nikko and Mahinpey, 2008[44]	Fluidized	Aspen Plus	Entire bed	Hydrodynamics and kinetics nested
De Kam et al., 2009[62]	Fluidized	Aspen Plus	Entire bed	Equilibrium method was used
Sharma, 2008[71]	Downdraft	Matlab	Reduction zone	Presented a thermodynamic and finite-rate kinetic model for char conversion

Table 1. Summary of experimental investigations on downdraft gasifier and process simulations on all bed types in the past decades (cont.)

Zhong and Mei, 2009[72]	Fluidized	Matlab	Entire bed	Equilibrium in thermolysis step and kinetics for gasification step
Roy et al., 2009[73]	Downdraft	Matlab	Entire bed	Finite rate kinetic-controlled chemical reactions in the reduction zone
Doherty et al., 2009[38]	Circulating fluidized	Aspen Plus	Entire bed	Drying and pyrolysis were instantaneous, equilibrium blocks were used for bed calculation
Ramzan et al., 2011[59]	Updraft	Matlab	Entire bed	Equilibrium method was used
Abdelouahed, et al., 2012[74]	Dual fluidized	Aspen Plus	Entire bed	Pyrolysis was calculated by mass yield ratios.
Kuo et al., 2014[61]	Downdraft	Aspen Plus	Entire bed	The paper used thermodynamic equilibrium model to simulate the performance of raw and torrefied bamboo wood.
Mendiburu et al., 2014[75]	Downdraft	Matlab	Entire bed	Model M1 was developed based on equilibrium model, M2-M4 considered equilibrium model constrained by correlating experimental data, apparent gasification rate, and both of them.

Table 1. Summary of experimental investigations on downdraft gasifier and process simulations on all bed types in the past decades (cont.)

Keche et al., 2015[60]	Downdraft	Aspen Plus	Entire bed	Equilibrium method was used.
Jangsawaing et al., 2015[76]	All types	GASEQ	Entire bed	Provided optimum equivalence ratio for two cases: (1) excess carbon present and (2) excess gasifying agent with all the carbon completely gasified.
Kaushal and Tyagi, 2017[46]	Fluidized	Aspen Plus	Entire bed	Used two separate CSTRs coupled with kinetics to calculate gasification step. The devolatilization step was calculated by the ratio of reaction rates.

2. MODEL DESCRIPTION

2.1. MINIMIZING GIBBS ENERGY MODEL (GEM MODEL)

The GEM Model predicts the composition of syngas by applying the thermodynamic equilibrium approach. The non-stoichiometric chemical equilibrium methodology is performed through minimization of the Gibbs free energy. Total Gibbs energy (Gt) of a closed system at constant temperature and pressure decreases during an irreversible process and, when equilibrium is reached, Gt attains its minimum value[77], which means:

$$(dGt)_{T,P} = 0 \quad (1)$$

When applying Eq. (1), it is essential to maintain the overall mass balance of each element, meaning that element mass in biomass and air must be equal to the total element mass in the product, plus ash and tar:

$$\sum_{i=0}^N a_{i,j} n_i = A_j \quad (2)$$

It is assumed the final syngas product has the same composition as at the equilibrium point. For the Aspen Plus model, an RGIBBS block is used to accomplish this work when the pressure and the temperature of the block are given. The RGIBBS block is limited since it does not account for reactor geometry, plus all the chemical reactions are assumed to reach chemical equilibrium before the syngas leaves the reactor. Be specific to the gasification process, the RGIBBS block does not have the ability to predict the amount and compositions of the tar, since tar is an intermediate product.

2.2. REACTION MODEL (KINETIC MODEL)

The Kinetic model and the less accurate GEM Model were each compared to experimental data to assess their performance and accuracy. The Kinetic Model uses detailed kinetic parameters for each reaction, with the rate of reaction is changing by the variation of its rate coefficient at different temperatures. The kinetic reaction rate for species “i” in reaction “r” is expressed as:

$$r_{i,r} = k_r \prod_{i=1}^N [c_{i,r}]^{\alpha_{i,r}} \quad (3)$$

Where k_r is computed using the Arrhenius expression:

$$k_r = A_r T^\beta e^{-\frac{E_a}{RT}} \quad (4)$$

Only H₂, O₂, N₂, CO, CO₂, CH₄, H₂S, H₂O, char and ash are considered, with other possible components assumed to be negligible in both reaction pathways and in syngas production.

2.3. SIMULATION STRATEGY AND DETAILS

2.3.1. Test Cases. Two experiments were selected as simulation test cases to validate the kinetic model. Case 1 considered the experiment [33] in a downdraft gasifier for hazelnut shells. The internal reactor diameter of the oxidation zone was 0.45m and the total bed height was 0.81m. A hazelnut shell mixture with size of 17.9mm×16.5mm ×8.5mm was used. The proximate and ultimate analysis of the shells are shown in Table 2. Case 2 considered the experiment using a reactor of 1.3m height and 0.35m inner diameter for pine wood gasification [19]. The biomass particles prepared with an average size of

3cm × 3cm × 3cm. The proximate and ultimate analyses for the biomass are shown in Table

2.

Table 2. Proximate and ultimate analysis of hazelnut shell [33]

Proximate (wt.% wb ^a)		Ultimate (wt.% DAF ^b)	
Volatile matter	62.70	Carbon	46.76
Fixed carbon	24.08	Hydrogen	5.76
Ash	0.77	Oxygen	45.83
Moisture	12.45	Nitrogen	0.22
GCV(MJ/kg)	17.36	Sulfur	0.67
Bulk density (kg/m ³)	319.14		
Absolute density(kg/m ³)	944.84		

a: Wet basis b: Dry-Ash-Free basis

Table 3. Proximate and ultimate analysis of pine wood [19]

Proximate Analysis (wt. %, db ^a)		Ultimate Analysis (wt. % DAF)	
Moisture	8	Carbon	50.54
Volatile Matter	82.29	Hydrogen	7.08
Fixed Carbon	17.16	Oxygen	41.11
Ash	0.55	Nitrogen	0.15
Bulk density (kg/m ³)	222	Sulfur	0.57
Absolute density (kg/m ³)	556		

a: Dry basis b: Dry-Ash-Free basis

2.3.2. Structure of Downdraft Gasifier. The downdraft gasification system includes four sections: 1) fuel hopper, 2) reactor body, 3) air feeding system and 4) ash removal box. Some kind of gas cleaning apparatus (E.g., spray towers, cyclones, filters), is required to remove the tar and particles to optimize the utilizing the producer gas. Biomass is usually fed through the top or shoulder of the reactor, with air moving downwards concurrently.

In general, biomass gasification occurs in four zones as shown in Figure 1. In the drying zone (50°C - 150°C), raw biomass is dried by heat, either supplied by biomass combusting or the application of external heat. In the pyrolysis zone, a series of complex physical and chemical processes take place to generate char, tar, ash and light gases (H_2 , CO etc). The temperature in this zone is usually between 250°C - 550°C [27, 45]. The third step is oxidation (combustion), light gases and tar generated in previous sections are mostly burned with the feed air, generating CO_2 and H_2O . In this zone, temperatures range from 900°C to 1500°C , which provides sufficient heat to support the whole gasification process. The final zone is the reduction (gasification) zone, where the water-gas shift and the Boudouard reactions take place.

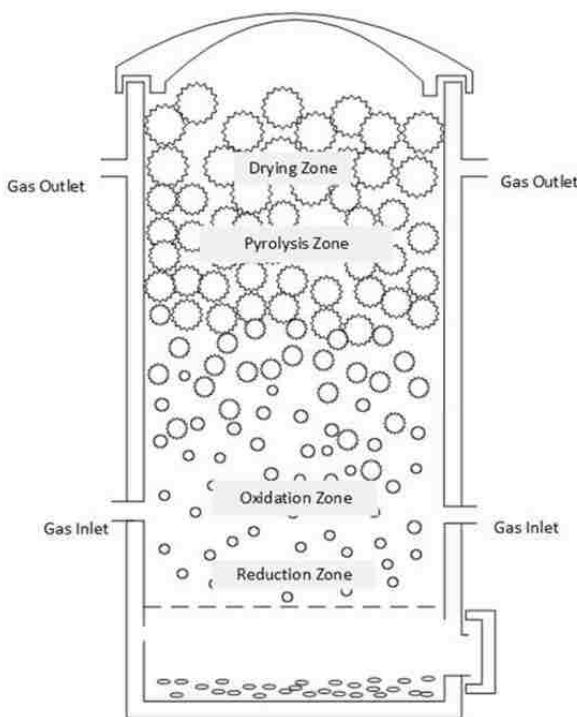


Figure 1. Schematic diagram of a downdraft gasifier

$$\sum_{i=0}^N a_{i,j,in} n_{i,in} = A_j = \sum_{i=0}^N a_{i,j,out} n_{i,out} \quad (5)$$

2.3.3. Aspen Plus Simulation (Kinetic Model). To model a downdraft gasifier using Aspen Plus, the overall process was broken down into a number of sub-processes. Each sub-process coordinates with the position and function of the four zones as mentioned before. Figure 2 shows the overall simulation scheme, Table 4 gives the description for all the operation units used in the Kinetic Model. The biomass stream passed through all of the four zones with different reaction temperatures. The biomass was decomposed gasified to yield the syngas product. For each operation unit, mass balance was considered as equation (5).

The Aspen Plus simulation flowsheet is shown in Figure 3. Biomass was specified as a non-conventional component and is defined using its ultimate and proximate analysis. The gasification process is modeled in three stages. In the first stage, RSTOIC model was used to simulate the drying process of the feed biomass, which was controlled by a FORTRAN block. In the second stage, the RYIELD block was used to simulate the biomass decomposition into its basic elements (C, H, O, S and N) by specifying yield distribution. The yield distribution was calculated according to the biomass element mass balance, details see Eq (6) and (7). The carbon was split into fixed carbon and volatile carbon, the split ratio of the char stream over the original follows Eq (8). The fixed carbon stays inert in the pyrolysis step. While the volatile carbon with H, O, N, and S was sent into an RGIBBS block to generate light gases (CO, CO₂, H₂, H₂O, N₂, CH₄, and H₂S).

Table 4. Lists the Aspen Plus units

Unit	Description [78]	Function
RSTOIC-1	Conversion reactor with known stoichiometry	Reduces the moisture content of the wet biomass
RFLASH	Performs rigorous two-phase equilibrium calculations	Separates the steam from the biomass
RYIELD	Yield reactor with known product yields	Decomposes dried biomass into basic elements
SSPLIT	Separates a stream into two streams, must specify each substream, for all but one outlet stream	Split char
RGIBBS	Multiphase chemical equilibrium reactor (non-stoichiometric)	Models gas-phase chemical equilibrium by minimizing Gibbs free energy
RPLUG	Plug flow reactor with known kinetics	Models a plug flow reactor. This unit was used to perform char-pyrolysis reaction when reaction kinetics is known
RCSTR	Continuous stirred tank reactor with known kinetics	Models a continuous-stirred tank reactor. This unit was used to perform gas-phase reaction when reaction kinetics is known
RSTOIC-2	Conversion reactor with excessive air	Models the full combustion of the product

$$W_m \% = D_m / \left(\sum_{m=1}^N D_m \right) \quad (6)$$

$$E_n \% = (1 - W_{H_2O} \% - W_{Ash} \%) \times U_n \% \quad (7)$$

$$SR = W_{Fixed\ Carbon} / E_{Carbon} \quad (8)$$

In the third stage, air was injected. The biomass gasifier is usually considered as a tubular flow reactor, since both the air and the biomass enter and flow axially down the reactor. However, the air goes through the reactor much faster than the biomass. In Case 2, the resident time of the biomass is approximately 700 times more than that of the air. In other Aspen Plus simulations[44-46], researchers used simple CSTR with kinetic

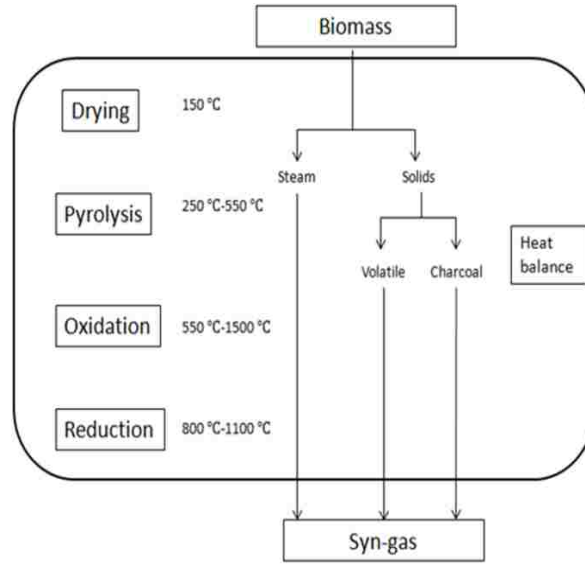


Figure 2. Model scheme of a downdraft gasifier

information to simulate the syngas production, which might cause simulation errors. In order to build a simulation that better describes the gasification process, the Kinetic Model adopted four similar sections. Each section consisted of two blocks: an RCSTR block for heterogeneous reactions and an RPLUG block for homogeneous reactions. In this way, each section is a CSTR-PFR combined unit, and when repeated four times, it imitates the PFR for combustion and gasification zones[79]. In every heterogeneous block, one fourth of char was consumed, a DESIGN SPEC block was used to control the char reduction. For each RPLUG reactor calculation, the reactor diameter was set to be the same as the modeled gasifier. Reactor lengths were calculated using Eq. (9) and Eq. (10). In each section RCSTR and RPLUG have the same length

$$L_{hm} = L_{rt}t_{ht}/t_{total} \quad (9)$$

$$t_{total} = \rho V_{rt}/F_{bio} \quad (10)$$

The temperatures were estimated according to the normal combustion and gasification temperatures (1000°C) for the first three gasification sections. In the last section, the temperature was calculated after applying the law of energy conservation. Table 5 gives the heterogeneous and homogeneous reactions considered in this work, with their frequency factor (A) and activation energy (E_a) as specified. Heterogeneous reaction kinetics were only activated in heterogeneous blocks. Homogeneous reaction kinetics were only activated in homogeneous blocks.

In Figure 3, stream “syngas” was considered as the final product. The following process simulated full syngas combustion, as experimentalists normally burn the product gas using excessive air instead of releasing syngas directly to the atmosphere.

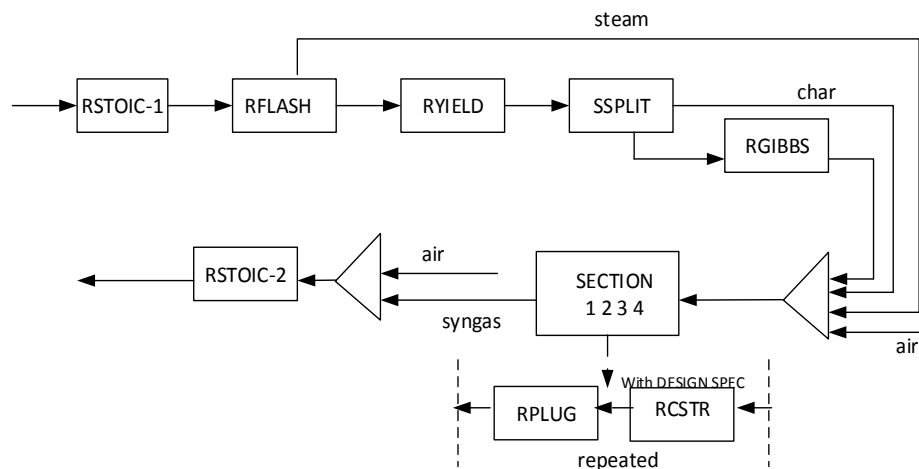


Figure 3. Aspen Plus flowsheet for downdraft biomass gasification with air

Table 5. Reactions involved in biomass gasification and their kinetic parameters

Reactions		Kinetic Parameters		
Heterogeneous Reactions		Ar	Ea	
Boudouard[80, 81]	$C+CO_2 \rightarrow 2CO$	589T	222829	
Water gas shift[80, 82]	$C+H_2O \rightarrow CO+H_2$	5.714T	129706	
Combustion I[83, 84]	$C+0.5O_2 \rightarrow CO$	0.002	79000	
Combustion II[85]	$C+O_2 \rightarrow CO_2$	7.96×10^{-7}	27118	
Methanation[86]	$C+2H_2 \rightarrow CH_4$	0.0342T	129706	
Naphthalene cracking I[87]	$C_{10}H_8 \rightarrow 10C+4H_2$	7.0×10^{14}	360000	
Homogeneous Reactions		Ar	Ea	
Combustion III[88]	$CO+0.5O_2 \rightarrow CO_2$	$1.3 \times 10^{11} C_{H_2O}^{0.5}$	125600	
CO shift[80, 82, 89]	$CO+H_2O \leftrightarrow CO_2+H_2$	Fr	2.78	12560
		Rr	104.830	78364
Steam methane reform[90]	$CO+3H_2 \leftrightarrow CH_4+H_2O$	Fr	312	30000
		Rr	6.09×10^{14}	257000

Table 5. Reactions involved in biomass gasification and their kinetic parameters (cont.)

Combustion IV[80, 91]	$\text{H}_2 + 0.5\text{O}_2 \rightarrow \text{H}_2\text{O}$	$3.53 \times 10^{8.4}$	30514
Methane burning[80, 92]	$\text{CH}_4 + 1.5\text{O}_2 \rightarrow \text{CO} + 2\text{H}_2\text{O}$	$10^{11.7}$	24357
Propionic acid cracking[93]	$\text{C}_3\text{H}_6\text{O}_2 \rightarrow 0.5\text{C}_6\text{H}_6\text{O} + 1.5\text{H}_2\text{O}$	10^4	136000
Acetone cracking[87, 93]	$\text{C}_3\text{H}_6\text{O} + 0.5\text{O}_2 \rightarrow 0.5\text{C}_6\text{H}_6\text{O} + 1.5\text{H}_2\text{O}$	10^4	136000
Phenol cracking[87, 93]	$\text{C}_6\text{H}_6\text{O} \rightarrow 0.5\text{C}_{10}\text{H}_8 + \text{CO} + \text{H}_2$	10^7	100000
Toluene cracking	$\text{C}_7\text{H}_8 + \text{H}_2 \rightarrow \text{C}_6\text{H}_6 + \text{CH}_4$	3.3×10^{10}	247000
Naphthalene cracking II	$\text{C}_{10}\text{H}_8 + 4.75\text{H}_2 \rightarrow 1.25\text{C}_6\text{H}_6 + 2.5\text{CH}_4$	10^{11}	324000

3. RESULTS AND DISCUSSION

The model validation simulations were conducted using the gasifier geometry described in the original cases. For all analysis to determine parameter effects, a cylindrical reactor with 0.4m diameter and 1.0m height were considered. Biomass feed was set at 2kg/h. Since air was used as the gasification agent, carbon monoxide was expected to be maximized.

The operation parameter, ER, is usually introduced in biomass gasification simulations. ER is known to have a significant effect on the final syngas composition, it is defined as the ratio of oxygen provided to oxygen required for stoichiometric combustion:

$$(dGt)_{T,P} = 0 \quad (11)$$

$$ER = \frac{\text{actual air/fuel ratio}}{\text{air/fuel ratio for stoichiometric combustion}} \quad (12)$$

3.1. MODEL VALIDATION

Product concentrations, such as volume fraction of CO, H₂ and CH₄ for different ERs were computed and compared with experimental data. The comparison of test cases 1 and 2 are shown in Figure 4a-4c and Figure 4d, respectively. As shown, the Kinetic Model corresponds more closely to the experiment for CO composition than the GEM model. For case 1, the Kinetic Model CO fraction increases from 0.17 at ER= 0.248, gives a peak around 0.205 at ER=0.264 and then decreases to 0.10 at ER=0.296. For case 2, the peak was located at ER=0.25. While, the GEM model gave a roughly linear trendline decreasing from 0.214 at ER= 0.248, to 0.208 at ER=0.296. For the GEM model, there was a big

discrepancy with the measured data, plus no peak was observed. Based on this comparison, the Kinetic Model appears to have a more accurate prediction.

A slight discrepancy is observed between the prediction and the experiment, where the Kinetic Model gives different ER values when CO is at the highest point. This can be explained in three ways. First, the kinetic expressions used in the simulation were inaccurate, which significantly effects on the prediction. Second, although the whole gasification process must follow the law of energy conservation, temperature information is still not sufficient. For the first three gasification sections, the temperatures were assumed based on operating with experience, and only the temperature in the fourth section was calculated. Third, the species concentrations in the experimental reactor are not well mixed, while the simulation assumes the entire section to be uniformly mixed. This may also explain the small amount of oxygen remaining in the experiment, while oxygen concentrations are always zero in the simulated cases.

As for the case 1, the H₂ composition values are in good agreement with the experimental data. The kinetic results are lower than the experimental data at lower ERs, and correspond with the measured data between ER=0.26-0.27, then run lower again when ER>0.27. The GEM model decreases continuously as ER goes higher, it performs poorly at ER<0.27, but it has smaller error than the Kinetic Model when ER>0.27. As shown in Figure 4d, the methane composition is predicted to be higher than it is in the experiment. The biggest error for the RXN model occurs at ER=0.273 for 52%, while for the GEM Model the error is more than 95%. This difference is explained by examining a few assumptions. For example, the simulation used the ideal gas law, and allowed no tar

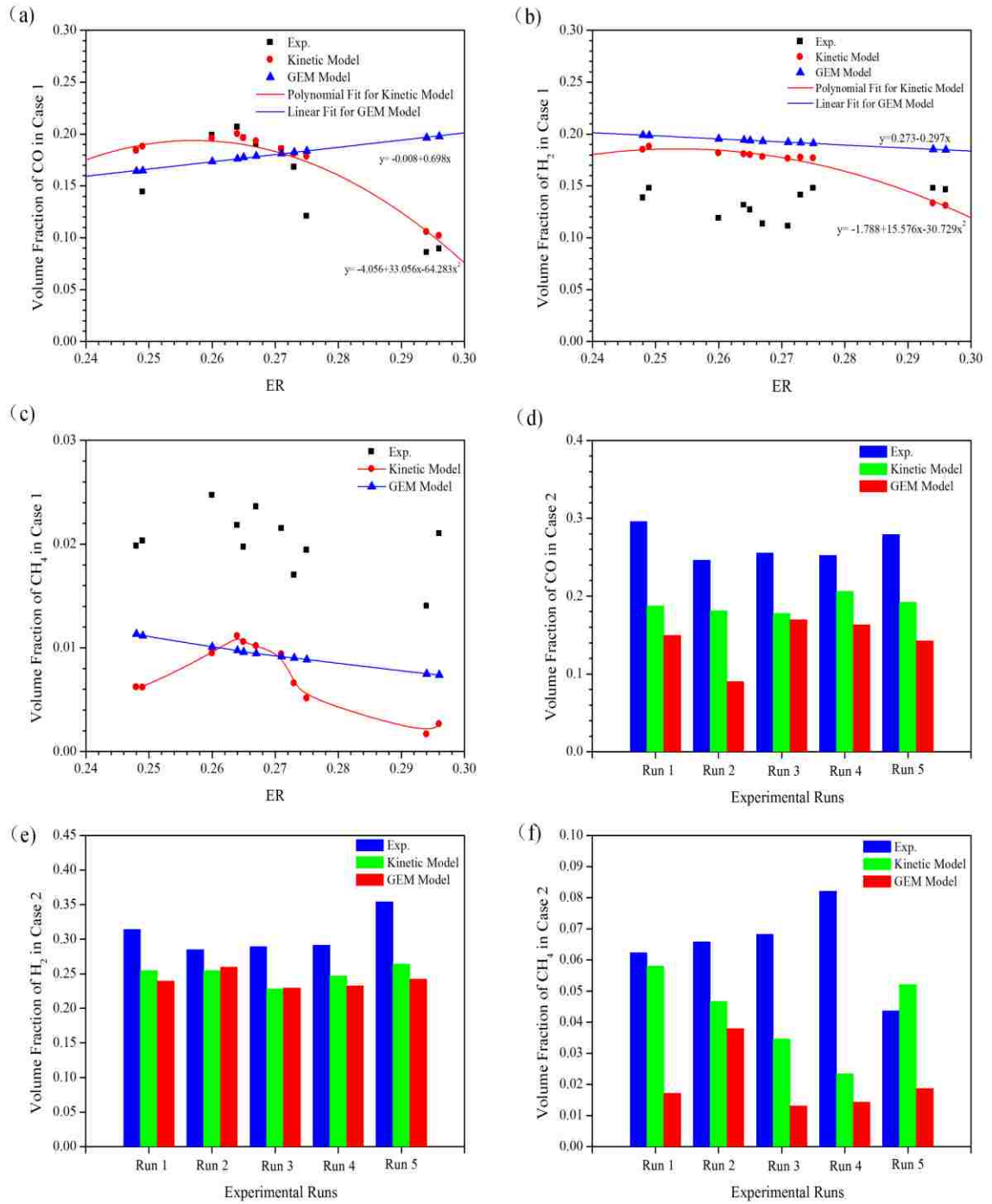


Figure 4. Comparison among experimental data, Kinetic Model and GEM Model results on (a)CO (b)H₂ (c)CH₄ of case 1; (d) CO (e)H₂ (f)CH₄ of case 2

formation during the process. This has also been a common problem in previous biomass gasification models [63, 64].

Table 6 summarized some models developed in the recent years. The errors of each model may vary due to the different model parameters (i.e. gasifier temperatures and biomass types). Errors are usually around 10-70%, an average upper error is 18.3% for CO, 25.3% for H₂, 53.9% for CH₄. The kinetic simulation has biggest CO error of 20% at ER=0.27, H₂ error is 27% at ER=0.273, CH₄ error at 44% at ER=0.273 (there is a big chance the experimental CH₄ volume fraction at ER=0.295 or 0.30 is a bad point). So, the Kinetic Model upper errors are smaller than the average upper error for referenced models. As shown, the comparisons between the Kinetic Model predictions are basically corresponding with the experimental results. The Kinetic Model is able to provide useful guidelines for industrial gasification process design, optimization, scaling up and operations.

Table 6. Analysis and errors for other Aspen Plus models

Authors and references	Comparison objects	Error analysis
Nikko and Mahinpey, 2008 [44]	Simulation results were compared with experimental data for product gas composition versus five different temperatures in the range of 700–900 C.	For H ₂ , CO and CO ₂ , the model gives bigger errors at 700 C and smaller errors at 900 °C; it is the opposite for CH ₄

Table 6. Analysis and errors for other Aspen Plus models (cont.)

		H ₂ : 70% at 700°C, 7% at 900 C CO: 27% at 700 C, 0% at 900°C CO ₂ : 57% at 700°C, 30% at 900°C CH ₄ : 2% at 700°C, 33% at 900°C
Doherty et al., 2009 [38]	Model was compared with one set of syngas compositions	Most compositions are in good match with experiment, but methane prediction is unacceptable higher than experiment. H ₂ :3.6%, N ₂ :6.9%, CO:1.1%, CH ₄ :125%, CO ₂ :2.5%
Ramzan et al., 2011 [59]	The model used food waste, municipal solid waste and poultry waste as the raw biomass to produce syngas, the results were compared with experiments	N ₂ : <14.4%, O ₂ : <37.1%, CO: <33.5%, CO ₂ : <13.5%, H ₂ : <19.7%, CH ₄ : <83.6%
Abdelouahed, et al., 2012 [74]	The author developed models with 1) WGS kinetic, 2) optimized WGS kinetic, and results were compared with experiments	H ₂ : 25%, 2% CO ₂ : 30%, 5%, CO: 19%, 5% CH ₄ : 15%, 18%,
Kaushal and Tyagi, 2017 [46]	Simulation results were compared with experimental data for product gas composition versus five different temperatures in the range of 700°C, 770 C,820°C	H ₂ : 8.3%, CO:11.1%, CO ₂ :47%, CH ₄ : 10%

3.2. ER EFFECT

ER influences the product compositions from two aspects: combustion and temperature. During combustion, if the ER increases, the biomass becomes more fully combusted using more available oxygen, which increases CO_2 composition. For the temperature aspect, a higher quality combustion results in more heat being generated thus increasing the reaction temperature; at the same time, extra air absorbs the heat which decreases overall temperature. Temperature also affects composition through the reaction rate, which is why close control of the ER is essential to good operation of a biomass gasifier.

During each of the experiments described above, CO mass fraction increased with the ERs to peak values and then decreases, which is consistent with the results reported by other researchers[10, 24, 32]. When a small amount of air is provided, biomass is combusted to a limited degree, resulting in low gasifier temperature. As more air is fed, combustion reactions occur at much higher rates, thus increasing bed temperature significantly. Although more CO_2 is produced in the combustion zone, it is more likely to be consumed by reacting with char in gasification zone to produce CO. Higher temperatures also help the water gas shift reaction to move right, and CO shift reaction to move left. If the ER keeps increasing, more CO is burnt to CO_2 , large amounts of cold air also stops the gasifier temperature from increasing, causing the CO amount to decrease. This explains the typical optimal ER appearance. At the ER where CO is at its peak, the energy is preferentially preserved in the final product.

However, in the GEM model, the CO composition decreases with ER increasing, which means that the GEM model is only valid in a very narrow ER range (approximately

from 0.255 to 0.270 if 15% CO simulation error is acceptable). This model considers all the reactions taking place in infinite time scales and that the system achieves equilibrium states. This is usually not the case in reality. The Kinetic Model approximates this curve more accurately.

3.3. TEMPERATURE EFFECT

A biomass gasifier generally produces sufficient energy required to be self-sustaining. The temperature in the reduction zone is set by the reactor design, feeding materials, biomass and air feed rate. The temperature profile can also be adjusted by using an external heat source, such as steam which can be used to control reactor wall temperature. The Kinetic Model estimates gas compositions at different temperatures are shown in Figure 5. The reduction zone temperature is the calculated temperature of the last block. This shows that the CO and H₂ content increase as temperature goes up. As for the steam methane reforming reaction, higher temperatures push the reaction backwards. Although increasing the temperature is beneficial to achieve a higher quality product, it requires extra energy from the gasifier to sustain the higher temperatures. For some types of biomass feedstocks that are lower in carbon content and heating value, measured bed temperatures are relatively low, therefore CO and H₂ content in the syngas is also low.

Higher temperature is shown to lead to better gasifier performance (more syngas production). Adding extra heat would be very helpful in improving the syngas quality and reducing tar content. Higher operating temperatures are also good when there is some waste heat available from existing process in chemical plants. Yet, for the biomass contents with a high heating value, the reaction bed temperature is normally very high (>1800°C),

therefore, the CO and H₂ contents do not change much after a sufficient amount of heat is added. Using external electricity or other fossil fuel to achieve higher reactor temperature is not advisable under this circumstance, due to the high cost of these resources. LHV also goes to an optimal and then decrease.

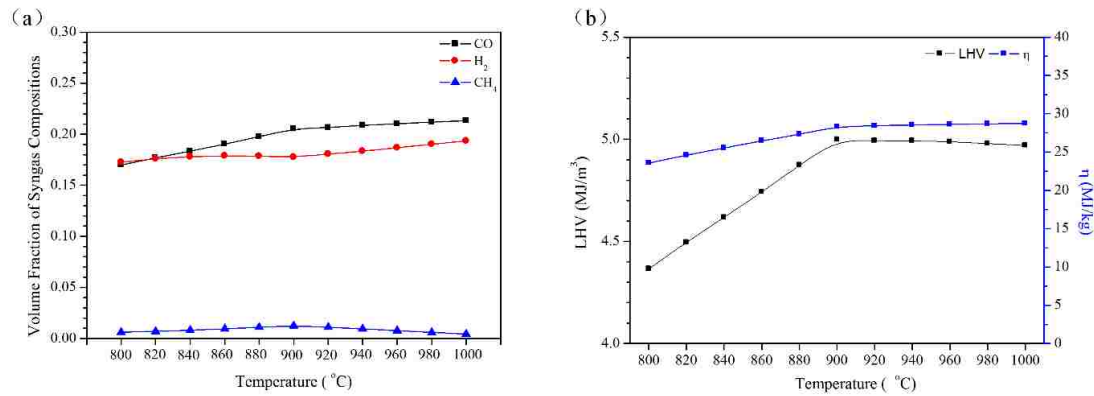


Figure 5. (a) Syngas compositions, (b) LHV and η at different reduction zone temperature

3.4. MOISTURE CONTENT EFFECT

To evaluate the impact of moisture on syngas product composition, four hypothesized biomass samples were examined in separate simulations. Their hypothetical ultimate and proximate analyses are shown in Table 7. Compositions of biomass samples 1-4 are the same, except that the moisture increases from 5% to 20%, which aligns closely to the moisture content of biomass feedstocks used for the gasification experiments. The simulated CO, CO₂ and H₂ compositions are shown in Figure 6. The volume fraction of CH₄ was 0 for each biomass in samples 1-4 with ER 0.20-0.35. As moisture content increases, the volume fraction of CO decreases, and H₂ and CO₂ increase. For each biomass

sample, CO reaches a maximum value between ER=0.20 and ER=0.30; as more oxygen is supplied, the concentration of H₂ decreases. For biomass samples 1, 2 and 3, CO₂ concentration decreases until it reaches a minimum, and then increases, which is opposite to the CO fraction; for biomass sample 4, CO₂ concentration decreases consistently. The volume fraction of methane remains zero, since the total water fraction is small and the system temperature remains low when air is the oxidizing agent.

Table 7. Composition analyses of biomass samples 1-8

Biomass Samples	Moisture (wet basis)	Proximate analysis (dry basis)			Ultimate analysis (dry basis)		
		Fixed Carbon	Volatile	Ash	C	O	H
1	0.05	0.20	0.75	0.05	0.40	0.50	0.10
2	0.10	0.20	0.75	0.05	0.40	0.50	0.10
3	0.15	0.20	0.75	0.05	0.40	0.50	0.10
4	0.20	0.20	0.75	0.05	0.40	0.50	0.10
5 (C/O=0.80)	0.05	0.20	0.75	0.05	0.40	0.50	0.10
6 (C/O=1.00)	0.05	0.20	0.75	0.05	0.45	0.45	0.10
7 (C/O=1.25)	0.05	0.20	0.75	0.05	0.50	0.40	0.10
8 (C/O=1.57)	0.05	0.20	0.75	0.05	0.55	0.35	0.10

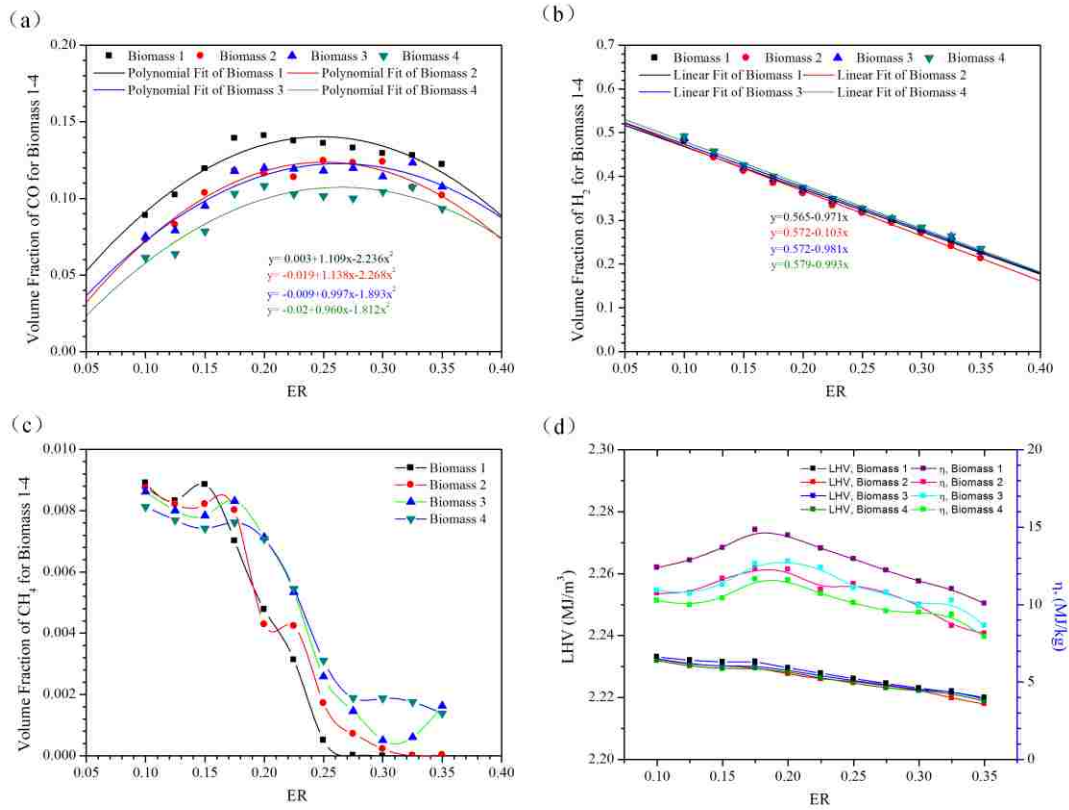


Figure 6. Product composition of (a) CO, (b) H₂, (c) CH₄, and (d) LHV and η for Biomass 1-4

3.5. EFFECT OF BIOMASS COMPOSITION

Gasification of different types of biomass yield different syngas compositions, which has a significant influence on downstream product amounts and quality. Biomass usually contains 40% - 55% carbon, 35% - 55% oxygen, around 5% hydrogen and negligible nitrogen and sulfur. The biomass proximate analysis shows fixed carbon usually accounts for around 20% of the total mass, volatiles account for 70%-90%, and ash for 0%-4%. Bulk density of biomass is around 300kg/m³. Biomass samples 5-8, listed in Table 7,

are shown to have compositions in the ranges listed above. Product composition and the optimized ERs for each biomass sample are shown in Figure 7.

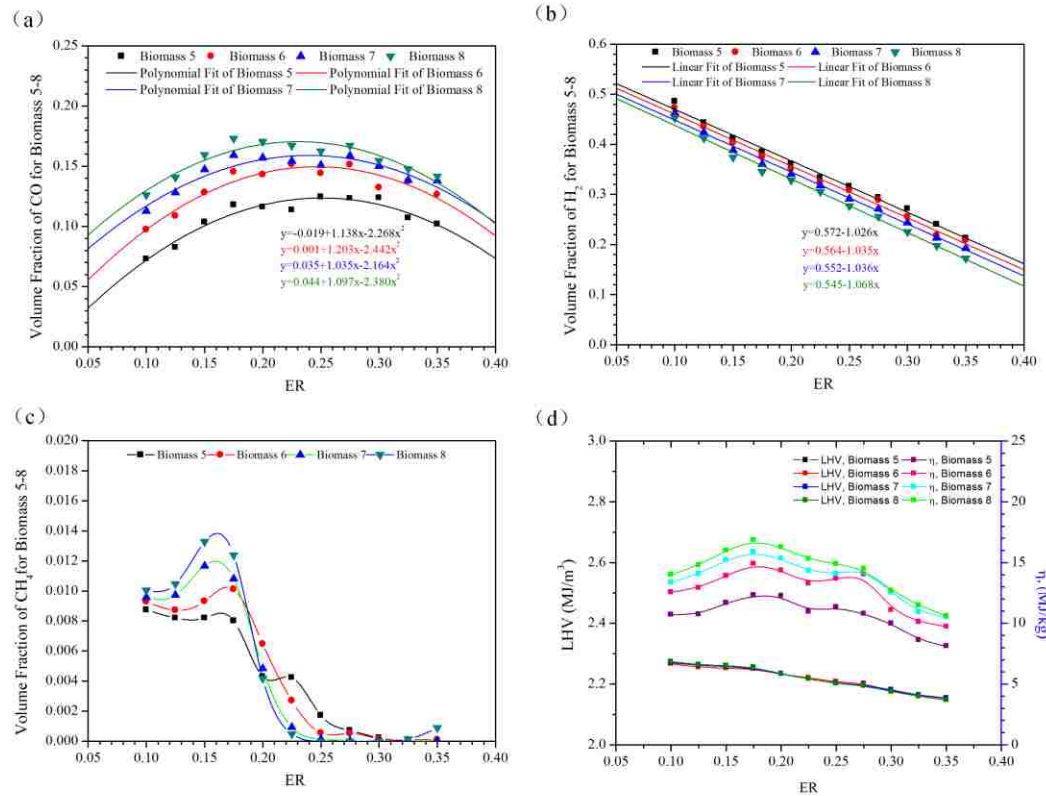


Figure 7. Product composition of (a) CO, (B) H₂, (c) CH₄, and (d) LHV and η for Biomass 5-8

Four biomass samples are expected to produce syngas compositions at 22%-27% CO, around 15% CO₂ and less than 5% methane. Hydrogen varies between 7% and 25%. Increasing carbon concentration in the biomass is shown to produce a higher CO volume fraction, as expected since more carbon is added to the system, which also causes an increased temperature in the gasifier bed. The kinetics for the water gas shift reaction

appears to be very important, since it controls the H_2/H_2O composition, which indirectly influences the yield of CO/CO_2 . Biomass samples 7 and 8 produce nearly the same CO product but increasing CO_2 fractions. This appears to be due to decreasing hydrogen pushing the water gas shift reaction to the right. As the original carbon composition increases from 0.40 to 0.55, more air is fed for the same ER value, so that more oxygen is consumed by hydrogen to produce more water. Thus, the hydrogen composition decreases from Biomass sample 5-8. Methane volume fraction increases since the biomass produces more methane in the volatiles, which are not burned in the combustion section.

3.6. TAR

Tar is the mean unfavorable byproduct of the gasification process. It is a complex mixture of condensable hydrocarbons, which includes hydrocarbons, oxygen-containing hydrocarbons and complex poly aromatic compounds (PAH) [94]. It is usually condensed to dark liquid of high viscosity when the syngas stream is cooled below $100^\circ C$. Tar residues do harm to the pipelines and downstream facilities [95], and this problem is considered the main barrier of commercialization of biomass-based power generation [96]. The implantation of kinetic information makes reasonable tar prediction possible. Several dominant tar components, including acetone, benzene, naphthalene, propionic acid, toluene and phenol. The tar could be thermally cracked above $700^\circ C$ [97]. For example, El-Run et al. reported phenol loses its stability as temperature increases [98]. The simulation results tell among all the simulated tar compositions, acetone takes approximately 50%, together with benzene, naphthalene are the main components of tar in the downdraft gasifier. It can be seen in Figure 8(a) that the tar amounts decrease slightly due to the increasing

gasification temperatures, this corresponds with findings of several literature that tar cracking is more effective at higher temperatures [97, 99, 100]. Figure 8(b) gives similar result, as the tar amount is lower at a higher ER. This is predictable as a higher ER means more oxygen is provided, so the combustion process is more performed and brings the reactor core to a higher temperature. Figure 8(c) and 8(d) illustrates the tar amount decreases when the biomass reserves more water, and increases when it contains more carbon. Yu and Smith [101] developed a RXN Model for updraft gasifiers, it is compared with the proposed downdraft Kinetic Model. According to literature reports, updraft gasifiers usually produce 10-15 g/Nm³ tar [102], which is more than 2 g/Nm³ for downdraft gasifiers [103]. Figure 9 shows the comparison of tar amount and components for Biomass 1 at different ERs, it is obvious to see that the updraft gasifier produce larger amount of tar with more complex components.

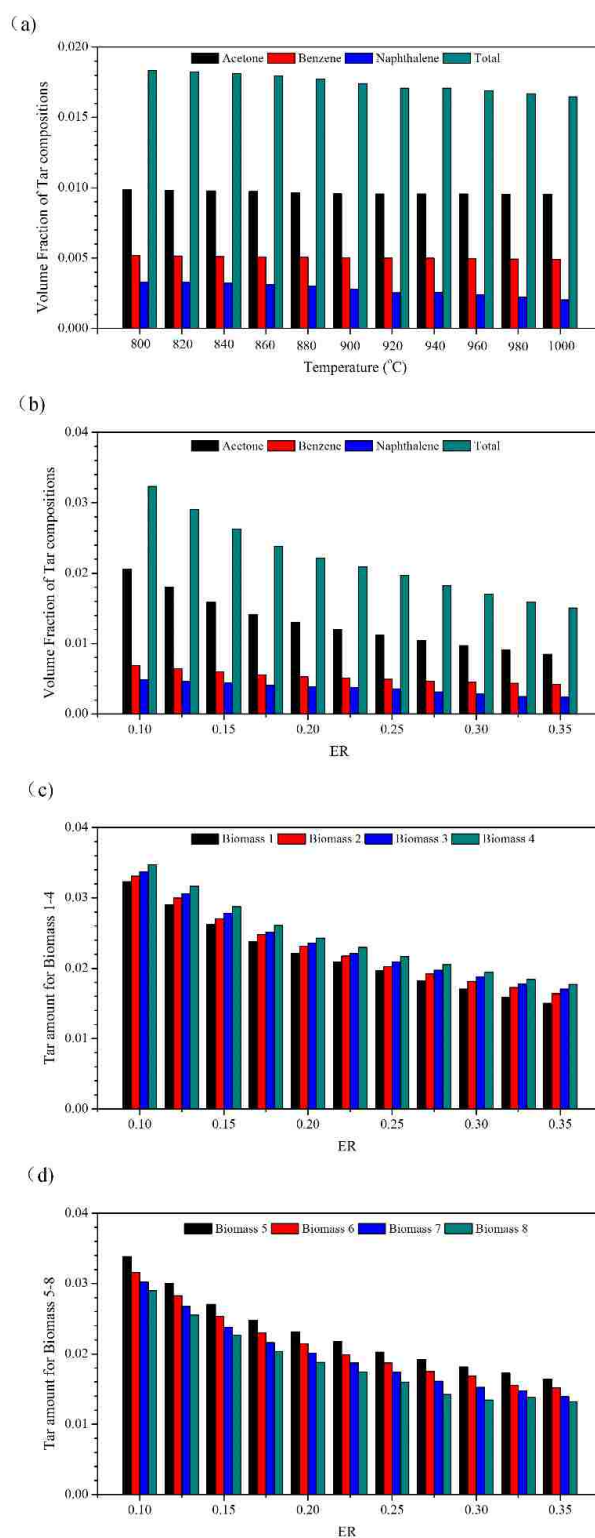


Figure 8. Volume fraction of tar for (a) Biomass 1 at different gasifying temperatures, (b) Biomass 1 at different ERs, (c) Biomass 1-4, (d) Biomass 5-8

4. CONCLUSIONS

A steady-state Kinetic Model was developed to simulate downdraft biomass gasifiers using Aspen Plus. In the Kinetic Model, syngas compositions were calculated using a series of chemical reactions with kinetics, which is fundamentally more accurate than a standard equilibrium model. Higher temperatures, higher carbon content and lower moisture were found to improve gasifier performance. Maximum CO production was predicted to occur for Equivalence Ratios (ER) between 0.20 and 0.30. Reactor geometry related hydrodynamic characteristics were not considered in the present model. Future work includes implementing this model into a CFD flow model to account for local mixing and reactions phenomena.

ACKNOWLEDGEMENTS

The authors gratefully acknowledge financial support from the Wayne and Gayle Laufer Endowment.

NOTATION

a	number for atoms
A	total number of atoms entering the reactor
A_r	frequency factor ($\text{mol}^{(1-\alpha)}\text{m}^{(3\alpha-3)}\text{s}^{-1}$)
C	concentration (mol/m^3)
E_a	activation energy (kJ/kmol)
D	proximate analysis value of a single category, dry basis
E	mass fraction of each proximate analysis category
F	feed rate (kg/s)
G_t	total Gibbs energy of system (kJ/mol)
k	reaction rate coefficient
L	reactor length (m)
n	moles (mol)
q	energy change for operation unit
R	gas constant ($\text{kJ}/\text{kmol K}$)
r	rate of reaction
SR	split ratio, the ratio of fixed carbon stream over the total carbon
t	residence time (s)
T	temperature (K)
U	ultimate analysis of each element
V	volume (m^3)
W	mass fraction of each category

Greek letters

α	reaction order
ρ	bulk density of biomass (kg/m ³)
β	temperature exponent

Subscripts

bio	biomass
i	species index
j	element index
m	category index of proximate analysis
n	element index of ultimate analysis
r	reaction index
rt	reactor
hm	homogeneous reaction
ht	heterogeneous reaction
total	total reaction

REFERENCES

1. Zhao, Y., et al., Characteristics of rice husk gasification in an entrained flow reactor. *Bioresource technology*, 2009. 100(23): p. 6040-6044.
2. Zhou, J., et al., Biomass–oxygen gasification in a high-temperature entrained-flow gasifier. *Biotechnology advances*, 2009. 27(5): p. 606-611.
3. Hernández, J.J., G. Aranda-Almansa, and A. Bula, Gasification of biomass wastes in an entrained flow gasifier: Effect of the particle size and the residence time. *Fuel Processing Technology*, 2010. 91(6): p. 681-692.
4. Turn, S., et al., An experimental investigation of hydrogen production from biomass gasification. *International Journal of Hydrogen Energy*, 1998. 23(8): p. 641-648.
5. Lv, P., et al., An experimental study on biomass air–steam gasification in a fluidized bed. *Bioresource technology*, 2004. 95(1): p. 95-101.
6. Rapagna, S., et al., Steam-gasification of biomass in a fluidised-bed of olivine particles. *Biomass and Bioenergy*, 2000. 19(3): p. 187-197.
7. Saravanakumar, A., et al., Experimental investigations of long stick wood gasification in a bottom lit updraft fixed bed gasifier. *Fuel processing technology*, 2007. 88(6): p. 617-622.
8. Plis, P. and R. Wilk, Theoretical and experimental investigation of biomass gasification process in a fixed bed gasifier. *Energy*, 2011. 36(6): p. 3838-3845.
9. Chen, W., et al., Updraft fixed bed gasification of mesquite and juniper wood samples. *Energy*, 2012. 41(1): p. 454-461.
10. Dogru, M., et al., Gasification of hazelnut shells in a downdraft gasifier. *Energy*. 27(5): p. 415-427.
11. Lv, P., et al., Hydrogen-rich gas production from biomass air and oxygen/steam gasification in a downdraft gasifier. *Renewable Energy*, 2007. 32(13): p. 2173-2185.
12. Zainal, Z., et al., Experimental investigation of a downdraft biomass gasifier. *Biomass and bioenergy*, 2002. 23(4): p. 283-289.
13. Janajreh, I. and M. Al Shrah, Numerical and experimental investigation of downdraft gasification of wood chips. *Energy Conversion and Management*, 2013. 65: p. 783-792.

14. Gai, C. and Y. Dong, Experimental study on non-woody biomass gasification in a downdraft gasifier. *International Journal of hydrogen energy*, 2012. 37(6): p. 4935-4944.
15. Pérez, J.F., A. Melgar, and P.N. Benjumea, Effect of operating and design parameters on the gasification/combustion process of waste biomass in fixed bed downdraft reactors: An experimental study. *Fuel*, 2012. 96: p. 487-496.
16. Papadikis, K., A. Bridgwater, and S. Gu, CFD modelling of the fast pyrolysis of biomass in fluidised bed reactors, Part A: Eulerian computation of momentum transport in bubbling fluidised beds. *Chemical Engineering Science*, 2008. 63(16): p. 4218-4227.
17. Ruiz, J., et al., Biomass gasification for electricity generation: review of current technology barriers. *Renewable and Sustainable Energy Reviews*, 2013. 18: p. 174-183.
18. Bridgwater, A., The technical and economic feasibility of biomass gasification for power generation. *Fuel*, 1995. 74(5): p. 631-653.
19. Reed, T. and A. Das, *Handbook of biomass downdraft gasifier engine systems*. 1988: Biomass Energy Foundation.
20. Basu, P., *Combustion and gasification in fluidized beds*. 2006: CRC press.
21. Doherty, W., A. Reynolds, and D. Kennedy, The effect of air preheating in a biomass CFB gasifier using ASPEN Plus simulation. *Biomass and Bioenergy*, 2009. 33(9): p. 1158-1167.
22. McKendry, P., Energy production from biomass (part 3): gasification technologies. *Bioresource technology*, 2002. 83(1): p. 55-63.
23. Corella, J., J.M. Toledo, and G. Molina, A review on dual fluidized-bed biomass gasifiers. *Industrial & Engineering Chemistry Research*, 2007. 46(21): p. 6831-6839.
24. Li, X., et al., Biomass gasification in a circulating fluidized bed. *Biomass and bioenergy*, 2004. 26(2): p. 171-193.
25. Lucas, J., C. Lim, and A. Watkinson, A nonisothermal model of a spouted bed gasifier. *Fuel*, 1998. 77(7): p. 683-694.
26. Hosseini, M., I. Dincer, and M.A. Rosen, Steam and air fed biomass gasification: comparisons based on energy and exergy. *International journal of hydrogen energy*, 2012. 37(21): p. 16446-16452.
27. Inayat, A., M.M. Ahmad, and M.A. Mutalib. Effect of process parameters on hydrogen production and efficiency in biomass steam gasification with in-situ CO₂ capture. in *Preceedings of Internatiional Conference on Process Engineering and Advanced Materials*. 2010.

28. Jaojaruek, K. and S. Kumar, Numerical simulation of the pyrolysis zone in a downdraft gasification process. *Bioresource technology*, 2009. 100(23): p. 6052-6058.
29. Nikoo, M.B. and N. Mahinpey, Simulation of biomass gasification in fluidized bed reactor using ASPEN PLUS. *Biomass and Bioenergy*, 2008. 32(12): p. 1245-1254.
30. s.A.N.M., San Diego, CA, United States, April 1-5, 2001 Abdelouahed, Lokmane, et al., Detailed modeling of biomass gasification in dual fluidized bed reactors under Aspen Plus. *Energy & Fuels*, 2012. 26(6): p. 3840-3855.
31. Kaushal, P. and R. Tyagi, Advanced simulation of biomass gasification in a fluidized bed reactor using ASPEN PLUS. *Renewable Energy*, 2017. 101: p. 629-636.
32. Gómez-Barea, A. and B. Leckner, Modeling of biomass gasification in fluidized bed. *Progress in Energy and Combustion Science*, 2010. 36(4): p. 444-509.
33. Xue, Q., T. Heindel, and R. Fox, A CFD model for biomass fast pyrolysis in fluidized-bed reactors. *Chemical Engineering Science*, 2011. 66(11): p. 2440-2452.
34. Fletcher, D., et al., A CFD based combustion model of an entrained flow biomass gasifier. *Applied mathematical modelling*, 2000. 24(3): p. 165-182.
35. Gentile, G., et al., A comprehensive CFD model for the biomass pyrolysis. *Chemical Engineering Transactions*, 2015. 43.
36. Guo, B., et al., Simulation of biomass gasification with a hybrid neural network model. *Bioresource Technology*, 2001. 76(2): p. 77-83.
37. Hornik, K., Approximation capabilities of multilayer feedforward networks. *Neural networks*, 1991. 4(2): p. 251-257.
38. Psychogios, D.C. and L.H. Ungar, A hybrid neural network-first principles approach to process modeling. *AIChE Journal*, 1992. 38(10): p. 1499-1511.
39. Barker, R., et al., ASPEN modeling of the tri-state indirect-liquefaction process. 1983, Oak Ridge National Lab., TN (USA).
40. Jiang, Y. and D. Bhattacharyya, Plant-wide modeling of an indirect coal-biomass to liquids (CBTL) plant with CO₂ capture and storage (CCS). *International Journal of Greenhouse Gas Control*, 2014. 31: p. 1-15.
41. Xiangdong, K., et al., Three stage equilibrium model for coal gasification in entrained flow gasifiers based on Aspen Plus. *Chinese Journal of Chemical Engineering*, 2013. 21(1): p. 79-84.
42. Phillips, J.N., Study of the off-design performance of integrated coal gasification combined-cycle power plants. 1986, Stanford Univ., CA (USA).

43. Shen, L., Y. Gao, and J. Xiao, Simulation of hydrogen production from biomass gasification in interconnected fluidized beds. *Biomass and Bioenergy*, 2008. 32(2): p. 120-127.
44. Ramzan, N., et al., Simulation of hybrid biomass gasification using Aspen plus: A comparative performance analysis for food, municipal solid and poultry waste. *Biomass and Bioenergy*, 2011. 35(9): p. 3962-3969.
45. Keche, A.J., A.P.R. Gaddale, and R.G. Tated, Simulation of biomass gasification in downdraft gasifier for different biomass fuels using ASPEN PLUS. *Clean Technologies and Environmental Policy*, 2015. 17(2): p. 465-473.
46. Kuo, P.-C., W. Wu, and W.-H. Chen, Gasification performances of raw and torrefied biomass in a downdraft fixed bed gasifier using thermodynamic analysis. *Fuel*, 2014. 117: p. 1231-1241.
47. De Kam, M.J., R.V. Morey, and D.G. Tiffany, Integrating biomass to produce heat and power at ethanol plants. *Applied engineering in agriculture*, 2009. 25(2): p. 227-244.
48. Chen, J.-s., Kinetic engineering modeling of co-current moving bed gasification reactors for carbonaceous materials. 1986, Cornell Univ., Ithaca, NY (USA).
49. Wang, Y. and C. Kinoshita, Kinetic model of biomass gasification. *Solar Energy*, 1993. 51(1): p. 19-25.
50. Milligan, J., Downdraft gasification of biomass. 1994, Aston University, Birmingham, UK.
51. Giltrap, D., R. McKibbin, and G. Barnes, A steady state model of gas-char reactions in a downdraft biomass gasifier. *Solar Energy*, 2003. 74(1): p. 85-91.
52. Yang, Y., et al., Effects of fuel devolatilisation on the combustion of wood chips and incineration of simulated municipal solid wastes in a packed bed ☆. *Fuel*, 2003. 82(18): p. 2205-2221.
53. Di Blasi, C., Modeling wood gasification in a countercurrent fixed-bed reactor. *AIChE Journal*, 2004. 50(9): p. 2306-2319.
54. Dennis, J., et al., The kinetics of combustion of chars derived from sewage sludge. *Fuel*, 2005. 84(2): p. 117-126.
55. Gøbel, B., et al., The development of a computer model for a fixed bed gasifier and its use for optimization and control. *Bioresource Technology*, 2007. 98(10): p. 2043-2052.
56. Sharma, A.K., Equilibrium and kinetic modeling of char reduction reactions in a downdraft biomass gasifier: A comparison. *Solar Energy*, 2008. 82(10): p. 918-928.

57. Zhong, L.-D. and W.-H. Mei. Kinetic model establishment and verification of the biomass gasification on fluidized bed. in Machine Learning and Cybernetics, 2009 International Conference on. 2009. IEEE.
58. Roy, P.C., A. Datta, and N. Chakraborty, Modelling of a downdraft biomass gasifier with finite rate kinetics in the reduction zone. International Journal of Energy Research, 2009. 33(9): p. 833-851.
59. Abdelouahed, L., et al., Detailed modeling of biomass gasification in dual fluidized bed reactors under Aspen Plus. Energy & Fuels, 2012. 26(6): p. 3840-3855.
60. Mendiburu, A.Z., et al., Thermochemical equilibrium modeling of a biomass downdraft gasifier: Constrained and unconstrained non-stoichiometric models. Energy, 2014. 71: p. 624-637.
61. Jangsawang, W., K. Laohalidanond, and S. Kerdsuwan, Optimum equivalence ratio of biomass gasification process based on thermodynamic equilibrium model. Energy Procedia, 2015. 79: p. 520-527.
62. Smith, J., H. Van Ness, and M. Abbott, Introduction to Chemical Engineering Thermodynamics, (2001) and 7th ed.(2005). McGraw-Hill, New York.
63. Inc., A.T., Aspen Plus User's Guide. 2000.
64. Fogler, H.S., in Elements of Chemical Reaction Engineering. 2005, Prentice Hall.
65. Wu, Y., et al., Two-dimensional computational fluid dynamics simulation of biomass gasification in a downdraft fixed-bed gasifier with highly preheated air and steam. Energy & Fuels, 2013. 27(6): p. 3274-3282.
66. Hobbs, M., P. Radulovic, and L. Smoot, Combustion and gasification of coals in fixed-beds. Progress in Energy and Combustion Science, 1993. 19(6): p. 505-586.
67. Yoon, H., J. Wei, and M.M. Denn, A model for moving-bed coal gasification reactors. AIChE Journal, 1978. 24(5): p. 885-903.
68. Chen, W.-H., et al., A comparison of gasification phenomena among raw biomass, torrefied biomass and coal in an entrained-flow reactor. Applied energy, 2013. 112: p. 421-430.
69. Du, S.-W. and W.-H. Chen, Numerical prediction and practical improvement of pulverized coal combustion in blast furnace. International Communications in Heat and Mass Transfer, 2006. 33(3): p. 327-334.
70. Arthur, J., Reactions between carbon and oxygen. Transactions of the Faraday Society, 1951. 47: p. 164-178.

71. Gerber, S., F. Behrendt, and M. Oevermann, An Eulerian modeling approach of wood gasification in a bubbling fluidized bed reactor using char as bed material. *Fuel*, 2010. 89(10): p. 2903-2917.
72. Umeki, K., T. Namioka, and K. Yoshikawa, Analysis of an updraft biomass gasifier with high temperature steam using a numerical model. *Applied energy*, 2012. 90(1): p. 38-45.
73. Howard, J., G. Williams, and D. Fine. Kinetics of carbon monoxide oxidation in postflame gases. *Symposium (International) on Combustion*. 1973. Elsevier.
74. Macak, J. and J. Malecha, Mathematical model for the gasification of coal under pressure. *Industrial & Engineering Chemistry Process Design and Development*, 1978. 17(1): p. 92-98.
75. Robinson, P.J. and W.L. Luyben, Simple dynamic gasifier model that runs in Aspen Dynamics. *Industrial & engineering chemistry research*, 2008. 47(20): p. 7784-7792.
76. Varma, A.K., A.U. Chatwani, and F.V. Bracco, Studies of premixed laminar hydrogen air flames using elementary and global kinetics models. *Combustion and flame*, 1986. 64(2): p. 233-236.
77. Dryer, F. and I. Glassman. High-temperature oxidation of CO and CH₄. in *Symposium (International) on Combustion*. 1973. Elsevier.
78. Morf, P., P. Hasler, and T. Nussbaumer, Mechanisms and kinetics of homogeneous secondary reactions of tar from continuous pyrolysis of wood chips. *Fuel*, 2002. 81(7): p. 843-853.
79. Milne, T.A., R.J. Evans, and N. Abatzoglou, Biomass Gasifier "Tars": Their Nature, Formation, and Conversion. 1998, National Renewable Energy Laboratory, Golden, CO (US).
80. Devi, L., K.J. Ptasinski, and F.J. Janssen, A review of the primary measures for tar elimination in biomass gasification processes. *Biomass and bioenergy*, 2003. 24(2): p. 125-140.
81. Asadullah, M., Barriers of commercial power generation using biomass gasification gas: a review. *Renewable and Sustainable Energy Reviews*, 2014. 29: p. 201-215.
82. Fagbemi, L., L. Khezami, and R. Capart, Pyrolysis products from different biomasses: application to the thermal cracking of tar. *Applied energy*, 2001. 69(4): p. 293-306.
83. El-Rub, Z.A., E.A. Bramer, and G. Brem, Experimental comparison of biomass chars with other catalysts for tar reduction. *Fuel*, 2008. 87(10-11): p. 2243-2252.

84. Anis, S. and Z. Zainal, Tar reduction in biomass producer gas via mechanical, catalytic and thermal methods: A review. *Renewable and Sustainable Energy Reviews*, 2011. 15(5): p. 2355-2377.
85. Han, J. and H. Kim, The reduction and control technology of tar during biomass gasification/pyrolysis: an overview. *Renewable and Sustainable Energy Reviews*, 2008. 12(2): p. 397-416.
86. Yu, J. and J. Smith, Validation and application of a kinetic model for biomass gasification simulation and optimization in updraft gasifiers. *Chemical Engineering and Processing - Process Intensification*, 2018. 125: p. 214-226.
87. Nakamura, S., S. Kitano, and K. Yoshikawa, Biomass gasification process with the tar removal technologies utilizing bio-oil scrubber and char bed. *Applied Energy*, 2016. 170: p. 186-192.
88. Bui, T., R. Loof, and S. Bhattacharya, Multi-stage reactor for thermal gasification of wood. *Energy*, 1994. 19(4): p. 397-404.

III. EXPERIMENTAL INVESTIGATION OF TAR RECYCLING IN PILOT-SCALE BIOMASS GASIFIERS: PROSPECTS, OPERATING PROCEDURES, PROCESS VARIATIONS AND CONTROLS

*Jia Yu^{1, #}, Haider A. Al-Rubaye^{1, #}, Joseph D. Smith^{1, *}, Hasan J. Al-Abedi²*

¹ Department of Chemical and Biochemical Engineering, Missouri University of Science and Technology. 1101 North State Street, 110 Bertelsmeyer Hall, Rolla, MO 65401-09,
United States

² Department of Chemical Engineering, University of Technology, Baghdad, Iraq.

^{*}Corresponding Author

E-mail address: smithjose@mst.edu (*Dr. Joseph. D. Smith*)

[#] Jia Yu and Haider Al-Rubaye share equal contribution.

ABSTRACT

Tar is considered as the main barrier to commercial power generation using biomass gasification as it causes serious environmental issues even after efficient removal system. What's more, the existed tar compositions contain high energy amount, thus lower the heating value of produced syngas. In this paper, tar is blended with three types of plain biomass at ratios up to 0.1; biomass and tar are gasified together at different equivalence ratios. Tar recycling is found beneficial to the syngas compositions. The size distribution of the biomass feed and the gasified char have been studied. Experimental evidence shows that the isolation time of shutdown procedure is proportional to the volume of the gasifier cores. This paper discusses the operation procedure and troubleshoot for biomass gasifiers in detail, which can provide useful guidelines for practical research in the future.

1. INTRODUCTION

Tar is a complex organic mixture of condensable liquids, which is usually considered as a byproduct of the coal or biomass gasification processes. Tar will result in: 1) the shutdown of gasification facilities, internal combustion engines, and turbines; 2) losing heating value of the produced syngas; and 3) environmental pollution due to the toxicity of aromatic hydrocarbons. Gasification processes usually produce a significant amount of tar: around 2g/Nm^3 for downdraft gasifiers [1], $10\text{-}15\text{g/Nm}^3$ for updraft gasifiers [2], and 10g/Nm^3 for circulating fluidized bed (CFB) [3]. However, the maximum concentration of tar for a stable operated internal combustion engine must be less than 0.1g/Nm^3 [4, 5]. The tar compositions create process inefficiencies such as pipeline corrosion and blockage, thus it has to be cleaned from the syngas before feeding to downstream facilities. The tar removing is considered the current challenge for produced syngas utility [6].

Multiple tar control and removal technologies were developed during the past decades, and they can be broadly classified into primary and secondary methods. Primary methods refer to treatments during the gasification, such as thermal cracking by controlling the operating parameters (e.g. temperature, equivalence ratio and residence time), catalytic cracking using Ni-based catalysts, and plasma gasification. However, the primary methods incur high initial and running costs and thus are not implemented commercially [7]. Researchers also improved reactor design to overcome this barrier. Pan et al. [8] and Narvaez et al. [9] reported significant tar reduction by injecting secondary air. Cao et al. [7] developed a two-stage biomass gasifier, which consisted of sand fluidized region and

tar decomposition region, and reduced the tar from 1227 mg/Nm³ to 12.34 mg/Nm³. Secondary methods such as using scrubbers, centrifuges and filters, are relatively cheaper and easier to commercialize. However, the physical filtrations create two problems. First, physical tar removing will cause a huge pressure drop. Second tar contamination still exists as tar was collected instead of reducing its production.

The compositions of the tar were analyzed using GC–MS or NMR. Yu et al. [10] categorized tar compositions according to the following:

- (1) Polycyclic aromatic hydrocarbons (PAHs),
- (2) Benzene, toluene, ethylbenzene and xylene isomers (BTEX),
- (3) Phenols and its derivatives,
- (4) Miscellaneous hydrocarbons.

Among all the compositions above, benzene and toluene account for approximately 70% of the total GC-MS detected tar [11]. Although tar is collected before feeding into the downstream pipeline and applicators, it requires storage and strict deposit method to avoid environmental pollution. As can be seen in Figure 1, the PAHs occupied approximately 65%-90% of the total amount. PAHs usually are generated from the plant synthesis, forest fires and volcanoes, etc.[12], while the anthropogenic resources are primarily from the incomplete combustion of fossil fuels [13]. Many PAHs is mutagenic and carcinogenic. They are readily absorbed by intestinal tract of mammals and then go through metabolic formation, many PAHs forms carcinogenic bay- and K-region epoxides during this process[14]. Naphthalene, for example, is the first member of the PAHs, which was also considered in the Aspen Plus models as a main component of tar. It usually binds covalently to molecules and do harm to liver, kidney and lung tissues,

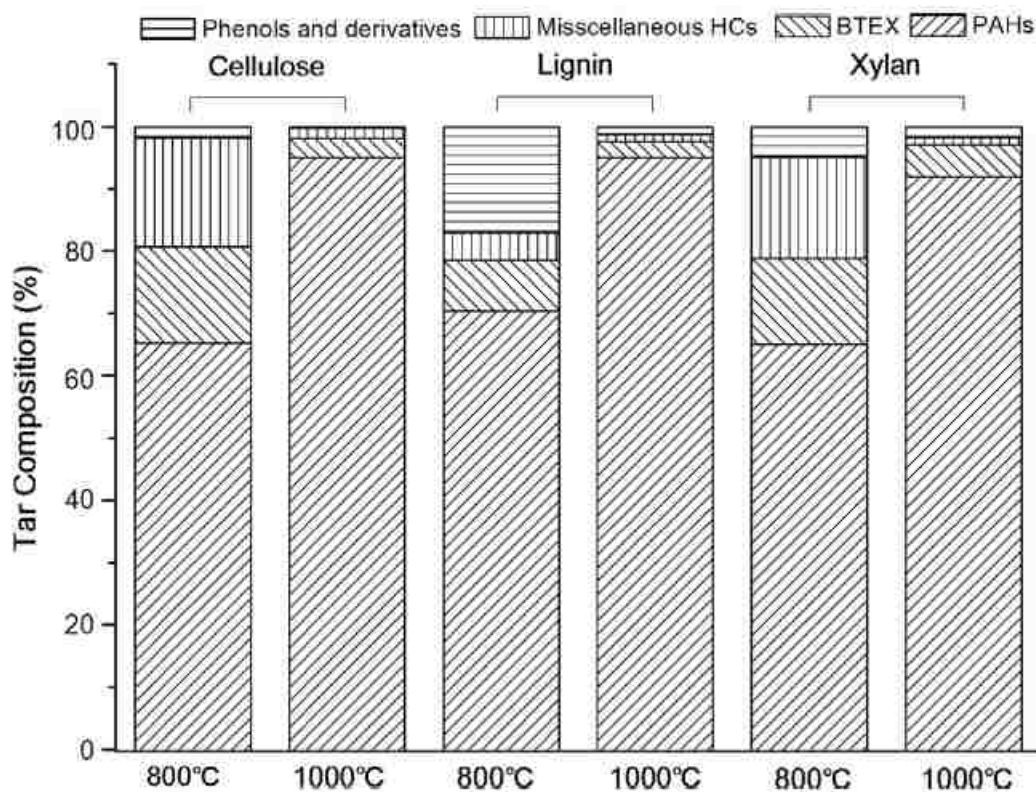


Figure 1. Relative content of different substance groups in gasification tar

and is also shown to sabotage energy conversion to adenosine triphosphate (ATP) [15]. Occupational exposures to high levels of pollutant mixtures containing PAHs have resulted in symptoms such as eye irritation, nausea, vomiting, diarrhea and confusion[16]. The PAHs also interfere the metabolism and photo-oxidation of the aquatic organisms, especially with the presence of ultraviolet light. PAHs are moderately persistent in the environment, yet it could be accumulated in the organisms such as fish and shellfish[17]. As hydrocarbons are not considered as hazardous waste in the US, they are usually disposed to a waste depot directly. Thus, it is important to reduce the amount of the tar to relieve the irritation to the environment.

2. METHODOLOGY

2.1. BIOMASS MATERIALS

Hardwood pellets, picks and flakes are fed into the gasifiers to investigate their influence on syngas compositions, heating values and bed performances. Five samples of each feedstock were taken randomly and go through the thermogravimetric analyzer (TGA) and CHN elemental analyzer. The physical properties, average proximate and ultimate analysis of each biomass are listed below in Table 1. Except for original plain biomass, biomass and tar blends are also prepared to test the gasification results. Tar and biomass are mixed at ratios 0.02, 0.04, 0.06, 0.08 and 0.10 w/w and then were fed into the gasifiers. Gasification tests were performed in three pilot-scale downdraft fixed bed gasifiers. These open-top gasification cores are cylinders of 19" height, 4", 8" and 12" diameter respectively. See biomass samples and reactor cores in Figure 2.



Figure 2. Biomass feedstocks and gasifier cores

Table 1. Proximate and ultimate analysis for feedstocks

Physical Properties	Pellets	Picks	Flakes
Bulk Density (kg/m ³)	664	146	42
Absolute Density (kg/m ³)	938	508	352
Bed void ratio	0.29	0.71	0.88
Proximate Analysis			
Volatile	65.98	66.88	73.47
Fixed Carbon	16.00	18.40	19.91
Ash	18.01	14.71	6.60
Moisture		35.19 (5.48 after dried)	
	7.56		11.01
Ultimate Analysis(DAF)			
C	49.03	48.81	48.24
H	5.58	5.96	6.15
O	0.06	0.26	0.06
N	45.33	44.98	45.55

2.2. EXPERIMENTAL DESIGN

The reactor cores are surrounded by a 20” reactor shell, which serves as a syngas plenum to reduce the ash and char residues carried by the syngas. A ¼” iron grate is attached 1” below the reactor core to support the biomass and dispose the ash. In addition, the produced syngas has a higher temperature than ambient air so that it helps to preserve the reaction core temperature. Three K-type thermocouples are inserted 4”, 8” and 12” above the grate and centered to obtain the temperatures of reduction, combustion and pyrolysis zones. The biomass is fed from the top of the gasifier. To safely monitor the bed

performances, one camera is installed above the bed to observe the movement of the bed, the other planted facing the burner to closely watch the syngas burning results. All the camera recordings, temperature and oxygen level data are monitored online using LabVIEW.

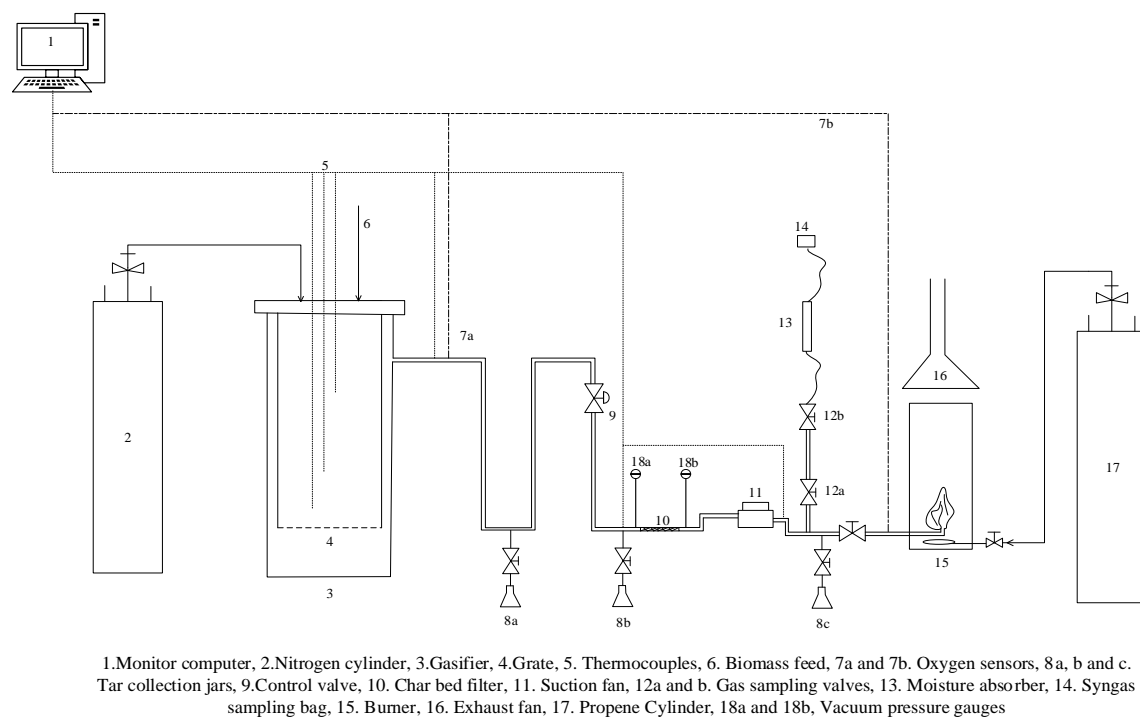


Figure 3. Flowsheet of the gasification process

A 2-inch syngas pipeline is connected to the reactor shell to transport the syngas into a draft fan. A ball valve is installed before the fan to control the syngas flow rate. The ball valve is calibrated to setting levels 0-8, see Table 2, where 0 is completely closed and 8 is completely open. The valve setting is controlled between 2 to 6 depends on different ER ratios and biomass feeds. Tar is condensed to liquid during this time as the syngas

temperature drops. As shown in Figure 3, the pipeline has two liquid trap jars and before the suction fan, one jar after the suction fan is used to collect produced tar. A char bed filter is also made to remove aerosol tar from the syngas as much as possible [2]. Two vacuum manometers are installed to measure the pressure drop of the char bed as an indicator for obstruction. Two oxygen sensors, one after the gasifier and the other one before the burner, are employed to record the oxygen residues inside the pipeline to secure safety issues. Syngas is carried to the burner and completely combusted to minimize the air contamination.

Table 2. Calibrated gas flow for the control valve setting

Valve Setting	Gas Flow (L/min)
Setting 0	0
Setting 1	90
Setting 2	200
Setting 3	256
Setting 4	269
Setting 5	282
Setting 6	295
Setting 7	307
Setting 8	320

2.3. GAS SAMPLING AND MEASURING SYSTEM

The gas goes through the open valve when gas samplings are required, followed by a moisture absorption column and aluminum sampling bags. Gas samples are collected after the gasifier reaches steady state, three samples are taken when pure biomass is fed, while two samples are taken when the biomass-tar blend is fed. The syngas samples are analyzed by gas chromatograph. The equipment uses a TCD detector and helium as the carrier gas. The contents of H_2 , CO, CO_2 and CH_4 and some other light hydrocarbons were detected, N_2 is calculated by the volume difference. The GC is calibrated by the calibration gas before it is used in analyses. The recommended GC testing details for syngas analysis is attached in Appendix B.

Each run is fixed at one reactor scale (4", 8" and 12"), one biomass feedstock (pellets, picks and flakes) and one equivalence ratio (0.15, 0.20, 0.25), but biomass with 6 levels of tar contents are fed in one run. The combusted propane gas provides a stable flame to ignite any produced syngas during each experimental run. The LabVIEW and exhaust fan should be working before propane is ignited. The experiment starts with loading 5-10lb of plain biomass into the gasifier bed. Approximately 30ml of charcoal light fluid is poured onto the surface of the biomass bed to help the ignition. The suction fan is turned on when the top layer biomass should catch fire and glow. At this time, the combustion zone temperature is at around 1000°F, and the control valve is usually set between 5 to 6 for startups. The investigators can now feed new plain biomass to build the drying layer for the bed. As the reaction proceeds, the bed temperature increases from the room temperature to 1200-1700°F. Then the valve is set to the testing setting, the bed is usually stabilized in 30 mins at this setting. An obvious drop of oxygen is observed as soon as the suction fan

starts working, two oxygen measuring points at most time keep identical oxygen levels around 0.6-1%. Six different feedstocks of plain biomass, 2%, 4%, 6%, 8% and 10% will be introduced into the gasifier in order. At least two gas samples are taken for each biomass feeds after both the bed and zone temperatures are stabilized. The collected tar is weighed every 15 mins. Longitudinal vibration is provided to help the bed move down and avoid piling.

After all the data and gas samples are collected, the gasifier must shutdown before the experimentalists leave the facility, it includes all the actions to safely seal the gasifier. A seal plate is placed onto the top of the gasifier to prevent any fresh air flowing into the core. 1 scfm N_2 is introduced into the bed and the valve is opened fully so that the reactor core is flushed completely by the N_2 gas. It usually takes 5-30mins, depending on different operating conditions, for the bed temperature to fall under 600°F. It is now safe to turn off the N_2 gas and seal the control valve completely closed, as the reactor core is filled with inert gas and the temperature is low enough to eliminate any combustion. The suction fan, propane cylinder and exhaust fan are shut down in an orderly sequence after no combustible gas is produced and the control valve is closed. The temperatures of combustion and reduction zone are monitored until the bed temperature goes below 300°F.

To close the mass balance, cleanup procedures is required after the reactor is cooled down to the room temperature. Reopening of the system is only recommended after the bed temperature drops below 100°F, otherwise the fresh oxygen will enhance a slow gasification and takes at least three times longer than keeping a closed system to reach the room temperature. All the unburnt biomass and char are moved from the reactor core by a vacuum machine. The reactor core also needs to be dismantled so the ash can be retrieved

from the air plenum. Tar is collected from the collection jars and all the above are weighted. Char samples are taken at different height of reactor core to measure the size for all runs. The feed rate of the biomass is calculated by the total biomass consumed after the ignition over the total operating time.

3. RESULTS AND DISCUSSION

3.1. EQUIVALENCE RATIO

Equivalence ratio (ER), defined as the ratio between the supplied air and the stoichiometric air for complete combustion. The values of ER for the different experiments carried out are approximately constant (0.1–0.35).

$$ER = \frac{\text{the actual air/fuel ratio}}{\text{air/fuel ratio for stoichiometric combustion}} \quad (1)$$

The equivalence ratio is the most critical parameter to control in the gasification process. This balance between the air flow and the biomass feed will influence, most importantly (1) the syngas compositions; (2) the bed temperature and gasification speed; (3) bed performance. During each experiment run, the ER should stay the same. However, the conductor sometimes needs to change the valve setting the control the movement of the bed or to control gasifying temperature, or test the respond of the process to identify the possible causes when there is a problem.

3.2. THE SYNGAS COMPOSITIONS

To assess the process technology, the following variables were defined and calculated by [18] as below

$$\eta_c = \frac{1000V_{\text{gas}}*(CH_4\%+CO\%+CO_2\%+2(C_2H_4+C_2H_6+C_2H_2)*12/22.4)}{W(1-X_{\text{ash}})*Carbon\%} \quad (2)$$

$$LHV = CO \times 12.636 + H_2 \times 10.798 + CH_4 \times 35.818 + C_2H_4 \times 59.036 + C_2H_6 \times 63.772 \quad (3)$$

Readers can achieve the syngas compositions after this paper is accepted by a journal.

3.3. TEMPERATURE PROFILE

The cooldown time during the shutdown system has a significant dependence on the reactor size and biomass type.

Figure 4 below shows a typical temperature profile of the gasification process. The temperature increases rapidly after the ignition, it only takes 2~3mins for the gasification zone to reach the desired gasification temperature. The whole system takes about 40 mins to achieve stability. The temperature starts to decrease after we feed biomass with tar due to the increasing moisture. When shutdown procedure starts, both combustion and gasification temperatures will decrease.

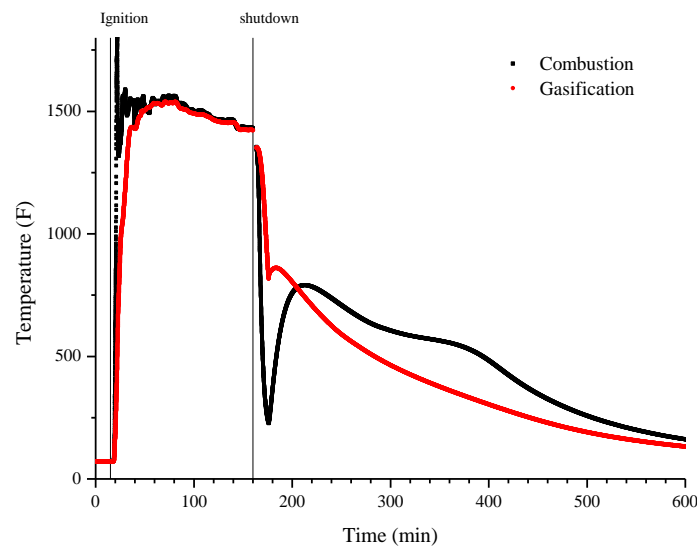


Figure 4. Typical temperature profiles

3.4. TAR

Bio-tar is a dark liquid of high viscosity, see Figure 5. It has a significant amount of miscible water for about 30-70%. The water has a negative effect on syngas production when fed back into the gasifier, researchers may consider over dry the tar before recycling. In this experimental setup, a small amount of tar enters the furnace, burning along with the syngas and generate soot. The hard soot rock lays on the syngas outlet and causes blockage.



Figure 5. Bio-tar produced during the gasification

3.4.1. Tar Compositions. The tar samples are collected and analyzed by H^1 -NMR to examine the difference before and after the tar recycling. Additionally, a thermal cracking investigation of the tar residue is performed. 2 ± 0.1 g of tar samples are heated to 800°F for 2s, 4s, 6s and 8s. All the tar samples are diluted 1:200, and are then analyzed by NMR.

3.4.2. Tar Amount. The tar amount has a significant relationship on the running time, see Figure 6. The tar production runs the highest within the first 15 mins of the startup. In this region, the biomass bed is still accumulating heat and increasing its temperature, this match the claim that the tar is produced at lower temperatures. When the bed temperature keeps climbing and getting stabilized between 15-30min, the tar amount reduces significantly. And then tar amount stays almost the same for 30-45min and 45-60min, as there is slightly temperature fluctuation at this stage. Among all the biomass feedstocks, the pellets produce the most tar at start up session, as pellets has big density thus needs more time to stabilize. But, they produce least tar after being stabilized, as they achieve higher operation temperature than the other two feedstocks.

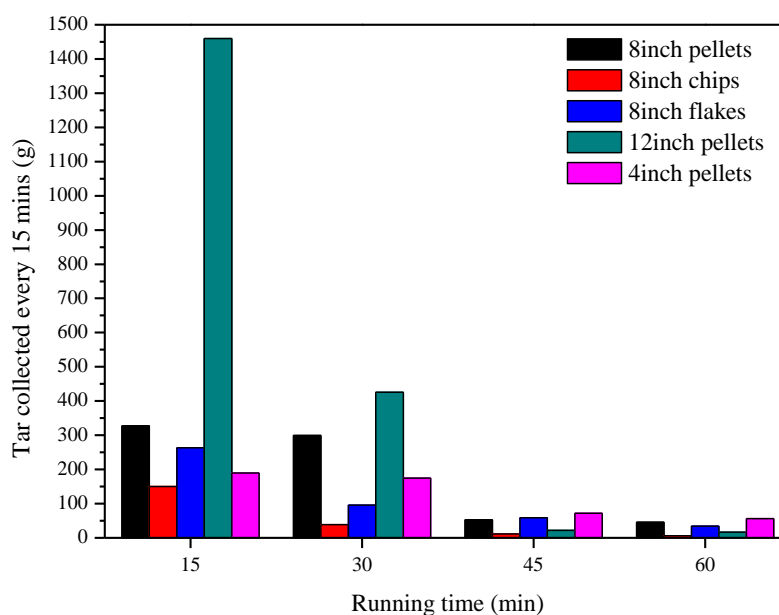


Figure 6. Amount of tar production every 15mins

3.5. CHAR SIZE DISTRIBUTION

Since plenty of researchers are simulating the gasification process using computational fluid dynamics, the void ratio and size distribution are important numerical parameters. Biochar is the leftover stable solid inside of the reactor core, which is rich in carbon. Table 3 gives the measured physical properties of char. When compared to Table 1, it is obvious that biomass beds increase their void ratios.

Table 3. Physical properties of gasified char

Physical Properties	Pellets Char	Picks Char	Flakes Char
Bulk Density (kg/m ³)	234	73	24
Absolute Density (kg/m ³)	779	359	379
Void Ratio	0.70	0.80	0.94

During the process of gasification, the biomass starts to be gasified from the surface to the core, causing the shrinkage and increased porosity of the biomass. The plain biomass and the gasified char are separated by sieves of different sizes, the meshes are 1mm, 2mm, 3mm, 4mm, 5mm, 6mm, 8mm. The separated biomass and char are weighted and recorded at the average size intervals, in other words 0.5mm, 1.5mm, 2.5mm, 3.5mm, 4.5mm, 5.5mm, 7mm, and 8.5mm. Figure 7 is a photo of the pellet char after the combustion.

Figure 8 illustrates the size distribution of all three types of biomass. These distributions have been fitted into Gaussian distribution curve, and the curve parameters

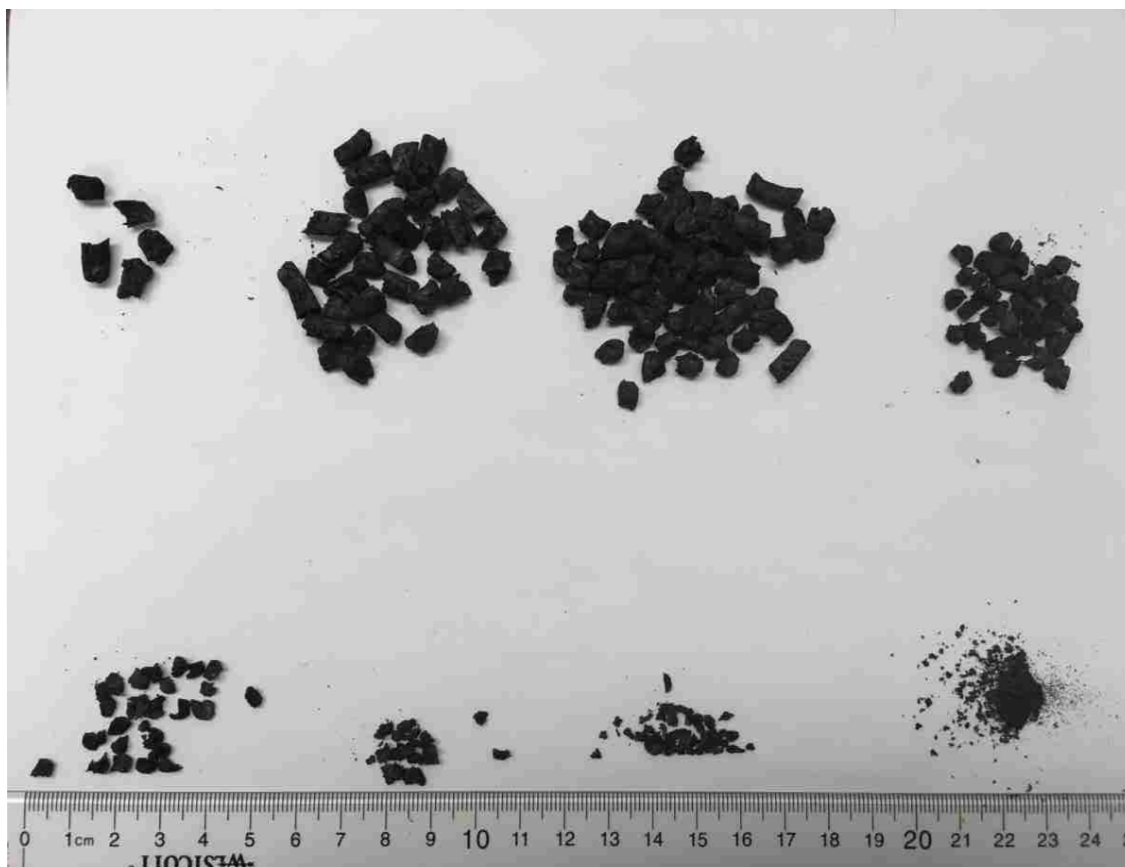


Figure 7. Char particles after sieving

are also listed below. As can be seen, the plain pellets and flakes have wider size span, their peaks are also located at the same position, say 6.8~7mm. However, the distribution peak of the picks is higher, which means their lengths are more centralized to about 7.3mm. Figure 9 gives the size distribution of biochar. Generally speaking, the biomass at the top receives shorter gasifying time than the biomass lies in the middle, the bottom char has the longest gasifying time. The size distribution confirmed this in another way- the peaks moving to smaller sizes as we dig deeper into the bed. At the same time, the gasification process also changed the standard deviation of the biomass size in various ways: it

centralizes the pellets, disperses the picks and flakes. Moreover, the pellets and picks char particles do not disappear at small sizes, they stopped pyrolysis reaction while the particle size $< 2\text{mm}$, so that the weight starts to accumulate. However, the flakes do not have this phenomenon.

3.6. THE AGGLOMERATION PHENOMENA OF THE CHAR PARTICLES

Agglomeration of bed material is a major operational problem in the gasification process. Agglomeration can result in biomass bridging inside the bed, as well as low carbon utility due to the decreased surface area of carbon particles. Among all types of gasifiers, fluidized bed might be the one most sensitive to the agglomeration. According to Lackner et al., the presence of low melting chemical compounds during the gasification process, the liquids increase particle stickiness and thus cause the agglomeration. In our case, the agglomeration exists for all the biomass, see Figure 10. The flakes form biggest agglomerated bulks, but they are the easiest to breakdown when interfered.

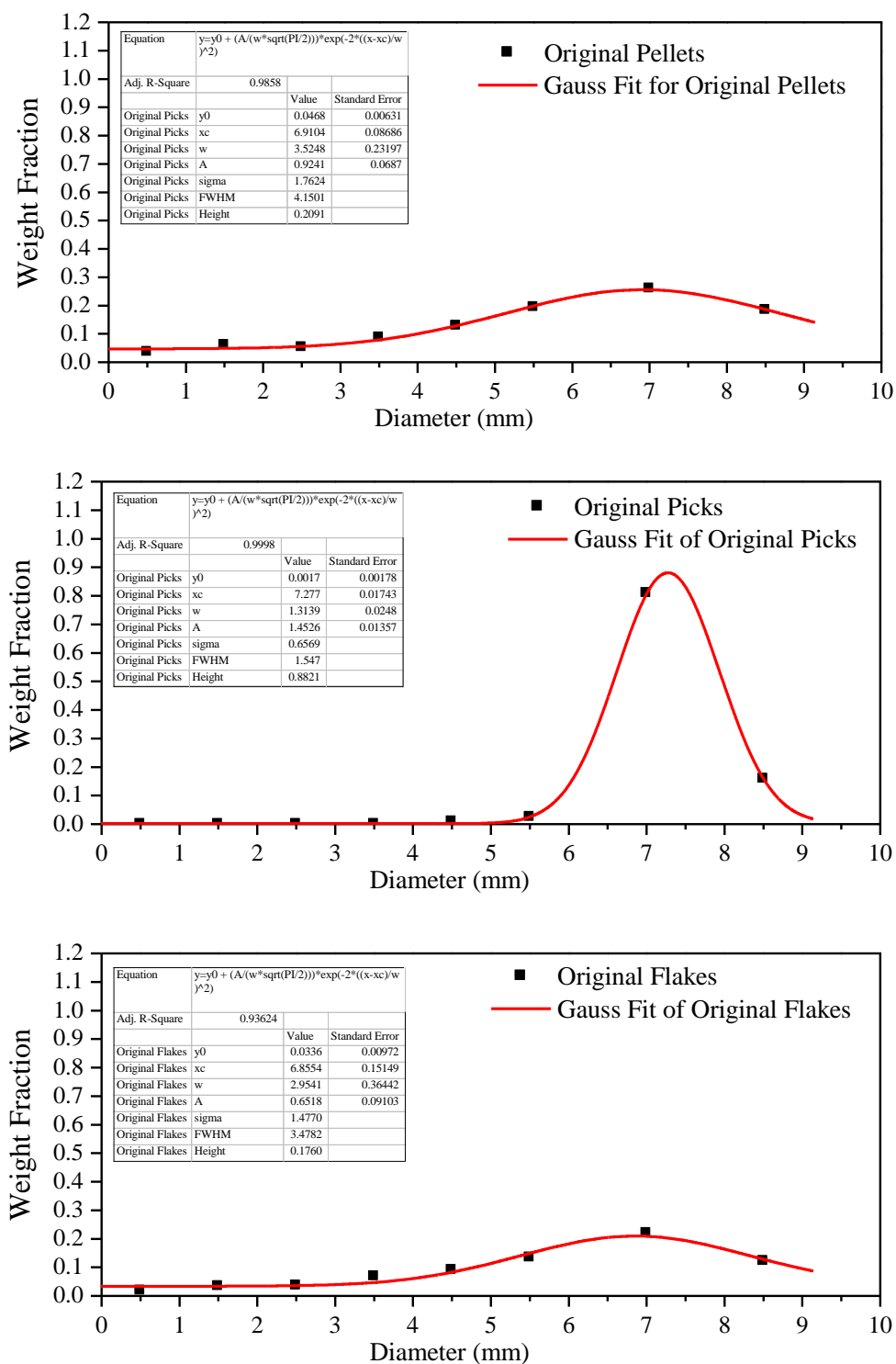


Figure 8. Size distribution for three types of feedstock

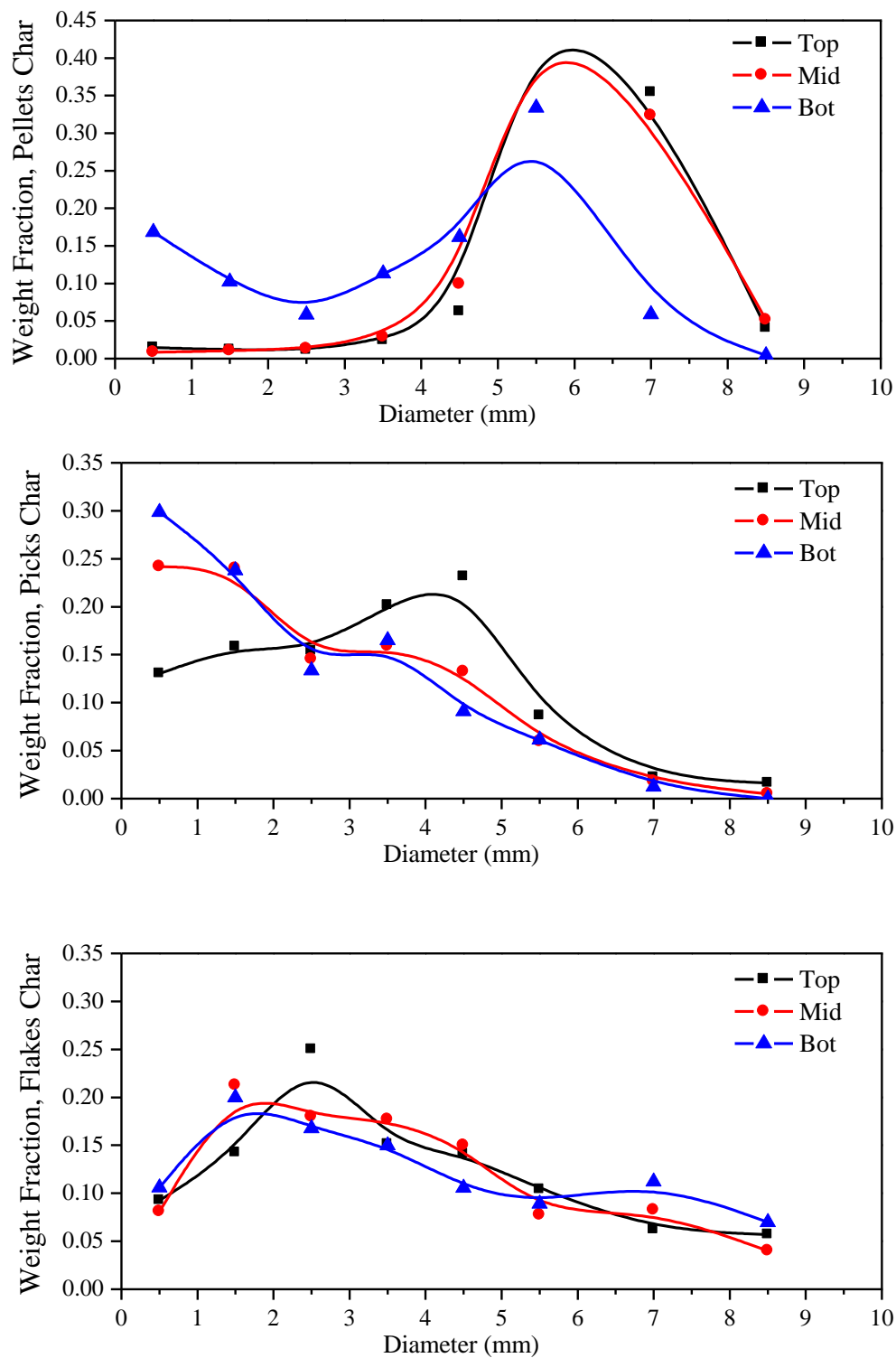


Figure 9. Char size distribution



Figure 10. Agglomeration phenomena for pellets, picks and flakes

4. PROCESS CONTROL

4.1. PREPROCESSING OF THE BIOMASS

The goal of pre-processing options for the biomass is to make the overall system works better or to be more cost-effective. The pre-processing includes pre-drying, chipping and pelletizing for the biomass. Biomass with a high moisture content has a high failure ratio on ignition. In our case, the original picks refuse to catch fire, they are air dried before feeding. Bridging is more common for picks and flakes than pellets and is more likely to exist around the thermocouples, see Figure 11. Pelletizing or baling the biomass can avoid this processing problem.



Figure 11. Bridging phenomenon when processing picks

4.2. TROUBLESHOOTING

Troubleshooting during the experiment is critical when (1) the experiments do not yield the expected results, and (2) the system is operating under unsteady state, the collected results could not be trusted. Experimental failure causes loss of time and money. However, due to the involvement of big amount of equipment and controlling parameters, troubleshooting is not easy. The first step is to properly distinguish normal and abnormal scenario.

The normal scenario refers to the system fluctuations that are not drastic and controllable. They are usually not fatal to the system and can be self-stabilized after a short time. They include: (1) temperature drop when adding new batches of biomass, (2) elevated temperature with increasing ER.

Abnormal scenario is the ones requires an immediate response or/and emergency shutdown. Table 4 lists the difficulties this setup experienced during the investigation.

Table 4. Troubleshooting and rectification

Problem Statement	Possible Causes and Recommendations
<i>Startup Process</i>	
Temperature does not increase after ignition.	<ol style="list-style-type: none"> 1. System blockage, due to the tar accumulation; 2. Check the fan and make sure it is working properly; 3. system leakage, due to the unsecured tar collection jars or pipe connections; 4. During the initial ignition step, the flow rate of the air should be carefully controlled. Intensive air blows the flame down, while the low-velocity air causes the flame to burn upwards, which prevent heat accumulation inside

Table 4. Troubleshooting and rectification (cont.)

	of the bed. Experiment conductors can put a flame at the open inlet of the bed, the flame should go downwards slightly, rather than upwards.
Harsh temperature drop/bed shutdown after loading new feed.	temperature drop within 100°F is acceptable after new loads of biomass. However, it might result in a harsh temperature drop if there is not enough preserved heat in the bed before adding new biomass batches. Avoid adding new biomass before the combustion zone temperature achieves 100°F.
Ignition difficulty	The biomass may result in ignition difficulty if the biomass contains high moisture (>20%). To process this kind of biomass, either 1. dry the biomass before loading into the reactor, or 2. Put another layer of drier and smaller size biomass (e.g. sawdust) on the top to pass the flame forward.
Bed height lost after ignition.	<ol style="list-style-type: none"> 1. Decrease the valve setting; 2. Change to a smaller grate to avoid biomass falling to the ash tray; 3. Avoid the vibration of the bed.
<i>Steady State Process</i>	
Syngas stream is not stable.	<ol style="list-style-type: none"> 1. Fan is not working continuously; 2. Cavities inside of biomass bed when elongate biomass is used. These cavities may cause localized oxygen building up, even a small-scale explosion. Vibration is needed for this case to dismiss the bridging.

Table 4. Troubleshooting and rectification (cont.)

Temperature drops continuously, and it could not be improved significantly by increasing valve setting.	<p>This usually indicates there is no sufficient air passing through the bed, Usually due to a block in burner due to the tar accumulation.</p> <ol style="list-style-type: none"> 1. Consider unclogging the burner first, and enhance the tar collection efficiency to prevent further block. 2. Check the tar collection jars and see if they are full. Sometimes those jars are not replaced on time, the tar pile up inside the pipeline and thus weakens the air suction.
Bed temperatures do not respond to valve setting, the oxygen sensor 7(b) has higher read than 7(a).	The unidentical oxygen reads imply a leakage in the pipeline. In our setup, since the tar collection jars need to be replaced every 15 mins. The fresh air may slip in from the jars rather than the pipe joints.
Tar amount reduced significantly compared to other runs, and/or lighter color tar is produced.	Jam in tar collection jar. Dismantle the pipeline and clean the inner surface. Tar is sticky and has difficulty dissolving in kerosene, gasoline or degreaser. Thanks to the thermal cracking of tar, propane torch could be used to heat up the tar and convert it into soot. The soot can then be removed from the surface using a metal brush easily.
Solid biomass is ejected from the opening top	This reflects a serious bridging phenomenon inside of the packed bed, resulting in local areas with high O ₂ , hence produces local syngas explosion. When this happens, start vibrating the bed first, if the problem persists, shutdown the system.
The drying zone temperature is higher than the normal drying temperature (500°F).	This indicates a pile up of the biomass bed. The bed should be maintained at a stable level to achieve a continuous production. The main idea of solving this is to increase the biomass consumption of the process.

Table 4. Troubleshooting and rectification (cont.)

	<ol style="list-style-type: none"> 1. Vibration should be enhanced to increase the biomass passing through ratio at the grate; 2. increase the grate mesh; 3. increase the valve setting.
Temperatures inside the bed are lower than any/all temperature(s) in the pipeline. A slow bed shutdown may be observed.	A leakage should be considered between the bed and the gas pipeline. In our case, this leakage is located between the reaction core and the gasifier shell. The air goes in and relocates the combustion zone to the shell plenum, the combustion heat mostly transferred to the environment rather than the biomass bed. The biomass bed is left to burn with very limited air by natural convection.
<i>Shutdown Process</i>	
Smoke comes out from the seal plate.	The proper seal of the shutdown plate should always be a priority if this scenario exists. However, one can still shut down the bed in time by controlling valve setting as an alternative. First open the valve completely when N ₂ purge starts, keep this until the temperature drops to ~800°F. Then close the valve completely, and slowly increase the valve setting to a level that the smoke just stops coming out from the seal plate. Keep it until the gasification temperature is lower than 300°F. Then shut down the N ₂ and close the valve, seal the system completely. In this way, there is no fresh air leaking into the system due to the plate gap.
It takes 2-3 days to shut down a pilot-scale gasifier	The reactor is not properly sealed, check the reactor body, seal gate and the valve to make sure there is no air going into the gasifier.

5. THE SHUTDOWN TIME

Shutdown is one of the most important steps when a gasifier is running. In the process of experimental investigation of the pilot scale gasifiers, shutdown is always needed when we have an overheated bed, or when one run is completed. In industry, the gasifier might need a shutdown due to time to time inspection or a catalyst refill, even there is no sign of abnormal operation. In this paper, the N_2 gas is fed into the bed at 1scfm, using as the inert gas to kill the active reactions. Some other researchers used a vacuum fan or machine to dilute the gas phase and accelerate the shutdown process. Figure 12 illustrates the comparison of the shutdown time among biomass feeds and gasifier sizes. For 8" reactor, pellets take longer than flakes and longer than the picks. For different sizes, the 12" reactor takes longest to shut down and the 4 inch takes shortest. After the shut the N_2 purge and the valve, the whole reactor becomes a closed system full of inert gas. There is a temperature revival after this, the possible reasons involve: (1) Both the thermocouples and the N_2 inlet are placed very near to the center of the reactor, the thermocouples are more likely detecting the temperatures of the N_2 could flow rather than the average zone temperature; and (2) The cold N_2 gas goes through the bed with the void between the biomass and decrease the biomass temperature from the surface, the heat inside of the biomass core must conduct along the diameters to transport to the surface, thus the biomass cores thus have higher temperatures than the surfaces. When the N_2 is shut, the heat from the biomass will increase the temperature of the gas phase until reaches the heat balance. The larger the gasifier is, the drastic this temperature revolve will be, and for sure will take longer for the whole reactor to reset to the room temperature.

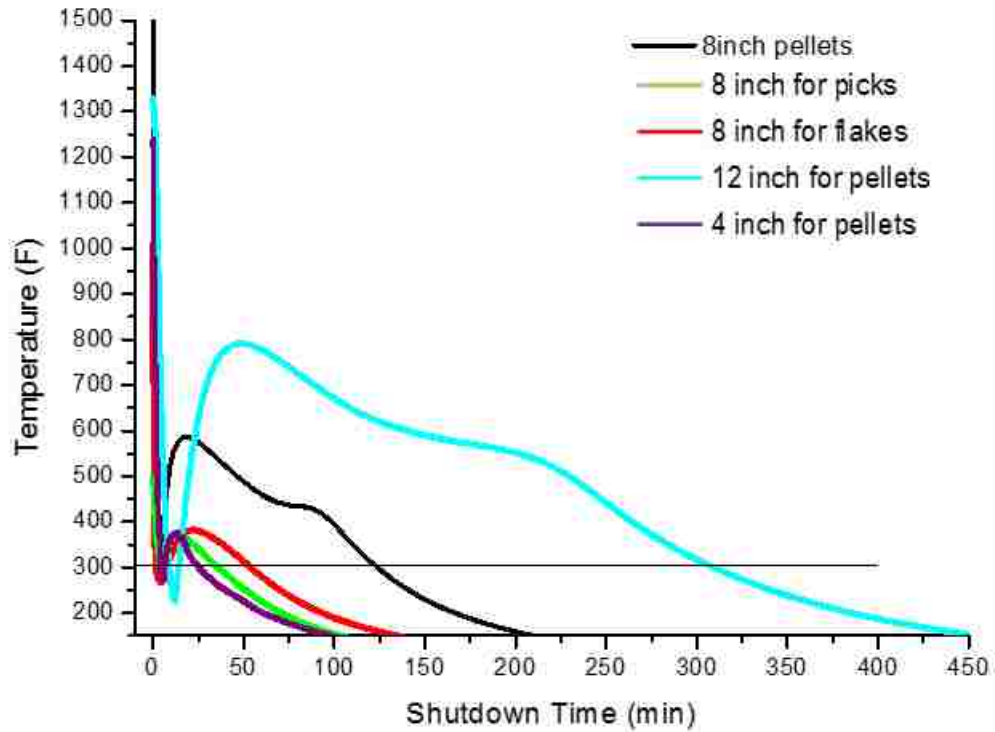


Figure 12. Shutdown time comparison

In our case study, the N_2 purge time is defined the time from the beginning of shutdown to the time that gasification zone temperature drops to 250°F. Since the speed of N_2 is stable during the flushing, N_2 consumption is proportional to the purging time. From Table 5. It can be known that the N_2 purge time does not vary a lot for pellets and picks, but takes much shorter for flakes. And, it does not change from 4" to 8", but doubled from 8" to 12". The isolation time is the duration from system closing to when the gasification temperature goes below 300°F. The cooldown time is exponentially related to the reactor diameter, or proportional to the reactor volume. Say,

$$\text{Isolation Time} \propto \text{reactor volume} \quad (4)$$

Table 5. The cooling down time for each gasification setups

	N ₂ Purge Time (min) / Isolation Time (min)		
	4" Reactor	8" Reactor	12" Reactor
Pellets	4.40 / 56	4.40 / 163	8.48 / 374
Picks		4.70 / 66	
Flakes		1.40/ 92.6	

An industrial syngas plant that consumes 1ton biomass per hour may have a reactor size 500 times more than our 12" reactor, then it takes approximately 3 months to cool down to 300°F. Due to this reason, a gasification plant should always perform a shutdown only when necessary. At the same time, they may modify the procedure to minimize the shutdown time. For example, purging the N₂ gas for 1-2 days instead of shutting down at a specific temperature, purging the system several times instead of only once, and/or using a fan to vacuum the system.

6. CONCLUSION

Experimental investigations of biomass gasification in downdraft fixed bed gasifiers of three different sizes are carried out using three different biomasses (pellets, picks and flakes) under various operating conditions. This paper reported the syngas compositions, tar compositions and their concentrations, biomass and gasified char size distributions and the agglomeration phenomena. The pellets produced the largest amount of tar at low temperatures. The original biomass size could be fit using a Gaussian distribution, while the gasified char size distribution derives from the Gaussian distribution. Agglomeration is a main process problem in the runs and the size of the agglomerated bulks are reported.

As the study of the general procedure and process control is lacking in the literature, this paper elaborates the detailed procedure of all the three stages for a single experimental run, including startup stage, steady-state stage, as well as the shutdown stage. In the process control section, experimental issues are separated into normal and abnormal scenarios; the recommended solutions are provided for each problem. The shutdown process is not favorable unless it is necessary, as it takes months for an industrial plant to return to ambient temperature.

REFERENCES

1. Bui, T., R. Loof, and S. Bhattacharya, Multi-stage reactor for thermal gasification of wood. *Energy*, 1994. 19(4): p. 397-404.
2. Nakamura, S., S. Kitano, and K. Yoshikawa, Biomass gasification process with the tar removal technologies utilizing bio-oil scrubber and char bed. *Applied Energy*, 2016. 170: p. 186-192.
3. Han, J. and H. Kim, The reduction and control technology of tar during biomass gasification/pyrolysis: an overview. *Renewable and Sustainable Energy Reviews*, 2008. 12(2): p. 397-416.
4. Milne, T.A., R.J. Evans, and N. Abatzoglou, Biomass Gasifier "Tars": Their Nature, Formation, and Conversion. 1998, National Renewable Energy Laboratory, Golden, CO (US).
5. Woolcock, P.J. and R.C. Brown, A review of cleaning technologies for biomass-derived syngas. *Biomass and bioenergy*, 2013. 52: p. 54-84.
6. Asadullah, M., Barriers of commercial power generation using biomass gasification gas: a review. *Renewable and Sustainable Energy Reviews*, 2014. 29: p. 201-215.
7. Cao, Y., et al., A novel biomass air gasification process for producing tar-free higher heating value fuel gas. *Fuel Processing Technology*, 2006. 87(4): p. 343-353.
8. Pan, Y., et al., Removal of tar by secondary air in fluidised bed gasification of residual biomass and coal. *Fuel*, 1999. 78(14): p. 1703-1709.
9. Narvaez, I., et al., Biomass gasification with air in an atmospheric bubbling fluidized bed. Effect of six operational variables on the quality of the produced raw gas. *Industrial & Engineering Chemistry Research*, 1996. 35(7): p. 2110-2120.
10. Yu, H., et al., Characteristics of tar formation during cellulose, hemicellulose and lignin gasification. *Fuel*, 2014. 118: p. 250-256.
11. Prando, D., et al., Characterisation of the producer gas from an open top gasifier: Assessment of different tar analysis approaches. *Fuel*, 2016. 181: p. 566-572.
12. Edwards, N.T., Polycyclic aromatic hydrocarbons (PAH's) in the terrestrial environment—a review. *Journal of Environmental Quality*, 1983. 12(4): p. 427-441.
13. Laflamme, R.E. and R.A. Hites, The global distribution of polycyclic aromatic hydrocarbons in recent sediments. *Geochimica et cosmochimica Acta*, 1978. 42(3): p. 289-303.

14. Samanta, S.K., O.V. Singh, and R.K. Jain, Polycyclic aromatic hydrocarbons: environmental pollution and bioremediation. *TRENDS in Biotechnology*, 2002. 20(6): p. 243-248.
15. Falahatpisheh, M., K. Donnelly, and K. Ramos, Antagonistic interactions among nephrotoxic polycyclic aromatic hydrocarbons. *Journal of Toxicology and Environmental Health Part A*, 2001. 62(7): p. 543-560.
16. Unwin, J., et al., An assessment of occupational exposure to polycyclic aromatic hydrocarbons in the UK. *Annals of Occupational Hygiene*, 2006. 50(4): p. 395-403.
17. Abdel-Shafy, H.I. and M.S. Mansour, A review on polycyclic aromatic hydrocarbons: source, environmental impact, effect on human health and remediation. *Egyptian Journal of Petroleum*, 2016. 25(1): p. 107-123.
18. Lv, P., et al., An experimental study on biomass air–steam gasification in a fluidized bed. *Bioresource technology*, 2004. 95(1): p. 95-101.

SECTION

2. OVERALL CONCLUSION

The key findings of this work are summarized in this section. The main objective of this work is to have a better understanding of the main troublemaker tar in the gasification system. To achieve this goal, this subject is divided into several aspects: formation, cracking and evolution mechanism, collection, disposal and recycling procedure.

In the Paper I and II, kinetic-based Aspen Plus models for both updraft and downdraft fixed bed gasifiers were developed to investigate the tar formation and cracking mechanism. The kinetics models are fundamentally superior to the traditional Gibbs Energy minimization model, thus can predict tar and syngas compositions more accurately. In Paper III, experimental investigations on tar recycling process in biomass gasifiers are carried out. This paper discusses the syngas composition, typical temperature profile, tar composition and amounts along the runtime. This study helps the reader to have a deeper understanding of tar.

This dissertation is also aiming to provide useful guidelines for other researchers working on biomass gasifiers. Note that there is a lack of reference focusing on the standard procedure and process control, this study reports the detailed procedure of the startup, steady state, and shutdown in Paper III. This paper also describes the problems experienced during the setup and provides the possible causes and recommends solutions.

APPENDIX A.

FORTRAN CODE IN THE PYROLYSIS CALCULATOR BLOCK

Calculation code:

$$\text{FACT} = (100 - \text{MOI}) / 100$$

$$\text{H}_2\text{O} = \text{MOI} / 100$$

$$\text{ASH} = \text{ULT}(1) / 100 * \text{FACT}$$

$$\text{PROPI} = 0.05$$

$$\text{ACET} = 0.05$$

$$\text{PHENOL} = 0.03$$

$$\text{TULENE} = 0.02$$

$$\text{C1} = \text{PROPI} / 74 * 36$$

$$\text{C2} = \text{ACET} / 58 * 36$$

$$\text{C3} = \text{PHENOL} / 94 * 72$$

$$\text{C4} = \text{TULENE} / 92 * 84$$

$$\text{CTAR} = \text{C1} + \text{C2} + \text{C3} + \text{C4}$$

$$\text{H21} = \text{PROPI} / 74 * 6$$

$$\text{H22} = \text{ACET} / 58 * 6$$

$$\text{H23} = \text{PHENOL} / 94 * 6$$

$$\text{H24} = \text{TULENE} / 92 * 8$$

$$\text{HTAR} = \text{H21} + \text{H22} + \text{H23} + \text{H24}$$

$$\text{O21} = \text{PROPI} / 74 * 32$$

$$\text{O22} = \text{ACET} / 58 * 16$$

$$\text{O23} = \text{PHENOL} / 94 * 16$$

$$\text{O24} = \text{TULENE} / 92 * 0$$

$$\text{OTAR} = \text{O21} + \text{O22} + \text{O23} + \text{O24}$$

$C = \text{ULT}(2)/100 * \text{FACT-CTAR}$

$H2 = \text{ULT}(3)/100 * \text{FACT-HTAR}$

$N2 = \text{ULT}(4)/100 * \text{FACT}$

$CL2 = \text{ULT}(5)/100 * \text{FACT}$

$S = \text{ULT}(6)/100 * \text{FACT}$

$O2 = \text{ULT}(7)/100 * \text{FACT-OTAR}$

APPENDIX B.

GC ANALYTICAL METHOD

Method A

The columns used are:

Thermo Scientific™ TracePLOT TG-BOND MSieve 5A, 30 m, 0.53 mm, 50 µm.

The precolumn is:

Thermo Scientific™ TracePLOT TG-BOND Q, 15 m, 0.53 mm, 20 µm.

The method used is listed in Table 1.

Table 1. GC analytical method

Oven Method	FID - Front Method
Initial temperature: 30.0 °C	Temperature: 250 °C
Initial hold time: 2.00 min	Ignition threshold: 1.0 pA
Number of ramps: 1	Air flow: 350.0 mL/min
Ramp rate: 20.0 °C/min	Hydrogen flow: 35.0 mL/min
Final temperature: 100.0 °C	Makeup gas flow: 40.0 mL/min
Ramp hold ti 2.00 min	TCD - Back Method
GSV - Front Method	Temperature: 100 °C
S/SL mode Split	Filament power on: Yes
Temperature enable: On	Filament temperature: 150 °C
Temperature: 120 °C	Reference gas enable: On
Split flow enable: On	Reference gas flow: 1.0 mL/min
Split flow: 5.0 mL/min	Carrier source: Front
GSV inj start time: 0.00 min	Acquire data: Yes
GSV inj duration: 0.50 min	Signal process: Standard Peaks
Carrier mode: Constant Flow	Negative polarity: No
Carrier flow 5.000 mL/min	Prep-run - TCD (Back): Autozero

Method B

The column used is:

Agilent J&W GS-CarbonPLOT column, 30 m, 0.320 mm, 3.00µm, part number

Method:

Helium at 27cm/sec (calculated off N₂ at 35°C)

Oven: -40 °C (below ambient temperature)

Injector: split 1:30, 185 °C, 250µL injection volume

Detector: TCD, 150 °C

REFERENCES

1. World Energy Council, World Energy Resources, Bioenergy, 2016. 2016.
2. Tilman, D., et al., Beneficial biofuels—the food, energy, and environment trilemma. *Science*, 2009. **325**(5938): p. 270-271.
3. Chum, H.L. and R.P. Overend, Biomass and renewable fuels. *Fuel processing technology*, 2001. **71**(1-3): p. 187-195.
4. Higman, C. and M. Van Der Burgt, *Gasification*. 2003: Gulf Professional Publishing.
5. Zhao, Y., et al., Characteristics of rice husk gasification in an entrained flow reactor. *Bioresource technology*, 2009. **100**(23): p. 6040-6044.
6. Zhou, J., et al., Biomass–oxygen gasification in a high-temperature entrained-flow gasifier. *Biotechnology advances*, 2009. **27**(5): p. 606-611.
7. Hernández, J.J., G. Aranda-Almansa, and A. Bula, Gasification of biomass wastes in an entrained flow gasifier: Effect of the particle size and the residence time. *Fuel Processing Technology*, 2010. **91**(6): p. 681-692.
8. Turn, S., et al., An experimental investigation of hydrogen production from biomass gasification. *International Journal of Hydrogen Energy*, 1998. **23**(8): p. 641-648.
9. Lv, P., et al., An experimental study on biomass air-steam gasification in a fluidized bed. *Bioresource technology*, 2004. **95**(1): p. 95-101.
10. Li, X., et al., Biomass gasification in a circulating fluidized bed. *Biomass and Bioenergy*, 2004. **26**(2): p. 171-193.
11. Breault, R.W., T. Li, and P. Nicoletti, Mass transfer effects in a gasification riser. *Powder technology*, 2013. **242**: p. 108-116.
12. Xiong, Q., S.-C. Kong, and A. Passalacqua, Development of a generalized numerical framework for simulating biomass fast pyrolysis in fluidized-bed reactors. *Chemical Engineering Science*, 2013. **99**: p. 305-313.
13. Collot, A., et al., Co-pyrolysis and co-gasification of coal and biomass in bench-scale fixed-bed and fluidised bed reactors. *Fuel*, 1999. **78**(6): p. 667-679.
14. Chopra, S. and A. Jain, A review of fixed bed gasification systems for biomass. 2007.
15. Atnaw, S.M., S.A. Sulaiman, and S. Yusup, Syngas production from downdraft gasification of oil palm fronds. *Energy*, 2013. **61**: p. 491-501.

16. Dogru, M., et al., Gasification of hazelnut shells in a downdraft gasifier. *Energy*, 2002. **27**(5): p. 415-427.
17. Gai, C. and Y. Dong, Experimental study on non-woody biomass gasification in a downdraft gasifier. *International Journal of hydrogen energy*, 2012. **37**(6): p. 4935-4944.
18. Janajreh, I. and M. Al Shrah, Numerical and experimental investigation of downdraft gasification of wood chips. *Energy Conversion and Management*, 2013. **65**: p. 783-792.
19. Lv, P., et al., Hydrogen-rich gas production from biomass air and oxygen/steam gasification in a downdraft gasifier. *Renewable Energy*, 2007. **32**(13): p. 2173-2185.
20. Pérez, J.F., A. Melgar, and P.N. Benjumea, Effect of operating and design parameters on the gasification/combustion process of waste biomass in fixed bed downdraft reactors: An experimental study. *Fuel*, 2012. **96**: p. 487-496.
21. Zainal, Z., et al., Experimental investigation of a downdraft biomass gasifier. *Biomass and Bioenergy*, 2002. **23**(4): p. 283-289.
22. Chen, W., et al., Updraft fixed bed gasification of mesquite and juniper wood samples. *Energy*, 2012. **41**(1): p. 454-461.
23. Pedroso, D.T., et al., Experimental study of bottom feed updraft gasifier. *Renewable energy*, 2013. **57**: p. 311-316.
24. Plis, P. and R. Wilk, Theoretical and experimental investigation of biomass gasification process in a fixed bed gasifier. *Energy*, 2011. **36**(6): p. 3838-3845.
25. Saravanakumar, A., et al., Experimental investigations of long stick wood gasification in a bottom lit updraft fixed bed gasifier. *Fuel processing technology*, 2007. **88**(6): p. 617-622.
26. Ueki, Y., et al., Gasification characteristics of woody biomass in the packed bed reactor. *Proceedings of the Combustion Institute*, 2011. **33**(2): p. 1795-1800.
27. Reed, T. and A. Das, *Handbook of biomass downdraft gasifier engine systems*. 1988: Biomass Energy Foundation.
28. Higman, C., *Gasification, in Combustion Engineering Issues for Solid Fuel Systems*. 2008, Elsevier. p. 423-468.
29. McKendry, P., Energy production from biomass (part 3): gasification technologies. *Bioresource technology*, 2002. **83**(1): p. 55-63.

30. Corton, J., et al., The Impact of Biomass Feedstock Composition and Pre-treatments on Tar Formation during Biomass Gasification. *Advances in Biofeedstocks and Biofuels: Biofeedstocks and Their Processing*, 2017: p. 33-53.
31. Rabou, L., Biomass tar recycling and destruction in a CFB gasifier. *Fuel*, 2005. **84**(5): p. 577-581.

VITA

Jia Yu grew up in Xi'an, which is the previous capital for more than 13 dynasties along the Chinese history. She received her B.S. in Chemical Engineering from East China University of Science and Technology (formerly known as East China College of Chemical Engineering) located in Shanghai, PRC. Jia landed on the US soil in 2012 and joined the research group of Dr. Joseph D. Smith in spring 2013. She received an M.S in Chemical Engineering in 2016 and Ph.D. in Chemical Engineering in May, 2018, both from Missouri University of Science and Technology in Rolla, Missouri.

Jia was a member of American Institute of Chemical Engineering. During her time in Missouri S&T, she served as teaching assistant in the chemistry department for more than 2 years. Her research specialized in the process modeling using Aspen Plus software, as well as experimental design and investigation specialized in biomass gasification process and hybrid energy systems.